TECHNISCHE UNIVERSITÄT MÜNCHEN

II. Medizinische Klinik und Poliklinik des Klinikums rechts der Isar

Transcription factors in acute pancreatitis

Patrick Thomas Neuhöfer

Vollständiger Abdruck der von der Fakultät für Medizin der Technischen Universität München zur Erlangung des akademischen Grades eines

Doktors der Naturwissenschaften

genehmigten Dissertation.

Vorsitzender: Univ.-Prof. Dr. U. Protzer

Prüfer der Dissertation:
1. Priv.-Doz. Dr. H. Algül
2. Univ.-Prof. Dr. H. Witt
3. Univ.-Prof. Dr. J. Adamski

Die Dissertation wurde am 20.06.2013 bei der Technischen Universität München eingereicht und durch die Fakultät für Medizin am 17.07.2013 angenommen.

Zusammenfassung

Das Ziel dieser Arbeit war es, molekulare Mechanismen der akuten Pankreatitis (AP) genauer zu untersuchen. Transkriptionsfaktoren scheinen eine wesentliche Rolle in der Pathogenese der akuten Pankreatitis zu spielen. Unter diesen Transkriptionsfaktoren nehmen NF-κB und Stat3 eine zentrale Rolle ein.

Im ersten Projekt dieser Arbeit wurde die Rolle von IκBα, dem Inhibitor von NF-κB, genauer untersucht. Vorversuche haben gezeigt, dass pankreasspezifische Inaktivierung von IκBα zu einer konstitutiven Aktivierung von RelA führt; die experimentelle AP in diesen Mäusen war attenuiert und die Trypsinaktivierung vermindert. Mit Hilfe von pankreasspezifischen Knockout Mäusen wurden anschließend NF-κB abhängige Gene identifiziert, die vor der Entstehung der AP schützen. Eines der identifizierten Gene war der Serinprotease Inhibitor 2A (Spi2A). SNP Analysen von *AACT*, dem humanen Analogon von *Spi2a*, in Patienten mit akuter und chronischer Pankreatitis zeigten jedoch keine Korrelation mit der Schwere der Erkrankung.

Im zweiten Projekt der Arbeit wurde die Rolle von IL-6 während der AP genauer untersucht. Es ist bekannt, dass IL-6 mit der Schwere der AP korreliert, jedoch ist nicht klar, ob IL-6 auch eine pathophysiologische Relevanz bei der AP besitzt. Um die Rolle von IL-6 genauer zu untersuchen wurde ein neues Model für eine schwere akute Pankreatitis etabliert. In diesem Model wurde gezeigt, dass IL-6 Trans-signaling und nicht der klassische IL-6 Signalweg den lokalen Schadens mit den systemischen Komplikationen der AP verknüpft. Durch die pankreasspezifische Inaktivierung von Stat3 bzw. Socs3 konnte die Bedeutung der IL-6-Trans-signaling/gp130/Stat3 Signalkaskade in der schweren AP gezeigt und charakterisiert werden. Pharmakologische Inhibitionsexperimente unterstrichen die Relevanz dieser Signalkaskade für mögliche Therapieansätze. Untersuchungen an Patienten mit milder und schwerer AP konnten die in den Mäusen gewonnenen Erkenntnisse bestätigen.

Parts of this thesis were submitted and accepted for publication:

Neuhöfer P., Liang, S. Einwächter, H. Schwerdtfeger, C. Wartmann, T. Treiber, M. Zhang, H. Schulz, H. U. Dlubatz, K. Lesina, M. Diakopoulos, K. N. Wörmann, S. Halangk, W. Witt, H. Schmid, R. M. and Algül, H. *Deletion of IκBα activates RelA to alleviate acute pancreatitis in mice through upregulation of Spi2A* Gastroenterology. 2013 Jan;144(1):192-201. doi: 10.1053/j.gastro.2012.09.058. Epub 2012 Oct 3.

Zhang H.*, **Neuhöfer P.***, Song L., Rabe B., Lesina M., Kurkowski MU., Treiber M., Wartmann T., Regnér S., Thorlacius H., Saur D., Weirich G., Yoshimura A., Halangk W., Mizgerd JP., Schmid RM., Rose-John S. and Algül H. *IL-6 trans-signaling promotes pancreatitis-associated lung injury and lethality* J Clin Invest. 2013 Mar 1;123(3):1019-31. doi: 10.1172/JCI64931. Epub 2013 Feb 15.
**these authors contributed equally to this work*

Table of content

1 Introduction

1.1 The Pancreas

1.1.1 Anatomy and physiology

The pancreas is located in the epigastrium between the spleen and the duodenum (Figure 1-1 A). It consists of two functional and histomorphologic compartments, the endocrine and the exocrine pancreas.

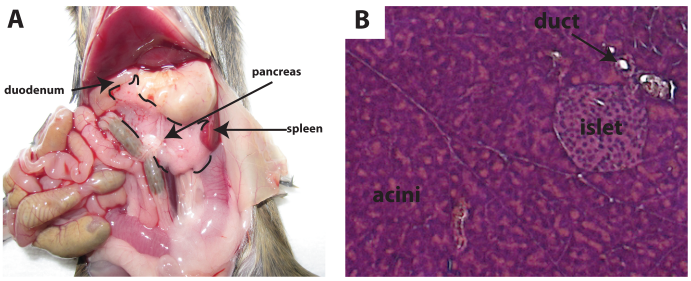

Figure 1-1: (**A**) Macroscopic localization of the pancreas in the abdomen. (**B**) Microscopic structure of the pancreas

Anatomically, the endocrine compartment is located in the islets of Langerhans, where hormones are produced by different cell types. Among those cells are glucagon-secreting α-cells, insulin-secreting β-cells, somastotatin-secreting δ-cells, pancreatic peptide-secreting pp-cells and ghrelin-secreting ε-cells. The islets of Langerhans play an important role in regulation of blood glucose levels and glucose metabolism. The other functional compartment, the exocrine pancreas, consists of acinar cells that are arranged in clusters called acini (Figure 1-1 B). Acini can be stimulated by the hormones secretin and cholecystokinin. Once secreted, the pancreatic juice is released into pancreatic ducts and from there into the duodenum. It contains precursor of the digestive enzymes, which are normally activated in the small intestine (Figure 1-2).

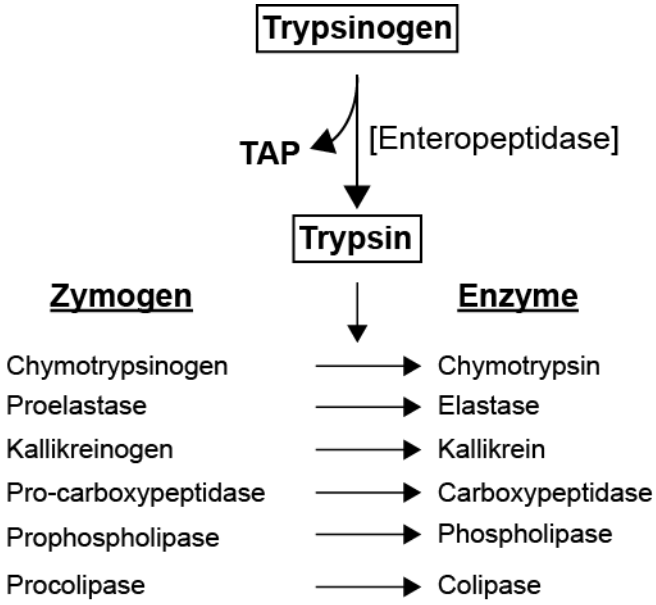

Figure 1-2: Pancreatic enzyme cascade.

1.2 Pancreatitis

Pancreatitis is a primarily sterile inflammatory disease of the pancreas. It can be divided into two different forms, acute pancreatitis (AP) and chronic pancreatitis (CP). While AP is a sudden inflammatory process of the pancreas, CP is characterized by chronic inflammation that progresses into irreversible morphological and functional damage of the exocrine and the endocrine pancreas.

1.2.1 Acute pancreatitis

In the United States, up to 210,000 patients per year are hospitalized due to AP (Baron and Morgan 1999). The most common causes for AP are gallstones and alcohol abuse. Other causes for AP are autoimmune pancreatitis, metabolic disorders as well as drug-induced AP. The disease can progress in two different ways. In the mild form of AP, patients recover without any complications, while in severe AP patients suffer from local as well as systemic complications (Frossard, Steer et al. 2008). While most patients develop a mild form of AP (70-80%), 20-30% of patients suffer from severe acute pancreatitis (SAP) with

an involvement of the immune system (termed: systemic inflammatory response syndrome “SIRS”). SIRS can develop into multiple organ failure (MOF) with mortality rates up to 50%. These systemic complications include acute lung injury (ALI) and sepsis. Currently, therapy is mostly symptomatic focusing on pain relief and fluid replacement, in serious cases with MOF, intensive care medicine is required.

Premature, intracellular activation of digestive enzymes is a central event during AP. The intrapancreatic conversion of trypsinogen to trypsin has been shown to play a crucial role in the onset of AP (Halangk and Lerch 2004). Activated trypsin in the acinar cells initiates the activation of a cascade of digestive enzymes, which leads to the autodigestion of the pancreas during AP (Figure 1-2) (Rinderknecht 1986). Although the concept of intrapancreatic trypsin activation as a trigger for pancreatitis appears to be conclusive, mutations in several members of the pancreatic enzyme cascade (PRSS1, SPINK1, CTRC*)* are associated with chronic (hereditary or idiopathic) pancreatitis rather than AP (Whitcomb, Gorry et al. 1996; Witt, Luck et al. 2000; Szmola and Sahin-Toth 2007; Rosendahl, Witt et al. 2008).

Beyond its implication in enzyme activation, trypsin has also been shown to be involved in modulating signaling pathways. MAPK signaling pathways, for example, were identified to be influenced by trypsin activity (Yoshida and Yoshikawa 2008). Specifically the phosphorylation of p-38, c-Jun/SAPK and Erk1/2 were correlated with trypsin conversion. Even more, trypsin also influences pro-inflammatory transcription factors, e.g., Ap1, Egr1 and nuclear factor κB (NF-κB). While there is a general consensus that the NF-κB signaling pathway is activated early during disease onset, its role in the course of the disease and its association with trypsin activity has still been under debate (Chen, Ji et al. 2002; Aleksic, Baumann et al. 2007; Algul, Treiber et al. 2007; Baumann, Wagner et al. 2007).

1.2.2 Chronic pancreatitis

Chronic pancreatitis (CP) is a disease that is characterized by inflammation-induced progressive pancreatic impairment that results in irreparable damage to

the exocrine as well as the endocrine compartment of the organ (Witt 2003; Witt, Apte et al. 2007). The incidence of CP in industrial countries ranges from 3.5-10 cases per 100.000 inhabitants. While 70-80% of these CP cases are caused by long term alcohol abuse, other causes such as hyperlipidemia, hypercalcemia and anatomical abnormalities are rare (Durbec and Sarles 1978; Ammann, Buehler et al. 1987). In 10-30% of CP cases, there is no apparent underlying condition, including heredity classifying these cases as idiopathic CP.

Over 100 years ago, Hans Chiari suggested that pancreatitis is a result of premature activation of pancreatic enzymes in the pancreas leading to autodigestion of the organ (Chiari 1896). The key role in the pancreatic enzyme cascade is attributed to the conversion of trypsinogen to trypsin, which leads to the conversion of all proteolytic enzymes to their active form (Figure 1-2)(Steer and Meldolesi 1987). Within recent years, mutations in genes regulating trypsinogen activation/inactivation have been linked to hereditary and idiopathic pancreatitis (Figure 1-3). Among the candidate genes, mutations in the cationic trypsinogen (*PRSS1*), the serine peptidase inhibitor Kazal type 1 (*SPINK1*), and the cystic fibrosis transmembrane conductance regulator (*CFTR*) have been found to be associated with chronic pancreatitis (Witt, Luck et al. 2000; Teich, Rosendahl et al. 2006; Rosendahl, Witt et al. 2008).

Clinically, three major features of CP are pain, exocrine insufficiency with maldigestion and endocrine insufficiency with subsequent diabetes mellitus type 3c (Ammann, Buehler et al. 1987). Abdominal pain is the most frequent clinical problem in patients with CP. Other clinical features include pseudocysts, weight loss and increased cancer risk. While recurrent or continuous pain is considered a hallmark of CP, pain can also originate from an acute attack of AP (Mullhaupt, Truninger et al. 2005). The development of pancreatic fibrosis, another cardinal feature of CP, is due to repeated attacks of pancreatic necroinflammation, with activation of pancreatic stellate cells playing a central role in fibrogenesis (Apte and Wilson 2004). Although there have been a lot of new and interesting results in CP research, therapy is usually still symptomatic, focusing on pain relief, oral enzyme substitution and insulin treatment for maldigestion and diabetes (Witt,

Apte et al. 2007). Only in cases with complications like duct congestion, pseudocysts or abscesses, surgery or endoscopic interventions are used.

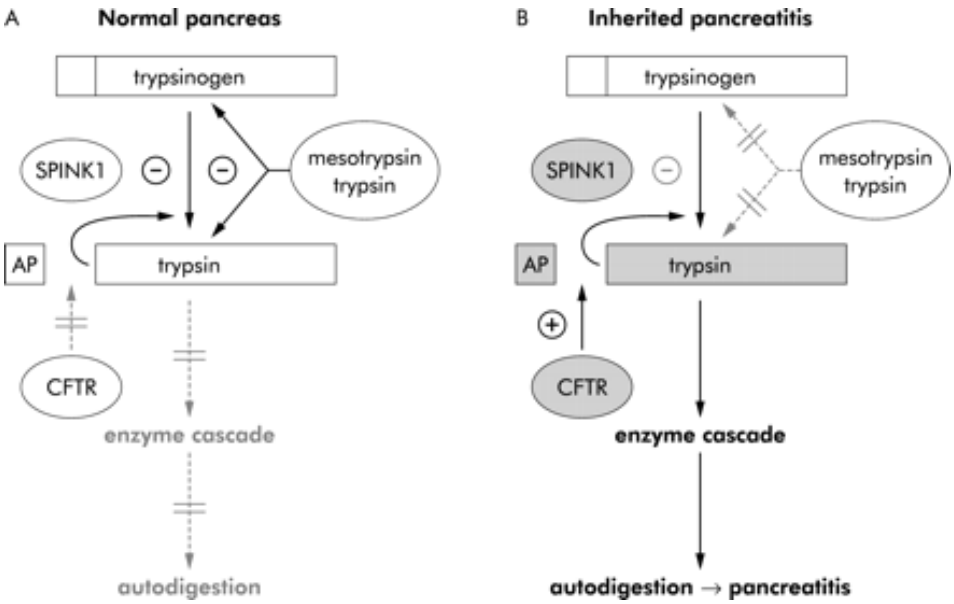

Figure 1-3: Role of digestive enzymes in pancreatitis. (**A**) Normal pancreas. SPINK1 and mesotrypsin inhibit autoactivation of trypsinogen within the pancreas. (**B**) Pancreatitis. Mutations in *SPINK1* and *PRSS1* lead to an imbalance of activated proteases in the pancreatic parenchyma, resulting in premature activation of pancreatic zymogens with subsequent autodigestion and inflammation. Adapted from (Witt 2003).

1.3 Experimental models of acute pancreatitis

1.3.1 Non-invasive models of acute pancreatitis

Several non-invasive models for experimental acute pancreatitis have been developed to investigate initiation, progression and possible treatment of AP.

1.3.1.1 Cerulein-induced pancreatitis

The cerulein-induced pancreatitis is the most common non-invasive AP model. Cerulein is a cholecystokinin analogue that causes AP in mice, rats, hamsters and dogs if applied in supraphysiological doses (Lampel and Kern 1977; Watanabe, Baccino et al. 1984; Niederau, Ferrell et al. 1985; Renner and Wisner 1986). Cerulein induces pancreatitis through intrapancreatic activation of digestive enzyme production and cytoplasmic vacuolization, leading to acinar

cell death and pancreatic edema (Yu, Kim et al. 2006). Cerulein can be injected intravenously, intraperitoneally or subcutaneously and allows control of timing and severity of AP by varying the concentration of cerulein administered and the number of injections (Su, Cuthbertson et al. 2006; Elder, Saccone et al. 2012). Pulmonary damage in cerulein-induced pancreatitis has been shown to mimic the early stages of acute lung injury (ALI) in the human disease (Guice, Oldham et al. 1988).

Taken together, cerulein-induced pancreatitis may be useful for evaluating pancreatitis-associated severe inflammatory response syndrome (SIRS) with mild ALI.

1.3.1.2 L-arginine-induced pancreatitis

Another non-invasive model for AP is the L-arginine-induced pancreatitis. In this model, L-arginine is administered twice intraperitoneally with one hour between the injections. This model leads to severe necrotizing pancreatitis with multiple organ damage within 72h (Dawra, Sharif et al. 2007). While the exact mechanism is still unknown, some data suggests that the conversion of L-arginine to nitric oxide may cause oxidative stress as well as endoplasmatic reticulum stress in the pancreas (Kubisch, Sans et al. 2006). Another possible mechanism of L-arginine-induced AP is the increase of pro-inflammatory cytokines (e.g. IL-6) (Huang, Wang et al. 2012). The advantages of the L-Arginine model are its high reproducibility, the non-invasiveness and the possibility to investigate early events during AP as well as the late phase (Su, Cuthbertson et al. 2006). The main disadvantages of L-arginine-induced pancreatitis are the unknown mechanism and that L-arginine is toxic to other organs. This toxicity makes it difficult to discriminate AP-related systemic complications from direct toxicity.

1.3.2 Invasive models of acute pancreatitis

Invasive models of AP were established to mimic the clinical situation more closely and provide animal models for severe AP. Most of the invasive models

of AP simulate the obstructive AP (e.g. biliary AP) observed in patients (Su, Cuthbertson et al. 2006).

The two best-established invasive models for AP are the taurocholate-induced pancreatitis as well as the pancreatitis model induced by bile duct ligation (Aho, Koskensalo et al. 1980; Awla, Abdulla et al. 2011). Sodium taurocholate is injected into the bilopancreatic duct, which leads to edema, necrosis and hemorrhage and late complications resembling clinical pancreatitis (Su, Cuthbertson et al. 2006). It also leads to leukocyte infiltration into the pancreas with acute inflammatory response. The model is however mostly used in bigger animals like dogs, cats and rats, since it is technically very challenging with high mortality rates. Acute pancreatitis may also be induced by ligation of the distal bile duct (Baxter, Jenkins et al. 1985). This creates an early development of acute pancreatitis, obstructive jaundice and cholangitis. The duct ligation model was developed in an attempt to resemble the clinical situation of gallstones. However, the complexity, technical difficulty, high cost, limited reproducibility and the analogy to chronic pancreatitis, have made the duct ligation model rarely used for evaluating acute pancreatitis (Su, Cuthbertson et al. 2006).

1.4 NF-κB signaling pathway

NF-κB is a family of inducible transcription factor that is found in almost all animal cell types. Specific NF-κB binding sites are found in the promoter/enhancer regions of a large number of genes. NF-κB mediates the transcription of genes that are involved in inflammation, cell survival, as well as the development and differentiation of immune organs (Rakonczay, Hegyi et al. 2008; Bollrath and Greten 2009). NF-κB consists of homodimers or heterodimers of its five members, p65(RelA), RelB, c-Rel, P105/p50 (Nf-κB1) and p100/p52 (NF-κB2). Under resting conditions NF-κB consists of dimeric subunits (e.g. NF-κB1 and RelA/p65) in complex with the corresponding inhibitor of κB proteins (e.g. IκBα), the negative regulators of the effector proteins (Karin 2008). IκBs retain the NF-κB dimers inactivated in the cytoplasm, by masking the nuclear localization site of NF-κB proteins and

blocking the DNA binding capacity of NF-κB. Upon a variety of stress signals the IκB kinase (IKK) complex, which consists of two catalytic subunits IKKα and IKKβ as well as the regulatory subunit IKKγ, becomes activated. NF-κB signaling can be divided into two different activation pathways, the canonical and non-canonical activation pathway (Figure 1-4). The canonical NF-κB activation, that promotes regulation of genes involved in inflammation and cell survival, depends on IKKβ and IKKγ kinase activity and leads to hyperphosphorylation of the inhibitor protein IκBα at the serine sites 32 and 36 (Traenckner, Pahl et al. 1995). Hyperphosphorylation of IκBα is followed by ubiquitination and subsequent proteasome-mediated degradation. This process allows NF-κB dimers to translocate into the nucleus and bind to specific κB binding sites, thereby regulating the expression of genes involved in inflammation, tissue injury and repair. In addition to the critical step of IκBα degradation, phosphorylation of the transactivating subunit RelA/p65 is a further essential regulatory step for transcriptional activity (Madrid, Wang et al. 2000). In contrast to the canonical activation, the non-canonical activation depends on IKKα activity, not IKKβ, and induces the processing of NF-κB2 dimers (Bollrath and Greten 2009).

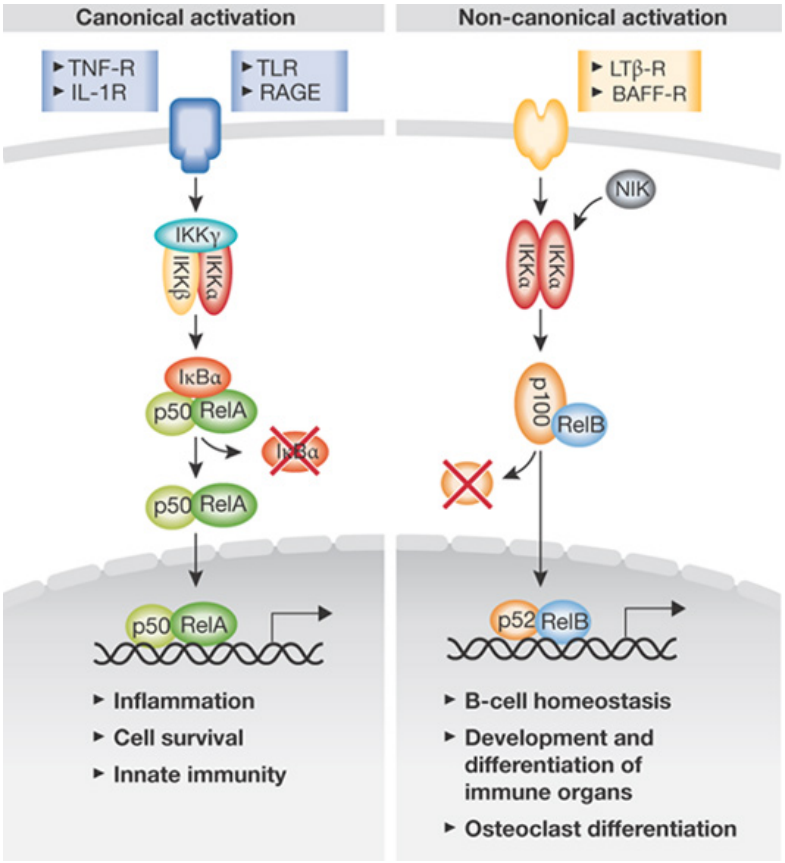

Figure 1-4: NF-κB signaling pathway. Canonical activation mostly regulates inflammation and cell survival, while non-canonical activation is involved by the regulation of B-cell developement. Adapted from (Bollrath and Greten 2009).

1.4.1 NF-κB and pancreatitis

It is well established that NF-κB is activated very early in the onset of AP, which leads to increased expression of inflammatory mediators (Gukovsky, Gukovskaya et al. 1998; Steinle, Weidenbach et al. 1999; Yu, Lim et al. 2002; Rakonczay, Hegyi et al. 2008). However, its role during AP remains controversial with studies supporting both protective and deleterious effects. Algül *et al.* used a mouse model with genetically inactivated RelA/p65 in the pancreas, to analyze the role of NF-κB (Algul, Treiber et al. 2007). In this model, the effector protein RelA/p65 was shown to play a protective role in the pancreas during AP, possibly by upregulation of the pancreatitis-associated protein 1 (PAP1). Other groups showed that pharmacologic inhibition of NF-κB led to contradictory results (Gukovsky, Gukovskaya et al. 1998; Steinle,

Weidenbach et al. 1999; Shi, Zhao et al. 2005). A mouse model with transgenic overexpression of the upstream kinase IKKβ was sufficient to activate NF-κB in the pancreas and induce pancreatitis (Baumann, Wagner et al. 2007).
While there is a general agreement that NF-κB is activated early during the onset of AP, its role during the disease is discussed controversial, with studies showing protective as well as deleterious effects.

1.5 IL-6/Stat3 signaling pathway

1.5.1 The IL-6 cytokine family

The IL-6 family of cytokines include IL-6, IL-11, leukemia inhibitory factor (LIF), oncostatin M (OSM), ciliary inhibitory factor (CNTF), cardiotropin-1 (CT-1), cardiotrophin-like related cytokine, stimulating neurotrophin-1/B-cell stimulating factor 3 (NNT-1), neuropoietin (NPN), IL-27 and IL-31. All IL-6 family members, with the exception of IL-31, share the membrane glycoprotein gp130 as a common receptor and signal transducer subunit (Heinrich, Behrmann et al. 2003). For signal initiation, IL-6 needs to bind to the membrane-bound IL-6 receptor (IL-6R) forming an IL-6/IL-6R complex, which associates with gp130, leading to gp130 homodimerization (Paonessa, Graziani et al. 1995). IL-11 initiates signal transduction the same way (with IL-11R respectively), while other family members (e.g. LIF, CNTF, OSM) signal via heterodimerization with gp130 (e.g. gp130/LIF-R heterodimer) (Taga and Kishimoto 1997).
While most soluble receptor molecules (e.g. OSM, LIF) are antagonists and compete with membrane-bound proteins for ligand binding, some soluble receptors (e.g. sIL-6R) of the IL-6 family are agonists (Scheller, Chalaris et al. 2011).

1.5.2 IL-6 signaling pathway

IL-6 can initiate signal transduction in two different ways. IL-6 signals are either mediated via gp130 through the classical IL-6 signaling pathway, where IL-6 binds to the membrane-bound IL-6 receptor (mIL-6R) or by complexation with the soluble IL-6 receptor (sIL-6R), which is termed IL-6 trans-signaling (Jostock,

Mullberg et al. 2001; Jones, Richards et al. 2005; Rabe, Chalaris et al. 2008). Classical IL-6 signaling is limited to a few cell types (mainly hepatocytes and leukocytes), since mIL-6R is only specifically expressed. IL-6 trans-signaling dramatically increases the number of potential IL-6 target cells, since sIL-6R can induce IL-6 signaling in virtually every cell via the blood flow (Jones, Richards et al. 2005).

Soluble IL-6R can be generated by two major mechanisms. The first mechanism is dependent on metalloprotease activity and involves proteolytic cleavage of the mIL-6R, while the second mechanism depends on the transcription of an alternative spliced IL-6R mRNA that is lacking the transmembrane and cytosolic domains (Lust, Donovan et al. 1992; Mullberg, Schooltink et al. 1993). Of note, the alternate spliced mRNA has only been described for humans so far and has not been identified in mice. The proteolytic cleavage (shedding) of IL-6R is catalyzed by proteases of the ADAM (a disintegrin and metalloprotease) family (Chalaris, Rabe et al. 2007; Chalaris, Gewiese et al. 2010). IL-6R has been described as a substrate for ADAM10 and ADAM17. While ADAM10 is slowly and constitutively shedding IL-6R, ADAM17 is activated by pro-inflammatory cytokines (e.g. IL-1β and TNF-α) and bacterial toxins (streptolysin O and hemolysin A) leading to rapid IL-6R proteolysis (Matthews, Schuster et al. 2003). A recent study showed that hepatocytes and hematopoietic cells are the main source of circulating sIL-6R (McFarland-Mancini, Funk et al. 2010). Interestingly, a soluble form of the signal transducer protein gp130 (i.e. sgp130) exists that is primarily formed by alternative splicing (Mullberg, Dittrich et al. 1993; Tanaka, Kishimura et al. 2000). Sgp130 inhibits IL-6-mediated trans-signaling by binding to the IL-6/sIL-6R complex without affecting classical IL-6 signaling (Jostock, Mullberg et al. 2001).

IL-6 signal transduction includes activation of the JAK/STAT, ERK, and PI3K signal pathways.

1.5.3 The Stat3 Signaling pathway

The Stat signaling family was first discovered in experiments that were analyzing the specificity of IFN receptors (Darnell, Kerr et al. 1994). Each family

member is activated by a different cytokine, suggesting that these proteins fulfill the requirements for intracellular signaling carriers (Levy and Darnell 1990). Cell culture experiments as well as experiments with genetically manipulated mice suggested a high degree of specificity for the family members towards its individual signaling pathway. Among the Stat proteins, Stat3 is the only family member that resulted in embryonic lethality if ablated in transgenic mice (Takeda, Noguchi et al. 1997).

The Stat3 signaling pathway is mainly activated by members of the IL-6 family (1.5.1), but also certain growth factors and IL-10 protein family members (Bollrath and Greten 2009). Dimerization of different receptor types (e.g. IL-6R and gp130) leads to the activation of receptor-associated Janus Kinases (Jak) (Zhong, Wen et al. 1994). After activation of Jak and the subsequent phosphorylation of Stat3 on Tyrosine residue 705, which leads to dimerization and subsequent translocation into the nucleus where Stat3-dependent target genes are transcribed (Aggarwal, Kunnumakkara et al. 2009). Non-receptor kinases, like Src and Abl, are also able to phosphorylate Stat3 at Y705 (Figure 1-5).

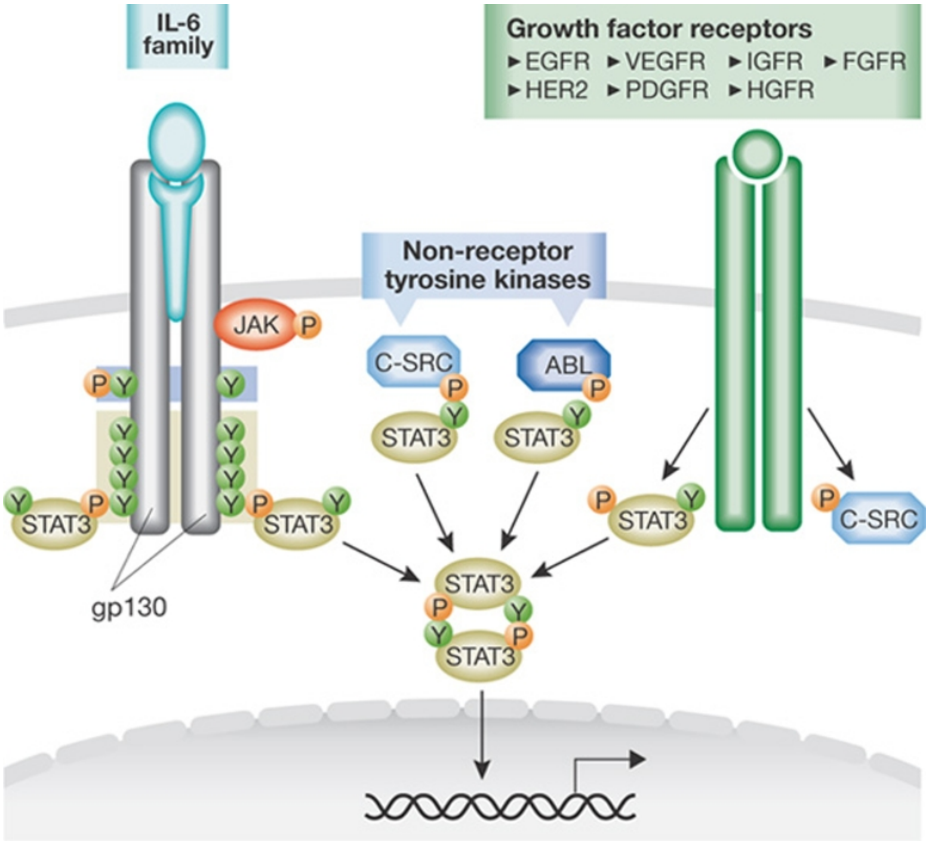

Figure 1-5: Stat3 signaling. On binding of IL-6 to IL-6R, which is followed by receptor heterodimerization with the gp130 receptor, JAKs are activated and phosphorylate tyrosine residues in the cytoplasmic region of gp130, which lead to the recruitment of Stat3 monomers. Stat3 can bind to gp130 through its SH2 domain and become phosphorylated before dimerization and translocation to the nucleus. Stat3 can also be activated by non-receptor tyrosine kinases Scr and Abl and growth factor receptors. Adapted from (Bollrath and Greten 2009)

The suppressor of cytokine signaling 3 (Socs3) is a negative regulator of Stat3 signaling that is induced by IL-6. Socs3 inhibits Stat3 activation by binding to Jak2 or a phosphopeptide corresponding to a region surrounding Y757 within gp130 (Krebs and Hilton 2001).

1.5.4 The role of IL-6 in disease

IL-6 is a cytokine that is mainly involved in inflammation and infection response (Scheller, Chalaris et al. 2011). IL-6 has been linked to several chronic inflammatory diseases, like chronic inflammatory bowel disease, rheumatoid arthritis and colitis-induced colon cancer (Atreya, Mudter et al. 2000; Nowell, Richards et al. 2003; Nowell, Williams et al. 2009; Matsumoto, Hara et al.

2010). Sgp130Fc, a chimeric designer cytokine receptor that consists of the entire extracellular portion of gp130 fused to the Fc region of human IgG1, forms dimers that act as a potent inhibitor of IL-6 trans-signaling with a 10-fold higher inhibitory potential compared to the monomeric natural occurring sgp130 form (Jostock, Mullberg et al. 2001). It has been shown in several models of inflammatory bowel disease that sgp130Fc was effective in blocking the inflammatory process (Atreya, Mudter et al. 2000). The application of sgp130Fc in two different models of arthritis inhibited the disease completely, suggesting an involvement of IL-6 trans-signaling rather than classical IL-6 signaling in the development of this autoimmune disease (Nowell, Richards et al. 2003; Nowell, Williams et al. 2009). While these data demonstrate the pro-inflammatory role of IL-6 trans-signaling, other studies showed a positive effect of IL-6 in regeneration. In a recent study of colitis-associated cancer, *Il-6*$^{-/-}$ mice showed an increased inflammatory score, compared to wildtype (Grivennikov, Karin et al. 2009). Here, IL-6 has a positive effect on regeneration of intestinal epithelial cells after induction of colitis. A regenerative effect of IL-6 was already demonstrated in a previous study with the enteric bacterial pathogen *Citrobacter rodentium* (Dann, Spehlmann et al. 2008).

Collectively, it seems that IL-6 trans-signaling mediates pro-inflammatory activities of IL-6 while classical IL-6 signaling is involved in regeneration and shows anti-inflammatory activities (Scheller, Chalaris et al. 2011).

1.6 Aim of this study

In this thesis, the molecular mechanisms of acute pancreatitis and pancreatitis-associated acute lung injury (ALI) are addressed in different approaches.

In the first part of this thesis, the role of NF-κB-dependent genes will be analyzed to identify potentially protective genes involved in AP by microarray analysis. To further scrutinize identified genes during AP, lentiviral-mediated overexpression of these genes will be investigated during AP. Additional screening of samples from patients with acute and chronic pancreatitis for mutations in the identified genes might be linked to the human disease.

In the second part of this thesis the systemic complication of severe acute pancreatitis (SAP) will be analyzed, focusing on ALI. Whether IL-6 describes only a marker for severity of AP or has any pathophysiological impact will be investigated in detail. To analyze the role of IL-6 during the disease, acute pancreatitis will be induced in different genetically altered mouse strains: in IL-6-deficient mice, where IL-6 signaling is completely blocked as well as in opt_sgp130Fc mice (transgenic mice overexpressing sgp130) where only IL-6 trans-signaling is inhibited. To further investigate the IL-6 signaling pathway, pancreas-specific knockout of Stat3 and its inhibitor Socs3 will be used to scrutinize a downstream target of IL-6 signaling that is activated during AP. Using pharmacological inhibitors of IL-6 signaling (e.g. IL-6 antibody, sgp130Fc and Stat3 inhibitors), the pathway will be evaluated for potential therapeutic treatment options.

2 Material and Methods

2.1 Mice

2.1.1 Mouse models

Il-6$^{-/-}$ (Kopf, Baumann *et al.* 1994):

The IL-6 gene was disrupted in the second exon (first coding exon) by insertion of a neomycin resistance cassette. This led to the ablation of a functional IL-6 protein.

opt_*sgp130Fc* (Rabe, Chalaris *et al.* 2008):

The optimized cDNA for the human fusion protein sgp130Fc (opt_sgp130Fc) was cloned into a plasmid and microinjected into pronuclei of fertilized eggs of B6D2 mice. Mice were screened for the presence of opt_sgp130Fc by southern blot.

Stat3$^{F/F}$ (Takeda, Kaisho *et al.* 1998):

A targeting vector was generated flanking exon 22, which encodes for a Tyrosine residue, with two LoxP sites. This results in expression of a truncated protein lacking the phosphorylation site Y705 that is necessary for activation of *Stat3* upon crossing with mice expressing Cre recombinase.

Socs3$^{F/F}$ (Yasukawa, Ohishi *et al.* 2003):

LoxP sites were introduced into intron 1 and the 3' untranslated region of exon 2 of the *Socs3* gene.

Rela$^{F/F}$ (Algul, Treiber *et al.* 2007):

Exons 7-10 of the *Rela/p65* gene were flanked with LoxP sites.

Ikba$^{F/F}$ (Rupec, Jundt *et al.* 2005):

Exons 1 and 2 of the *Ikba* gene were flanked with LoxP sites.

Ptf1a-Cre^{ex1} (Nakhai, Sel et al. 2007):

The Ptf1a locus was targeted with a vector replacing part of exon 1 (ex1) with the Cre recombinase. The integration of Cre at the ATG-start codon of the Ptf1a gene was verified directly by DNA sequencing.

Combination of mice:

Stat3$^{\Delta panc}$*:*

Stat3$^{F/F}$ mice were crossed with *Ptf1a-Cre*^{ex1} mice to generate mice lacking the Stat3 phosphorylation site Y705 in the exocrine pancreas.

Socs3$^{\Delta panc}$*:*

Socs3$^{F/F}$ mice were crossed with *Ptf1a-Cre*^{ex1} mice to generate mice with a total ablation of *Socs3* in the exocrine compartment of the pancreas.

Rela$^{\Delta panc}$*:*

Rela$^{F/F}$ mice were crossed with *Ptf1a-Cre*^{ex1} mice to generate mice with pancreas-specific inactivation of RelA/p65.

Ikba$^{\Delta panc}$*:*

Ikba$^{F/F}$ mice were crossed with *Ptf1a-Cre*^{ex1} mice deleting *I*κ*B*α in the exocrine pancreas.

2.1.2 Models of Acute Pancreatitis (AP)

2.1.2.1 Cerulein-induced pancreatitis

Age- and sex-matched littermates (8-12 week-old) were fasted for 12-18 hours but provided with water ad libitum. Mice received eight intraperitoneal (i.p.) injections of 50 µg/kg body weight cerulein (Sigma-Aldrich) in saline (0,9%). Mice were followed for up to 24 hours. Mice were sacrificed 30min, 1h, 90 min, 4h, 8h or 24h after the first injection of cerulein.

2.1.2.2 Severe acute pancreatitis (SAP)

Age- and sex-matched littermates (>25g) were fasted for 12-18 hours but provided with water ad libitum. Mice received 8 hourly i.p. injections of 50 µg/kg body weight cerulein (Sigma-Alrich) in saline (0,9%) per day for five consecutive days. Mice were sacrificed 72 hours and 120 hours after the first injection of cerulein.

2.1.2.3 Lentiviral transfection with AP

Per mouse around $1x10^6$ infectious units (ifus) (2.6.4) were concentrated and injected i.p. on day 1 and on day 4, according to the protocol in (Figure 3-8 A). On day 14 a cerulein pancreatitis was induced.

2.1.3 Blood pressure.

Blood pressure was noninvasively measured before the first injection of cerulein on days 1, 2, and 4 (n=4) during SAP by determining the tail blood volume with a volume pressure-recording sensor and an occlusion tail-cuff (CODA System, Kent Scientific)

2.2 Histological Analyses

2.2.1 Hematoxylin and eosin (H&E) staining

H&E staining was performed by deparaffinizing embedded paraffin sections (1,5-3µm) in xylol (X-TRA Solv, Medite GmbH) twice for five minutes. Afterwards, the sections were rehydrated in ethanol with decreasing concentration (100%, 96%, 70%; 3 minutes each). The slides were stained in haemotoxylin solution (Merck Millipore) for 3-4 minutes and washed with water for 10 minutes. Subsequently, the tissue was stained for two minutes in eosin solution (Waldeck GmbH). Slides were washed, dehydrated in 96% Ethanol Isopropanol xylol. Finally the slides were covert with mounting medium (pertex, Medite GmbH) and coverslips. Histologic images were taken with the Axiovert Imager (Zeiss).

2.2.2 Immunohistochemistry

Slides were deparaffinized and rehydrated as described (2.2.1). For antigen retrieval, slides were boiled in either citrate buffer (pH=6.0) or 1mM EDTA (pH=8.0) and sub-boiled for 15 min. Slides were cooled down at room temperature for 20 min and washed with water twice for 5 min. To quench endogenous peroxidase activity, sections were incubated with 3% H_2O_2 for 15 min. Later, slides were washed twice with TBS-T for 5 min. To block unspecific antibody binding, slides were incubated for 1h in TBS-T with avidin and 5% secondary antibody specific serum (e.g. goat serum for p-Stat3^{Y705}) (Table 2-1). After washing, slides were incubated with primary antibody in blocking solution with biotin over night at room temperature.

After washing twice with TBS-T, the secondary antibody (Vector laboratories) was applied in blocking solution 1:500 for 1h at room temperature. Signal detection was performed with the ABC solution kit (Vector laboratories) and DAB kit (Vector laboratories) according to the manufacturer´s protocol.

Subsequently, the slides were counterstained with hematoxylin (Roth) for 5 sec, dehydrated and mounted as described (2.2.1).

Table 2-1: Primary antibodies for Immunohistochemistry

Antibody	Dilution	Species	Company
p-Stat3^{Y705}	1:200	goat	Cell Signaling
IL-6	1:400	rabbit	Abcam
p-IκBα	1:1200	goat	Cell Signaling
p-p38	1:100	goat	Cell Signaling

2.2.3 Morphometric quantification of necrosis and edema.

Pancreatic tissue sections were stained with H.&E. Necrotic cells with swollen cytoplasm, loss of plasma membrane integrity, and leakage of organelles into the interstitium were counted and evaluated by 2 researchers in a blinded manner. Necrosis was expressed as the percentage of examined pancreatic parenchyma. Edema was calculated as interlobular and intraacinar fluid accumulation within the total pancreatic area using the Axio Vision Software

(Zeiss, Rel. 4.8). Morphometric quantification was performed with the assistance of Liang Song.

2.3 RNA/DNA Analyses

2.3.1 DNA isolation from mouse tails for genotyping

Tails were lysed in Tail Lysis Buffer (100mM TRIS/HCl (Sigma) pH 8.5; 200mM NaCl (Sigma); 5mM EDTA (Sigma) pH 8.0; 0.2% SDS (Sigma); 5% Proteinase K (Roche)) for 2-12 hours at 60°C. After the incubation samples were vortexed and incubated for 10 minutes at 95°C to inactivate the proteinase K. 900µl of dH_2O were added to dilute the DNA. 3-5 µl of DNA was used as template for genotyping PCR.

2.3.2 Genotyping PCR

All genotyping PCRs were performed using the RedTaq Ready Mix (Sigma) with 2-3 µl DNA template (2.3.1) with a standard PCR protocol (Table 2-2) and all primers (Table 2-3) at a final concentration of 10 pM. Mice were genotyped with the assistance of Karen Dlubatz.

Table 2-2: Genotyping PCR protocol

Step	Temperature	Time	
Pre Incubation	95°C	5 min	1x
Amplification	95°C 60°C 72°C	30 sec 30 sec 60 sec	35x
Cooling	4°C	∞	1x

Table 2-3: Genotyping primer

Name	Primer forward (5`-3`)	Primer reverse (5`-3`)	Product size
IL-6 WT	TTCCATCCAGTTGCCTTCTTGG	TTCTCATTTCCACGATTTCCCAG	174 bp
IL-6 KO	TTCCATCCAGTTGCCTTCTTGG	CCGGAGAACCTGCGTGCAATCC	380 bp
Ikba	CCAAGCAGAGACGTGTATTTCT	TCCAGACAGTAAGGGCCAGGT	450/500 bp
sgp130	GAGTTCAGATCCTGCGAC	TCACTTGCCAGGAGACAG	750 bp
Stat3	CCTGAAGACCAAGTTCATCTGTGTGAC	CACACAAGCCATCAAACTCTGGTCTCC	250/350 bp
Socs3	GCGGGCAGGGGAAGAGACTGTCTGGGGTTG	GGCGCACGGAGCCAGCGTGGATCTGCG	280/410 bp
RelA	GAGCGCATGCCTAGCACCAG	GTGCACTGCATGCGTGCAG	270/300 bp
Ptf1a	GTCCAATTTACTGACCGTACACCAA	CCTCGAAGGCGTCGTTGATGGACTGCA	1,3 kb

2.3.3 RNA isolation

After sacrificing mice, small tissue pieces were taken from each part of the pancreas and immediately transferred into RLT-buffer containing 1% β-Mercaptoethanol, homogenized and frozen in liquid nitrogen. The RNeasy Mini Kit (Qiagen) was used to isolate RNA, according to the manufacturer`s protocol. RNA concentration was measured in a NanoDrop 2000 spectrophotometer (Peqlab). Integrity of RNA was verified on a 1% Agarosegel.

2.3.4 cDNA synthesis

For cDNA synthesis, 1-5µg of total RNA was used. RNA transcription was performed using the Superscript™ II Reverse Transcriptase kit (Invitrogen) and oligo(dt)$_{12-18}$ primer according to the manufacturer's instruction. The concentration of cDNA was adjusted to 20ng/µl.

2.3.5 Quantitative RT-PCR

Quantitative RT-PCR was performed on a LightCycler 480 (Roche) using the LightCycler 480 Sybr Green Master Mix 1 (Roche) according to the protocol in Table 2-4. 100 ng cDNA were used as a template. Cyclophilin was used as a housekeeping gene for normalization (Table 2-5). Melting Curve analysis was

performed to verify primer specificity. Values were calculated using the following equation: $2^{DeltaCT(Cyclophilin) - DeltaCT(target\ gene)}$. *p*-values were calculated using the statistical software Prism 5 (GraphPad Software, Inc).

Table 2-4: RT-PCR Program:

Step	Temperature	Time	
Pre Incubation	95°C	10 min	1x
Amplification	95°C	10 sec	45x
	60°C	20 sec	
	72°C	10 sec	
Melting	95°C	1 min	
	55°C	1 sec	
	98°C	Continuous 0,11°C/s	5 Acquisitions / sec
Cooling	37°C	5 min	1x

Table 2-5: Primer used for RT-PCR:

Name	Primer forward (5`-3`)	Primer reverse (5`-3`)
Cyclophilin	ATGGTCAACCCCACCGTGT	TTCTGCTGTCTTTGGAACTTTGTC
IL-6	GAAGTAGGGAAGGCCGTGG	CTCTGCAAGAGACTTCCATCCAGT
Cxcl1	GGCGCCTATCGCCAAG	CTGGATGTTCTTGAGGTGAATCC

2.3.6 Microarray Analysis

Pancreases of unstimulated mice were dissected at 8 weeks. Total RNA was prepared as described above. Labeled cRNA was prepared using the Affymetrix – One-Cycle target Labeling Kit according to the manufacturer`s protocol. 10µg of labeled RNA was hybridized to mouse expression gene chip arrays (Affymetrix Mouse Genome 430A 2.0 Array) according to Affymetrix protocol. Gene Chips were scanned and analyzed using Affymetrix Microarray Suite 5.0 Software (MAS 5.0). Microarray analysis was perfomed with the assistance of Karen Dlubatz and Henrik Einwächter.

2.3.7 SNP analysis

2.3.7.1 Study subjects

The study was approved by the local medical ethical committees. All subjects gave their informed consent for genetic analysis. 242 CP patients, 219 AP patients and 401 controls were included all originating from Germany.

242 German patients (149 female, 93 male; mean age ± SD: 14.6 ± 11.0 years) with idiopathic or hereditary CP were enrolled in this study. The clinical diagnosis of CP was based on two or more of the following criteria: presence of a typical history of recurrent pancreatitis, radiological findings such as pancreatic calcifications and/or pancreatic ductal irregularities revealed by endoscopic retrograde pancreaticography or magnetic resonance imaging of the pancreas and/or pathological sonographic findings. Hereditary CP was diagnosed when two first-degree relatives suffered from recurrent acute or chronic pancreatitis without any apparent precipitating factor. Patients without a positive family history for CP were classified as having idiopathic disease when precipitating factors such as alcohol abuse, trauma, medication, infection, and metabolic disorders were absent. The acute pancreatitis (AP) group consisted of 219 German patients (82 female, 137 male; mean age ± SD: 53.7 ± 16.8) of alcoholic (n=57), biliary (n=84), idiopathic (n=43) or miscellaneous origin (n=35) (postoperative [n=15], trauma [n=5], ERCP-induced [n=8], hyperlipoproteinemia [n=5], hyperparathyroidism [n=1], drug-induced [n=1]). All AP patients were recruited at the university hospital Magdeburg, Saxony-Anhalt, between 1996 and 2003. AP was defined as acute abdominal pain with a typical clinical picture (severe abdominal pain / vomiting) and a serum amylase or lipase concentration of at least three times above the upper limit of normal and typical findings on imaging studies. Severity of AP was classified following the Atlanta symposium, 1992 (Bradley 1993). In accordance with this classification system, an attack was classified as mild (grade 1) if related with minimal organ dysfunction and an uneventful recovery. An attack was classified as severe if associated with local complications (grade 2) or systemic complications (grade 3). Thirty-six out of 219 (16.4%) patients showed mild (grade 1), 116/219 (53%) grade 2, and 67/219 (30.6%) grade 3 AP. Because the university hospital in Magdeburg represents a tertiary care center for pancreatic surgery, the AP patients were selected for severe pancreatitis. 401 German control subjects were recruited (236 female, 165 male; mean age ± SD: 31.4 ± 6.4 years). The controls consisted of subjects recruited for genetic associations studies in Berlin.

2.3.7.2 Mutation screening.

Genomic DNA was extracted from peripheral blood leukocytes. Primers for PCR amplification and DNA sequencing were designed from intronic sequences flanking the five SERPINA3 exons based on the published nucleotide sequence (GenBank #AL049839.3) (Table 2-6). Oligonucleotides were synthesized by TIB MOLBIOL, Berlin, Germany. PCR was performed using 0.75 U AmpliTaq Gold polymerase (Perkin Elmer), 400 µmol/L deoxynucleoside triphosphates, 1.5 mM/L MgCl2, and 0.1 µmol/L of each primer in a total volume of 25 µL.

The reaction mix was denatured at 95°C for 12 minutes followed by 48 cycles of denaturation at 95°C for 20 seconds, annealing at 64°C for 40 seconds, elongation at 72°C for 90 seconds, and a final extension step for 2 minutes at 72°C in a thermocycler.

PCR products were digested with shrimp alkaline phosphatase (USB) and exonuclease I (USB) and performed cycle sequencing using internal sequencing primers and BigDye terminator mix (Applied Biosystems). Reaction products were purified by ethanol precipitation and loaded onto an ABI 3730 fluorescence sequencer (Applied Biosystems). All five *SERPINA3* exons were sequenced in all 242 German CP patients and 52 German control subjects. In all other subjects only exon 2 of *SERPINA3* was analyzed by sequencing. The mutations were numbered according to the recommendations of the Nomenclature Working Group for human gene mutations (Antonarakis 1998). All mutations are numbered at the cDNA level, indicated by a "c." before the number. Position +1 corresponds to the A of the ATG translation initiation codon located at nucleotide 80 in the NM_001085.4 *SERPINA3* mRNA reference sequence. Mutation screens were performed by Prof. Dr. Witt.

Table 2-6: Primer sequences used for PCR amplification and sequencing of *SERPINA3* (*AACT*)

Exon	PCR forward	PCR reverse	DNA sequencing
1	AGCTGGGGTCTTCTCTGGGT	CCAGACACAGAGGATGCCTC	GAGCTAGTCCCATAACCAGG
2	GAGTGATGTGTGTCGGGTGC	CTGACTCAGACCAGAGGCTG	CCAGAGAGCACCTACCTGAG CTTGGCCTTCCTGTCTCTGG
3	TCCAAGCCTGCTGGGCTCTC	CCCAAAGCCATGTAGGCAGC	CCTCCTATGAGGGACTCTGG
4	CCCTGCTGGTGTGAAGGTGC	GCTGGGCTGTAACCTAGCTC	TTGGTGTGCTGCCTGGAGAC
5	ACCTCGATGGCTCTGGGCAA	GCTTAGGTAGTCCTGGGCAG	CAGGCCAGCACTAGGTGCTC

2.4 Proteinbiochemistry

2.4.1 Protein isolation from tissue or cells

MLB-buffer (5x):

50mM Hepes, pH 7.9 (Sigma); 150mM NaCl (Sigma); 1mM EDTA, pH 8,0 (Sigma); 0.5% NP-40 (Sigma); 10% Glycerol (Sigma); 1mM DTT (Sigma); 0.2% PMSF (Sigma); 1% Protease inhibitor cocktail (Roche)

Laemmli-buffer (5x):

300mM Tris-HCl, pH 6.8 (Sigma); 10% SDS (Sigma); 50% Glycerol (Sigma); 0.05% Bromphenol blue (Sigma); 5% β-Mercaptoethanol (Sigma)

For protein isolation the tissue/cells were kept on ice. MLB working solution (2ml MLB-buffer (5x) and 8ml Glycerol) was freshly prepared. 600µl of MLB working solution were given to the tissue/cells. Afterwards, the tissue/cells were homogenized and the sample was centrifuged at 4°C for 13.2 rpm for 10min.
Protein concentration was measured with the Bio Rad Protein Assay Kit (Bio Rad) and the samples were adjusted to 3µg/µl with 5x Laemmli buffer.

2.4.2 Immunoblot analysis

45µg of protein lysates were denaturated at 95°C for 5min and afterwards kept on ice. Protein separation was performed with a SDS-PAGE gel (Gel percentage depending on the protein size ranging from 7.5-15%) in running buffer at 120V in a Bio Rad Mini Protein Gel System chamber.
Gels consisted of two fractions, a Separating Gel (upper part of the gel) and a Running Gel (lower part). Loaded gels were run in running buffer.

Separating Gel (10%):
4ml 1.5 M Tris pH 8.8 (Sigma); 5.1ml 30% Acrylamide/Bis solution (Roth); 150µl 10% SDS (Sigma); 75µl 10% APS (Sigma); 25µl TEMED (Sigma), add 15.75 ml dH_2O

Running gel:
1.3ml 0.5 M Tris pH 6.8 (Sigma); 0.75ml 30% Acrylamide/Bis solution (Roth); 50µl 10% SDS (Sigma); 25µl 10% APS (Sigma); 10µl TEMED (Sigma), add 5.1 ml dH_2O

10x running buffer
10g SDS (Sigma), 30g TRIS (Sigma), 144g Glycin (sigma), add 1000 ml dH_2O

Protein transfer to a PDVF membrane (Milipore) was performed in transfer buffer at 390mA for 2h in a blotting chamber.

10x transfer buffer
144g Glycin (Sigma); 30g Tris-Base (Sigma) add 1l dH_2O

1x transfer buffer for wet transfer

100 ml	10x transfer buffer
200 ml	Methanol
700 ml	dH_2O

After transfer, membranes were incubated with 5% skim milk powder in TBS-T to block any unspecific antibody binding. Afterwards, the membrane was incubated with primary antibody in 5% skim milk in TBS-T over night at 4°C (Table 2-7).

Next, the membrane was washed 3-5 times with TBS-T and incubated with the species-specific HRP-coupled antibody in 5% skim milk in TBS-T for 1h at room temperature. After several washing steps with TBS-T, the protein band was visualized using the ECL Western Blotting Detection Reagents and Amersham Hyperfilms (both GE Healthcare).

10x TBS

80g NaCl (Sigma), 31.5g Tris-HCl (Sigma) add 1l dH_2O pH 7.6

TBS-T

1l 1xTBS (Sigma), 1ml Tween20 (Sigma)

Table 2-7: Primary antibodies for immunoblot analysis

Antibody	Dilution	Species	Company
Erk1	1:1000	rabbit	Santa Cruz
Erk2	1:1000	rabbit	Santa Cruz
β-Actin	1:5000	mouse	Sigma
IκBα	1:1000	rabbit	Santa Cruz
IκBβ	1:1000	rabbit	Santa Cruz
Stat1	1:1000	rabbit	Santa Cruz
p-Stat1^{Y701}	1:1000	rabbit	Cell Signaling
C-term Stat3	1:1000	mouse	BD
N-term Stat3	1:1000	rabbit	Cell Signaling
p-Stat3^{Y705}	1:1000	rabbit	Cell Signaling
p-Stat3^{S727}	1:1000	rabbit	Cell Signaling
RelA	1:1000	rabbit	Cell Signaling
ΔRelA			
p-RelA	1:1000	rabbit	Cell Signaling
PAP1	1:250	rabbit	(Algul, Treiber et al. 2007)
Spi2A	1:3000	armenian-hamster	Santa Cruz

2.4.3 CHIP- Chromatin immunoprecipation

After stimulation, pancreatic tissues were fixed at room temperature by the addition of formaldehyde (1%). Pancreatic tissues were washed twice with ice-cold PBS (Invitrogen), lysed in L1 buffer (50mM Tris, pH 8.0; 2mM EDTA; 0.1% NP-40; 10% glycerol; and a protease inhibitor cocktail diluted 1:200, P-8340, Sigma), and then transferred to a reaction tube. Nuclei were pelleted at 1,000 g and resuspended in L2 buffer (50mM Tris, pH 8.0; 5mM EDTA; 0.1% SDS; and protease inhibitor cocktail diluted 1:200). Chromatin was sheared into fragments of an average size of 400 bp with a sonicator (3 × 30 s at 60% maximum power; Bandelin), centrifuged to pellet debris, and diluted 10-fold with dilution buffer (50mM Tris, pH 8.0; 0.5mM EDTA; 0.2M NaCl; 0.5% NP-40; and protease inhibitor cocktail diluted 1:200). Each sample was precleared for 3 hours with 80 μl of salmon sperm–saturated protein A agarose (Upstate Biotechnology). Immunoprecipitations were performed overnight at 4°C. Anti-p65 and anti-H4 antibodies (Santa Cruz) were used and antibody-chromatin complexes were collected with 80μl of salmon sperm–saturated protein A agarose for 1 hour and washed 3 times each with highsalt buffer (20mM Tris, pH 8.0; 2mM EDTA; 0.5M NaCl; 0.1% SDS; and 1% NP-40), LiCl buffer (20mM Tris, pH 8.0; 1mM EDTA; 250mM LiCl; 0.5% NP-40; and 0.5% sodium deoxycholate), and 1x TE (10 mM Tris, pH 8.0, and 1 mM EDTA). Immune complexes were extracted with 1x TE containing 1% SDS at 65°C. After addition of NaCl (300mM final concentration), protein-DNA crosslinks were reverted overnight at 65°C. Proteins were digested with proteinase K for 2 hours. The DNA was extracted with phenol/chloroform and precipitated with ethanol. One-twentieth of the DNA was used in each PCR (35–38 cycles) with the κB primers (Table 2-8). Chip analysis was performed with the assistance of Karen Dlubatz.

Table 2-8: CHIP primer:

Name	Primer forward (5`-3`)	Primer reverse (5`-3`)
κB1	TCATTGGAGGTTGTTGGAGGGAAG	TCCTAGGAATCTCTTTATCTTCCCGG
κB2	GGCACAAATTATGCTATGACATAGTTT GTAAAA	AACTTACACCTACAATTTTTAATCTGCT CAGTTC

2.4.4 Protein purification

HEK cells were transfected with 2µg pCDNA3.1-Spi2A plasmid DNA (2.6.3) using Lipofectamine® 2000 (Invitrogen). $2x10^7$ cells were used for purification of Spi2A protein with the Ni-NTA Agarose Kit (Qiagen), according to the manufacturer's protocol.

2.4.5 ELISA - Enzyme linked immunosorbend assay

2.4.5.1 Mouse ELISAs

For the analysis of mouse serum, blood was taken from the *Vena cava inferior* after the mice were sacrificed. Serum was isolated using the „Microvette" (Sarstedt) at 12000 rcf at 4°C for 5 minutes. BALF for ELISA was obtained as described in 2.4.8.

The ELISA was performed according to the manufacturer's protocol (Table 2-9). The sIL-6R ELISA was performed with the assistance of Prof. Dr. Rabe.

Table 2-9: Mouse ELISAs

Antibody	Dilution	Company
IL-6	1:5-1:10	Ebioscience
Cxcl1	1:5	R&D
sIL-6R	1:5	R&D

2.4.5.2 Human ELISAs

Patients with AP who were admitted to Scania University Hospital in Malmö, Sweden, were included in the study. AP was defined as upper abdominal pain and elevated serum amylase levels (i.e., minimum 3 times the upper reference limit) and/or radiological findings that confirmed AP. No patients were referred from other hospitals. Patients were considered to have severe (n=10) or mild (n=20) pancreatitis based on the Atlanta criteria (Bradley 1993). Blood samples were place in PST tubes and centrifuged (2000 g, 25°C, 10 min), and the plasma was frozen at -80°C. Human plasma samples were a generous gift from Dr. Regnér and Dr. Thorlacious.

The ELISA was performed according to the manufacturer's protocol (Table 2-10). The sIL-6R ELISA was performed with the assistance of Prof. Dr. Rabe.

Table 2-10: Human ELISAs

Antibody	Dilution	Company
IL-6	1:5-1:10	Ebioscience
IL-8	1:5	Ebioscience
sIL-6R	1:5	R&D

2.4.6 Serum analyses

2.4.6.1 Amylase

Mouse serum was diluted 1:10 with 0.9% NaCl and Amylase content was assessed by standard protocol (AMYL2, Cobas).

2.4.6.2 Lipase

Mouse serum was diluted 1:10 with 0.9% NaCl and Lipase content was assessed by standard protocol (LIPC, Cobas).

2.4.6.3 BUN

BUN was determined in mouse serum by kinetic tests with urease and glutamate dehydrogenase (Roche).

2.4.6.4 AST

AST was measured in the serum Method according to the International Federation of Clinical Chemistry (IFCC), but without pyridoxal-5'-phosphate. AST in the sample catalyzes the transfer of an amino group between L-aspartate and 2-oxoglutarate to form oxaloacetate an L-glutamate. The oxaloacetate then reacts with NADH, in the presence of malate dehydrogenase (MDH), to form NAD^+. The rate of the NADH oxidation is directly proportional to the catalytic AST activity. It is determined by measuring the decrease in absorbance at 340 nm.

2.4.6.5 ALT

ALT was measured in the serum of mice according to the International Federation of Clinical Chemistry (IFCC), without pyridoxal-5-phosphate. ALT catalyzes the reaction between L-alanine and α-ketoglutarate (Roche). The

pyruvate formed is reduced by NADH in a reaction catalyzed by lactate dehydrogenase (LDH) to form L-lactate and NAD+. ALT catalyzes the reaction between L-alanine and α-ketoglutarate. The pyruvate formed is reduced by NADH in a reaction catalyzed by lactate dehydrogenase (LDH) to form L-lactate and NAD^+. The rate of the NADH oxidation is directly proportional to the catalytic AST activity. It is determined by measuring the decrease in absorbance at 340 nm.

2.4.6.6 Endotoxin

Endotoxin levels were analyzed in 100µl serum of C57BL/6 mice at different time points according to the protocol of the manufacturer (Limulus amebocyte lysate [LAL] QCL-1000, Lonza).

2.4.7 Assessment of pulmonary capillary permeability.

To measure airway permeability, mice were challenged with cerulein for 8h or 3 days. Along with the last i.p. injection of cerulein mice were injected with 200µl (5 mg/ml) of fluorescein isothiocyanate-dextran intravenously (FD4; Sigma). The mice were sacrificed; the BALF was recovered, and the alveolar permeability was measured via fluorescence.

2.4.8 BALF analysis.

Animals were killed by decerebration. The trachea was then exposed and intubated with a catheter. Afterwards, repeated (1-3) 0.8 ml injections of PBS were given to harvest bronchoalveolar lavage fluid (BALF). The collected BALF was centrifuged at 1,200 rpm for 10 min at 4°C, and the supernatant was frozen at −80°C for the subsequent analysis of total protein count (Bio-Rad protein analysis kit) and inflammatory mediators via ELISA (2.4.5.1). Cells in the pellet were resuspended in PBS for quantification.

2.4.9 Trypsin activity

Tissue for the measurement of pancreatic enzyme activities was thawed and homogenized in iced medium containing 5 mM MOPS (Sigma), 1 mM $MgSO_4$ (Sigma), and 250 mM sucrose (pH 6.5) (Sigma) with an Ultra-Turrax T25 (IKA-Werke, Staufen, Germany). Samples were sonicated and centrifuged for 5 minutes at 12,000g. Trypsin was measured in supernatants at 37°C using 30 µM BOC-Gln-Ala-Arg-7-amido-4-methylcoumarin (Bachem) as a substrate. To increase specifity, trypsin activity was expressed as fluorescence increase sensitive to 20 µM soybean trypsin inhibitor (Sigma-Aldrich). Trypsin activity was measured by Dr. Wartmann.

2.5 Cell Culture

2.5.1 Isolation of acinar cells

The following solutions were prepared before sacrificing mice:

Solution I:
McCoy's medium 5A (Sigma) with 0.1% BSA (Sigma)

Solution II:
McCoy's medium 5A (Sigma) with 0.1% BSA (Sigma) and 1,2 mg/ml Collagenase Type VIII (Sigma)

Culture medium:
DMEM + Ham's F12 (1:1) (Invitrogen) with 2mM Glutamine (Invitrogen), 1% Penicillin/Streptomycin (Invitrogen) and 10% FBS (Invitrogen)

The mouse was sacrificed, blood was removed from the portal vein and the pancreas was removed into cold sterile PBS (Invitrogen) in a petri dish. All further steps were performed in a sterile cell culture hood. The pancreas was washed twice with cold PBS, transferred into a new petri dish with 5ml of Solution II and minced into small pieces with a scalpel. The petri dish was kept

in a 37°C incubator for 10 min. The cell suspension was transferred into a 50ml falcon, the petri dish was washed with 10ml of Solution I and added to the cell suspension in the 50 ml falcon and centrifuged for 5 min at 0.3 rcf at room temperature. The pellet was resuspended in 5ml of Solution II and incubated for 10 min at 37°C. The cell suspension was filtered with a 100µm nylon mash and the petri dish was washed with 10ml of Solution I and filtered. The filtered cell suspension was centrifuged for 3min with 0.3 rcf at room temperature. The pellet was resuspended in 20ml of Solution I and centrifuged again. The cell pellet was resuspended in Culture medium and incubated for at least 30 min at 37°C.

2.5.2 Stimulation of acinar cells

Before isolating acinar cells for stimulation, the KRH working solution was prepared.

10x KRH-stock solution:
5.96g Hepes (Sigma), 6.096g NaCl (Sigma), 0.14g KH_2PO_4 (Sigma) and 0.296g $MgSO_4x7H_2O$ (Sigma) were dissolved in 100ml of water.

100mM $CaCl_2$:
0.735ml of $CaCl_2$ (Sigma) were dissolved in 50ml water.

KRH working solution:
10ml of the 10x KRH-stock solution were mixed with 2ml $CaCl_2$ (100mM), 1ml MEM (Invitrogen) and 1ml of L-Glutamine (Invitrogen). Water was added to 100ml and the pH was adjusted to 7,4. Than 45mg Glucose (Sigma), 200mg BSA (Sigma) and 10mg Trypsin Inhibitor (Sigma) were added. the KRH working solution was mixed and filtered through a 45µm sterile filter.

Acinar cells were isolated as previously described (2.5.1) but cells were suspended into KRH working solution instead of Culture medium and rested for at least 30 min at 37°C before stimulation.

Cells were stimulated with Cerulein (Sigma), IL-6 (Peprotech) and Hyper-IL-6 (Fischer, Goldschmitt et al. 1997) at different concentrations for various time intervals.

2.5.3 Flow cytometry

Before sacrificing mice, FACS buffer was prepared.

FACS buffer:
5% FBS (Invitrogen) with 2mM EDTA (Sigma) in PBS (Invitrogen)

Mice were sacrificed and the lung was placed into a petri dish with cold PBS. Single cells were prepared by digestion of the organ with Collagenase (Sigma). The cell suspension was dispersed using a 70µm cell strainer and the collagenase was then inactivated by adding 50ml of FACS buffer. The cells were centrifuged for 6 min at 0.3 rcf. The supernatant was discarded and the pellet was resuspended in 2ml of red blood cell lysis buffer (RBC lysis buffer) (Sigma), shaken for 90s and filled up with 20ml FACS buffer. The cell suspension was centrifuged (6min; 0.3 rcf) and the pellet was resuspended in 1-5ml FACS buffer.
Cells were stained with the PE-conjugated antibody to Gr-1 (clone RB6-8C5) (Ebioscience) and APC-eFluor 780-conjugated CD11b-specific antibody (clone M1/70) (Ebioscience). Cells were stained with propidium iodide (BD Biosciences) to assess viability. Flow cytometry analysis was performed on a Gallios flow cytometer (Beckman Coulter) after gating and excluding dead cells. Data were analyzed using FlowJo software.

2.6 Cloning

2.6.1 Ligation of Spi2A and pCDNA

Ligation was performed using 10-20 fmol of insert (Spi2A cds with a 5' His-Tag) and 5-10 fmol of vector (pCDNA 3.1; Invitrogen) and the T4 DNA Ligase Kit (NEB) according to manufacturer's protocol.

2.6.2 Transformation

Transformation was carried out according to the manufacturer's protocol (Top10 one shot; Invitrogen). For each transformation reaction 1-3µl of ligation product were used and plated out on LB agar plates with 100µg/ml ampicillin over night at 37°C. Colonies were picked and analyzed by colony PCR.

Table 2-11: Colony PCR primer

Name	Primer forward	Primer reverse
Spi2A cPCR	agcttacaaccagagacc	tagtcggtggagatgg

2.6.3 Isolation of plasmid DNA

Positiv clones of the transformation (2.6.2) were picked and incubated in LB-media (Sigma) o.n. at 37°C. DNA Miniprep isolations were performed according to the manufacturer's protocol (Invitrogen). Clones were tested via restriction enzyme digestion with HindIII (NEB) and a plasmid DNA was isolated from positive clones Maxiprep (Invitrogen).

2.6.4 Lentivirus production

The Spi2A cds was subcloned into the pQCXIP vector (Clonetech). The constructs pQCXIP and pQCXIP–Spi2a were transfected into the packaging cell line GP2-293 (Clontech) using turbofect transfection reagent (Fermentas).

3 Results

3.1 NF-κB-dependent upregulation of Spi2A alleviates acute pancreatitis

3.1.1 Severity of pancreatitis depends on RelA

Previous publications showed that the NF-κB pathway plays an important role in the onset of acute pancreatitis (Algul, Tando et al. 2002; Chen, Ji et al. 2002; Algul, Treiber et al. 2007; Baumann, Wagner et al. 2007). The role of NF-κB as the disease progresses is discussed controversial, with studies showing protective as well as aggravating effects (Algul, Treiber et al. 2007; Baumann, Wagner et al. 2007).

The inhibitor protein IκBα regulates NF-κB by masking the nuclear localization site of the NF-κB complex, hence keeping the complex inactive in the cytoplasm. Upon various stimuli, IκBα is phosphorylated by the IKK complex and degraded. This enables the NF-κB effector proteins to translocate into the nucleus where they bind to the DNA and NF-κB-dependent genes are transcribed. While the role of IKK subunits and RelA has been well established, the role of IκBα has not been addressed in acute pancreatitis so far (Algul, Treiber et al. 2007; Baumann, Wagner et al. 2007).

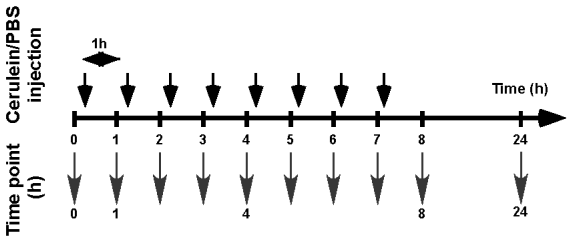

Figure 3-1: Model for cerulein-induced acute pancreatitis

To analyze the role of IκBα during the disease, acute experimental pancreatitis was induced in C57BL/6 mice by i.p. injections of cerulein according to the protocol in Figure 3-1. Histological sections of the pancreas of these wildtype mice were stained for phosphorylation of IκBα showing that IκBα is activated

early during AP; however phosphorylation of IκBα decreased as the disease progressed (Figure 3-2).

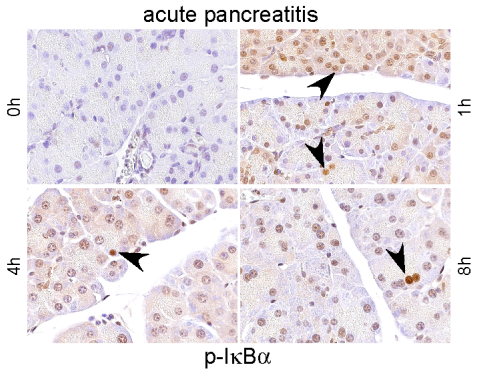

Figure 3-2: Phosphorylaton of IκBα during AP: Immunohistochemical detection of p-IκBα during pancreatitis at the indicated time points. Note the increase of p-IκBα –positive cells (black arrows) after 1 hour.

To further scrutinize the role of IκBα during AP, mice lacking IκBα in the pancreas (*Ikba*$^{\Delta panc}$ mice) were generated by crossing *Ptf1aCre*^{ex1} mice with *Ikba*$^{F/F}$ mice. This Cre/LoxP based system leads to recombination and consectutive inactivation of IκBα in the pancreas and not the lung or liver (Figure 3-3).

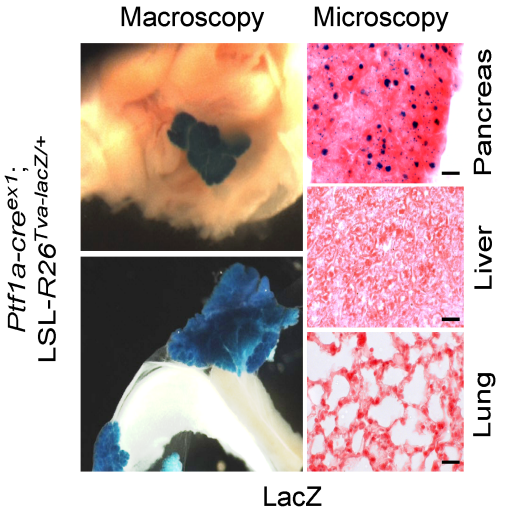

Figure 3-3: Tissue specificity of *Ptf1aCre*^{ex1}: Macroscopic images of X-Gal-stained liver, pancreas and small bowel. Microscopic images of nuclear lacZ activity in sections of the pancreas, liver, and lung. Scale bar represents 50µm.

Ikba$^{\Delta panc}$ mice developed normal, were fertile and did not show any phenotypical or histological abnormalities in the pancreas (Schwerdtfeger 2012). However, pancreas-specific inactivation of IκBα resulted in nuclear translocation of RelA (Schwerdtfeger 2012). Gene expression profiles showed an increase of a NF-κB-specific gene signature in *Ikba*$^{\Delta panc}$ mice compared to *Ikba*$^{F/F}$ mice. A pancreas-specific gene set showed no differences in pancreatic differentiation in both genotypes (Schwerdtfeger 2012).

These data suggest that inactivation of IκBα in the pancreas resulted in translocation of endogenous RelA into the nucleus and activation of NF-κB-dependent genes.

To scrutinize the impact of basal NF-κB activity in the pancreas, acute experimental pancreatitis was induced in *Ikba*$^{\Delta panc}$ mice. These mice showed significant amelioration of local damage and systemic complications in two different models of AP (Schwerdtfeger 2012). Intrapancreatic trypsin activation is considered as a key event in the onset of AP. *Ikba*$^{\Delta panc}$ mice showed a significant decrease of trypsin activity compared to floxed littermates (Schwerdtfeger 2012).

To evaluate the role of endogenous nuclear RelA in this setting, mice lacking both, IκBα and RelA in the pancreas were generated and analyzed. Additional inactivation of RelA reverted the phenotyp of the *Ikba*$^{\Delta panc}$ mice and led to a more severe AP (Schwerdtfeger 2012) (Figure 7-1).

Taken together, these data suggest that nuclear RelA mediates the protective effects of *Ikba*$^{\Delta panc}$ mice during AP.

3.1.2 Spi2A is upregulated in IκBα–deficient mice

To obtain a more global view on NF-κB-dependent genes in the pancreas that might be responsible for the observed effects, a genome-wide gene expression analysis was conducted, using RNA samples from *Ikba*$^{F/F}$, *Ikba*$^{\Delta panc}$ and *Rela*$^{\Delta panc}$ mice. Basal transcriptomes of the analyzed samples were significantly different (Figure 3-4).

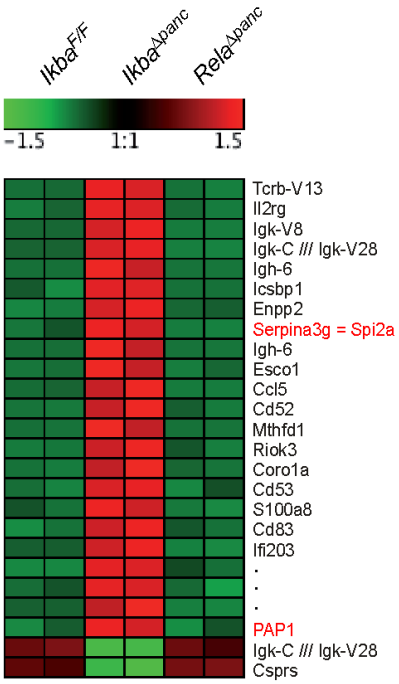

Figure 3-4: NF-κB-dependent genes: Expression analysis of 8-week-old pancreata from untreated *Ikba*$^{F/F}$, *Ikba*$^{\Delta panc}$, and *Rela*$^{\Delta panc}$ mice. Heat map of significantly regulated transcripts between IκBα-deficient and other pancreata.

The gene encoding for the pancreas-specific acute-phase protein pancreatitis-associated protein (*Pap1*) was significantly upregulated in *Ikba*$^{\Delta panc}$ mice. Previous studies showed that induction of PAP1 has a protective effect on AP (Algul, Treiber et al. 2007; Shigekawa, Hikita et al. 2012). To evaluate the role of PAP1 in the underlying model, mice lacking IκBα were injected with cerulein and PAP1 expression was analyzed using Western Blot analysis. There was an increase in PAP1 expression in *Ikba*$^{\Delta panc}$ mice compared to floxed littermates (Figure 3-5).

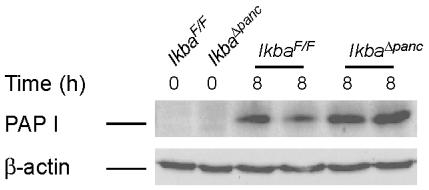

Figure 3-5: PAP1 expression during AP: Total pancreata of *Ikba*$^{F/F}$ and *Ikba*$^{\Delta panc}$ mice were isolated and homogenized to detect PAP1 at indicated time points. β-actin served as loading control (n=3).

Interestingly, the gene encoding for the serine protease inhibitor 2A (*Spi2a*), the homologue of the human α1-Antichymotrypsin (*AACT*), was highly upregulated in resting pancreata of *Ikba*$^{\Delta panc}$ mice.

To verify the data obtained by the microarray analysis, protein expression was evaluated in all three genotypes. Spi2A expression was increased in *Ikba*$^{\Delta panc}$ mice, while *Ikba*$^{F/F}$ and *Rela*$^{\Delta panc}$ mice showed only low basal level of Spi2A (Figure 3-6 A). Deletion of IκBα or truncation of RelA was confirmed on protein level for the relevant genotypes (Figure 3-6 A). Upon stimulation with cerulein, *Ikba*$^{F/F}$ and *Ikba*$^{\Delta panc}$ mice showed no difference in induction of Spi2A expression (Figure 3-6 B). Since Spi2A is also present in the serum and to rule out any contamination, analysis was extended to acinar cells. Acinar cells isolated from *Ikba*$^{\Delta panc}$ mice express Spi2A under resting conditions, while acinar cells isolated from *Ikba*$^{F/F}$ mice did not show Spi2A expression (Figure 3-6 C). To test whether Spi2A is regulated directly or indirectly during AP, *in vivo* as well as *in vitro* analyses were performed. Upon cerulein stimulation *in vivo*, Spi2A was induced in acinar cells isolated from *Ikba*$^{\Delta panc}$ mice (Figure 3-6 D). This finding could be replicated in acinar cells *in vitro*, thus showing that cerulein directly contributes to the up-regulation of Spi2A in acinar cells (Figure 3-6 D). Cerulein is known to activate the IKK/NF-κB pathway, further corroborating the RelA-dependent regulation of Spi2A. Thus, it was investigated next whether RelA directly interacts with the Spi2A promoter/enhancer region. Chromatin immunoprecipitations with a RelA antibody were performed using pancreas lysates from untreated pancreata. κB sites in the Spi2A promoter were localized using the matinspector online tool. Within a 30-kB fragment at

the 3' site of the mouse *Spi2a* gene, 3 κB 1 sites were found, one of them at 7.2 kB from exon 1 with very high affinity. This site was considered potentially relevant for regulation of Spi2A expression. Precipitated DNA was analyzed by PCR using primers surrounding the position of the κB site. RelA recruitment to the κB site in the Spi2A promoter was detectable in *Ikba*$^{\Delta panc}$ mice (Figure 3-6 E).

Taken together, among a cluster of potentially protective genes, identified by genome-wide analysis of resting pancreata, *Spi2a* was shown to be expressed basally in acinar cells lacking IκBα. Further studies showed that Spi2A is regulated by RelA and induced during AP.

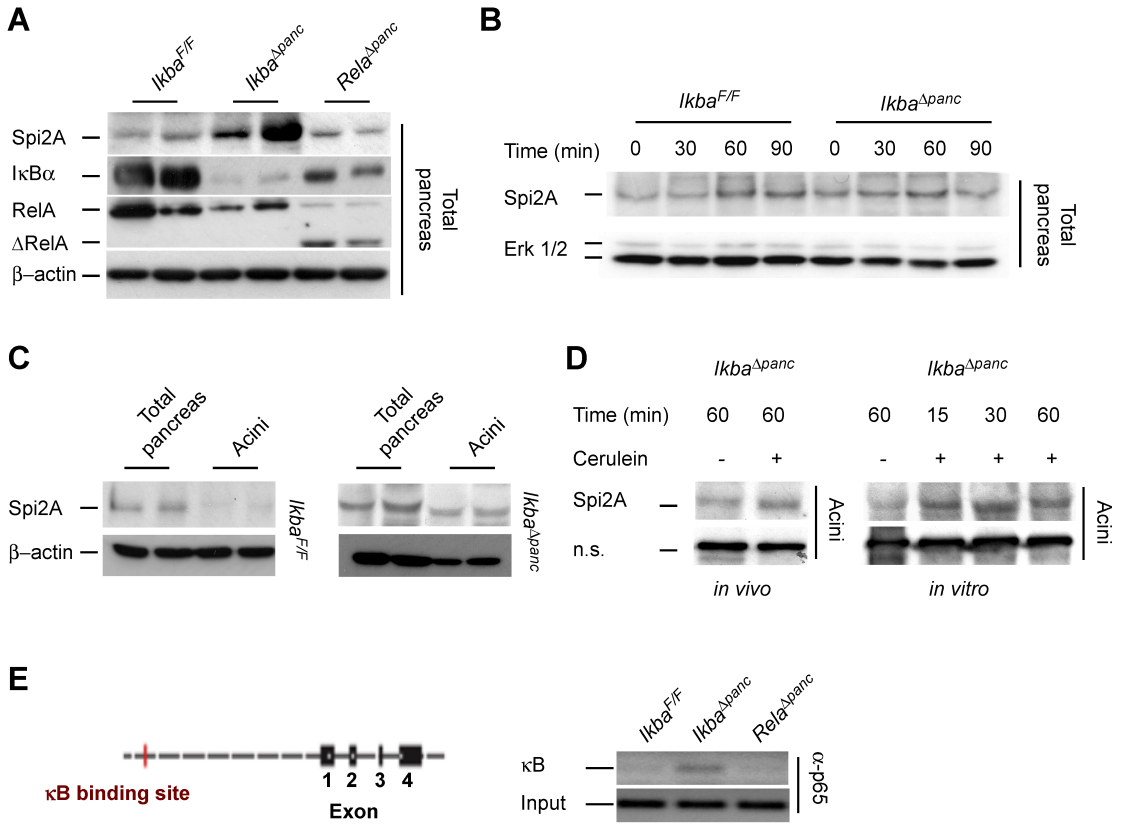

Figure 3-6: The role of Spi2A during AP (**A**) Pancreata from *Ikba*$^{F/F}$, *Ikba*$^{\Delta panc}$, and *Rela*$^{\Delta panc}$ mice were isolated and homogenized to detect Spi2A, IκBα, RelA, and truncation of RelA (ΔRelA) by Western blot. β-actin served as loading control (n=4). (**B**) Spi2A was detected in total pancreas lysates at the indicated time points. Erk 1/2 served as loading control (n=3). (**C**) Total pancreatic lysates and acinar cells were subjected to Spi2A expression analysis by Western blot. β-actin served as loading control (n=3). (**D**) *In vivo* and *in vitro* stimulated acinar cells were analyzed for Spi2A expression. NS, nonspecific band. (**E**) Chromatin immunoprecipitation experiments were performed with pancreatic tissue of the indicated genotypes using an antibody against RelA.

To evaluate the role of Spi2A during AP, the Spi2A coding sequence (cds) with a 5' His-Tag was cloned into the expression vector pCDNA3 to obtain the Spi2A-pCDNA3 construct. HEK cells were then transfected with the Spi2A-pCDNA3 construct. Using Ni-NTA agarose, Spi2A was purified from transfected cells (Figure 3-7). *In vitro* assays were performed to test the ability of the purified Spi2A to decrease cathepsin B and trypsin activity. Spi2A failed to affect both, cathepsin B and trypsin activity *in vitro* (data not shown), potentially due to the loss of bioactivity of the purified Spi2A.

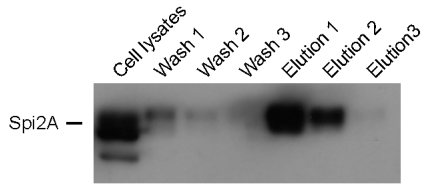

Figure 3-7: Purification of Spi2A: Western Blot of Spi2A from indicated steps during protein purification.

3.1.3 Lentiviral-mediated expression of Spi2A attenuates AP in mice

Since the purified Spi2A protein did not show any bioactivity and failed to clarify the role of Spi2A during AP, a lentiviral approach was selected to elucidate its role. The coding sequence of Spi2A was subcloned into the lentiviral expression vector pQCXIP (Clonetech) and virus was produced. Mice were injected twice with approximately $1x10^6$ infectious units (ifu) according to the protocol in Figure 3-8 A. The lentiviral transfection of the LV-Spi2A construct led to an increase in Spi2A expression in all analyzed organs, compared to mice transfected with the LV-empty construct, that did not contain the Spi2A coding sequence (Figure 3-8 B).

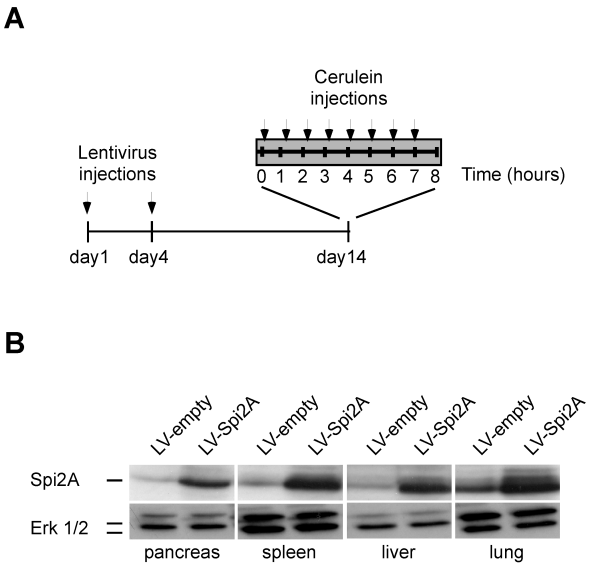

Figure 3-8: Lentiviral transduction model (**A**) Model of lentiviral transduction. C57BL/6 mice were injected with $1x10^6$ ifu of lentivirus on day 1 and day 4. Pancreatitis was induced on day 14. (**B**) Immunoblot analysis of Spi2A expression in mice injected with either LV-empty or LV-Spi2A in indicated organs. Note the increase of Spi2A expression due to lentiviral transduction of LV-Spi2A in all organs. Erk 1/2 served as loading control (n=3).

Next, mice transfected with either construct were challenged with 8 hourly injections of cerulein, to elucidate the effect of lentiviral-mediated overexpression of Spi2A during AP. Morphologically, mice infected with LV-empty showed normal features of pancreatitis, whereas mice transfected with LV-Spi2A revealed an attenuated experimental pancreatitis (Figure 3-9 A). Semi-quantitative analysis of necrotic and edematous tissue revealed a significant reduction of necrosis and edema in the LV-Spi2A group (Figure 3-9 B and C). Interestingly, trypsin activity was reduced in mice transfected with LV-Spi2A, suggesting a correlation of high Spi2A expression and trypsin activation (Figure 3-9 D).

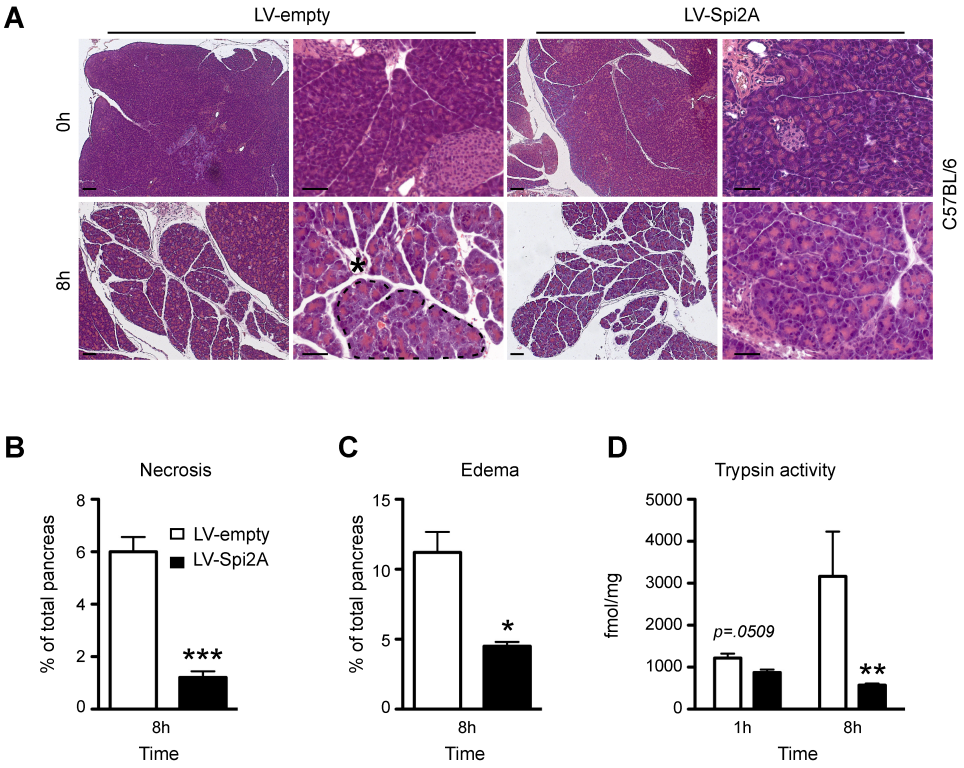

Figure 3-9: Lentiviral-mediated expression of Spi2A attenuates AP (**A**) Histological sections of H&E stained pancreatic tissue of mice injected with indicated lentiviral constructs. Note the increased necrosis (dashed line) and edema (black stars) in LV-empty mice. (**B**) and (**C**) Histological sections were analyzed to evaluate necrosis and edema in relation to total pancreatic area. (**D**) Trypsin activity was measured after 1 and 8 hourly injections in LV-Spi2A and LV-empty mice during AP. Note the low activity of trypsin in LV-Spi2A compared with LV-empty mice after 1 and 8 hours. Results are means ± SD (n=3 for each group). *P <05; **P<.005, and ***P>.001 was considered significant. Scale bar represents 50µm.

To verify the results obtained in C57BL/6 mice, mice harboring a disruption in the *Rela* gene (*Rela*$^{\Delta panc}$ mice) were transfected with the LV-Spi2A construct (Algul, Treiber et al. 2007). Transfection of LV-Spi2A showed an improvement of symptoms, even in this severe phenotype of AP. Necrosis, but not edema, was decreased significantly in *Rela*$^{\Delta panc}$ mice mice infected with LV-Spi2A (Figure 3-10 A-C).

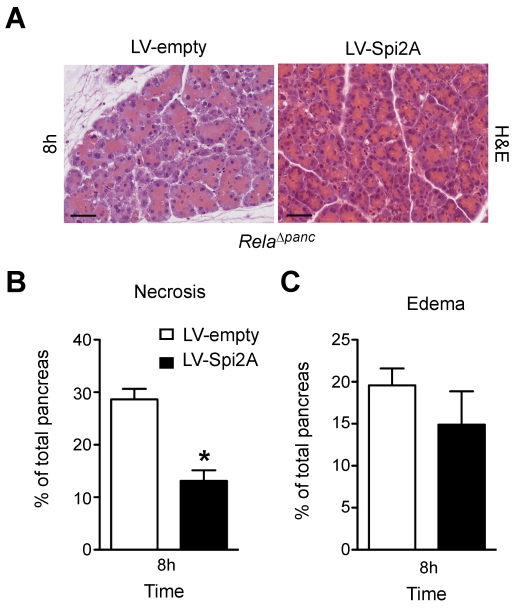

Figure 3-10: Lentiviral-mediated expression of Spi2A in RelA deficient mice (**A**) Histological sections of H&E stained pancreatic tissue of *Rela*$^{\Delta panc}$ mice injected with LV-empty or LV-Spi2A. (**B**) and (**C**) Histological sections were analyzed to evaluate necrosis and edema in relation to total pacreatic area. Results are means ± SD against LV-empty injected *Rela*$^{\Delta panc}$ mice, *p< 0.05 was considered significant. Scale bars represent 50µm.

Since these data show that Spi2A attenuates the severity of AP by interfering with trypsin activity, genetic alterations in the coding sequence of the human analogue *AACT* were evaluated for association with acute or chronic pancreatitis. 219 patients with AP, 242 patients with chronic pancreatitis, and 401 healthy control subjects were screened for *AACT* coding variants by direct DNA sequencing. 5 nonsynonymous and 8 synonymous variants were detected (Table 7-1). None of these alterations, however, were linked with either acute or chronic pancreatitis per se or with the severity of AP, according to the Atlanta criteria.

These data led to the conclusion that Spi2A attenuates AP by interfering with trypsin activity. Polymorphisms in the human analogue *AACT*, however, are not associated with either acute or chronic pancreatitis.

3.2 IL-6 trans-signaling promotes pancreatitis-associated lung injury and lethality

3.2.1 Establishing a new model for SAP-induced lethal ALI

The most suitable model for pancreatitis-induced lung injury is the cerulein model (Algul, Tando et al. 2002; Elder, Saccone et al. 2011; Elder, Saccone et al. 2012). Cerulein is a Cholecystokinin analogue that binds specifically to the acinar cell specific CCK-A receptor. When administered in supraphysiological doses, cerulein induces pancreatitis through intra-acinar activation of digestive enzymes (Algul, Treiber et al. 2007). With the exception of one study, multiple daily injections of cerulein cause nonlethal AP with mild lung injury (Cuzzocrea, Mazzon et al. 2002; Pandol, Saluja et al. 2007). To increase severity of lung injury and induce lethality the cerulein model was modified. In this new model for severe acute pancreatitis (SAP), mice were treated daily with 8 hourly injections of cerulein for 5 consecutive days (Figure 3-11 A). This new protocol resulted in SAP with multiple organ damage and lethal ALI, with mortality rates comparable to those in the human disease (Figure 3-11 B).

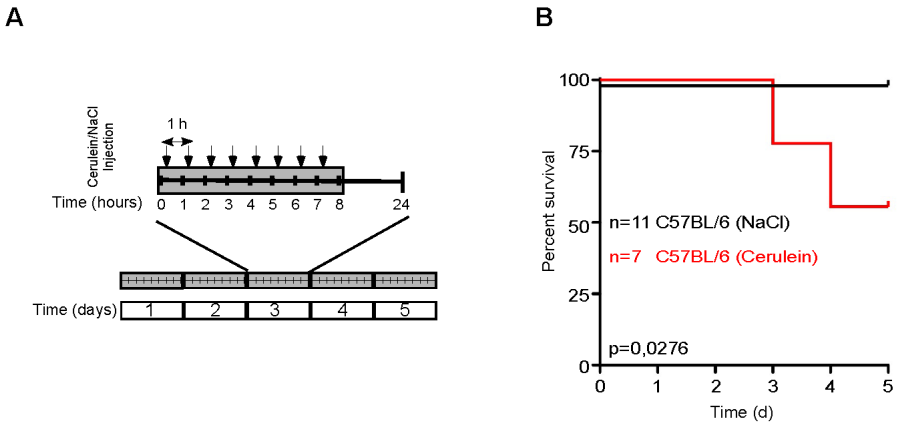

Figure 3-11: Model and survival for severe acute pancreatitis (SAP): (**A**) Schematic model of SAP. (**B**) Kaplan-Meier curves of cerulein-treated C57BL/6 (red), and sham-treated C57BL/6 mice (black) during SAP.

The pancreas showed an increase in cell death, necrosis and edema after 8 hours. However, pancreatic damage decreased after 3 days as seen in pancreatic histology and amylase, lipase level in the serum (Figure 3-12 A and B).

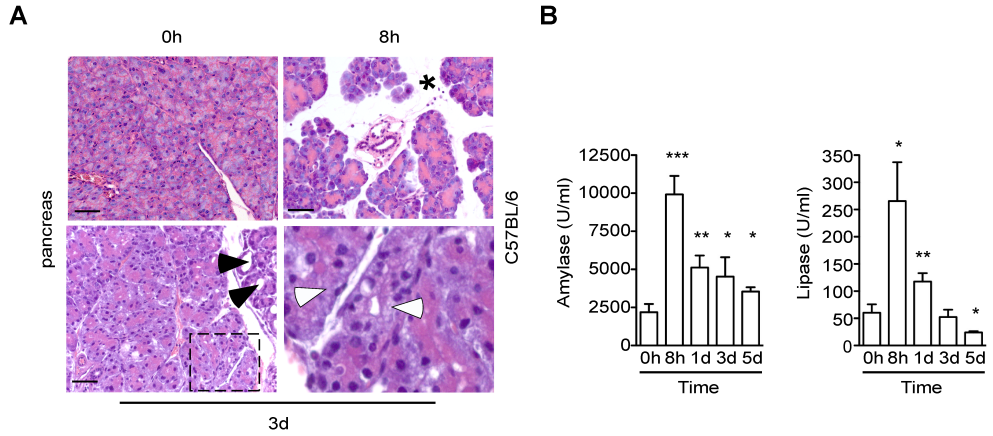

Figure 3-12: Pancreatic changes during SAP: (**A**) Histological sections of H&E stained pancreatic tissue of C57BL/6 mice at the indicated time points. Note the increase of edema (black stars) and necrosis (white arrows) after 8 hours and 3 days, as well as first signs of regeneration (black arrows) after 3 days. (**B**) Serum was removed for Amlyase and Lipase analysis at the indicated time points. Results are means ± SD (n=3 for each group). *P <05; **P<.005, and ***P>.001 compared to 0h was considered significant. Scale bars represent 50µm.

While the pancreas showed first signs of regeneration after 3 days, lung damage increased significantly over time as shown by histological changes in the lung (Figure 3-13 A). These morphological changes were verified by an increase of myeloperoxidase (MPO) activity in the lung, a marker for lung neutrophil infiltration (Figure 3-13 B). Since MPO is detectable in neutrophils and monocytes, flow cytometry experiments were performed. These experiments showed an increase of polymorphonuclear leukocytes (PMN) in the lung 8 hours after the first injection of cerulein (Figure 3-13 C). PMNs and macrophages could also be detected in the bronchoalveolar fluid (BALF) (Figure 3-13 C). Another marker for pulmonary damage is alveolar permeability. The extravasation of circulating FITC-dextran was measured, to evaluate the extend of alveolar permeability in the cerulein model. There was an increase of extravasation as the disease progressed (Figure 3-13 D). This increase of

alveolar permeability might also explain the increase in alveolar wall thickening that could be detected during SAP (Figure 3-13 E).

In line with these observations, an increase in cell numbers and protein content could be measured in the BALF (Figure 3-13 F and G). There was also an increase in cytokines (Cxcl1) and chemokines (IL-6) detectable in the BALF (Figure 3-13 H and I). These chemokines and cytokines are known to be important for inflammation and cellular recruitment (Hoth, Wells et al. 2011; Ahuja, Andres-Hernando et al. 2012).

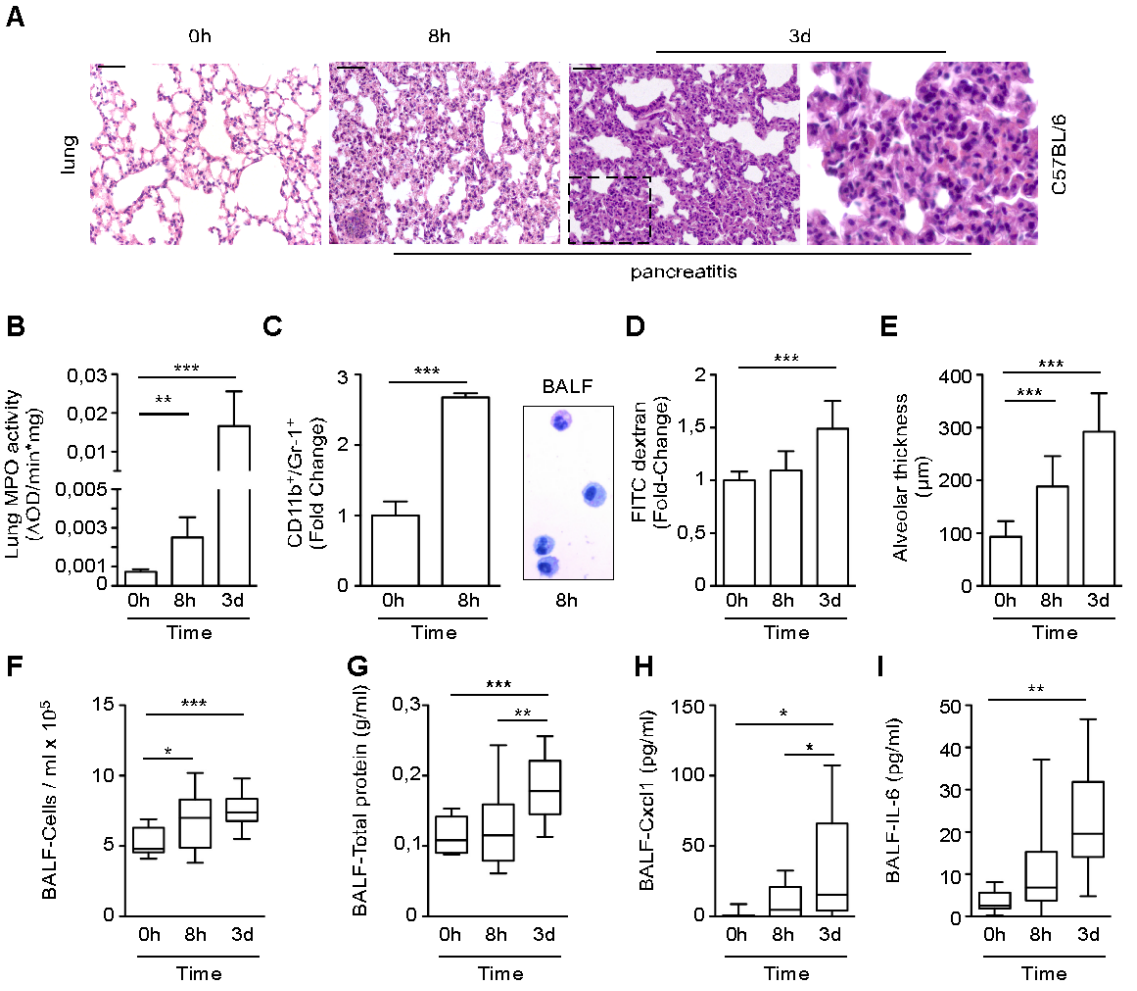

Figure 3-13: Lung damage during SAP: (**A**) Histological sections of H&E stained lung tissue during SAP. Note the increase of lung damage after 3 days as seen by alveolar wall thickening and alveolar collapse (Inset). (**B**) MPO activity (quantification of pulmonary neutrophil infiltration) in the lung tissue of C57BL/6 mice during SAP (n=5). (**C**) Flow cytometry analysis of $CD11b^{+}/Gr1^{+}$ cells in total lung tissue (n=6). Cytospin preparation of bronchoalveolar lavage fluid (BALF) in representative C57BL/6 mice after 8 hours. (**D**) Lung permeability, evaluated by FITC dextran clearance. (**E**) Interstitial lung accumulation, measured as capillary-alveolar membrane thickness (n=10). (**F-I**) Total cell count (**F**), total protein concentration (**G**), Cxcl1 concentration (**H**) and IL-6 (**I**) in BALF (n=1-3 per condition; 4 independent experiments). Results are means ± SD (n=3 for each group). *P <05; **P<.005, and ***P>.001 was considered significant. Scale bars represent 50µm.

To rule out hypotension and sepsis as causes for the lethality of SAP, blood pressure and serum endotoxin level were analyzed. While serum endotoxin level mildly increased during SAP with a significant increase only after 5 days, blood pressure analysis did not show any significant changes (Figure 3-14 A and B). Since most mice died after 3 and 4 days (Figure 3-11 B), sepsis can be ruled out as the main reason for lethality.

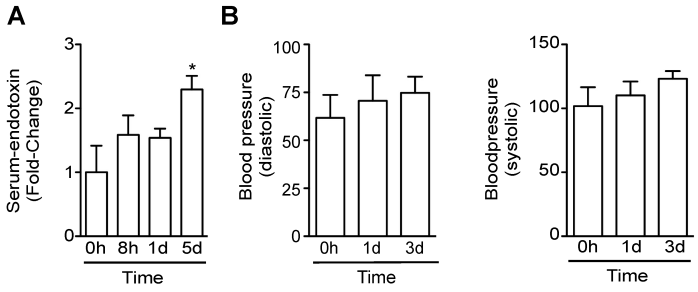

Figure 3-14: Systemic complications during SAP: (**A**) The endotoxin activities of different serum samples were determined assay at indicated time points. (**B**) Blood pressure was analyzed in mice during SAP. Results represent mean ± SD, *p< 0,05, versus 0 h.

Consistent with these findings systemic complications to the liver and kidney were only transient (Figure 3-15 A-E). While some necrosis could be found in the liver after 3 days, the level of the liver transaminases ALT and AST did not increase throughout SAP.

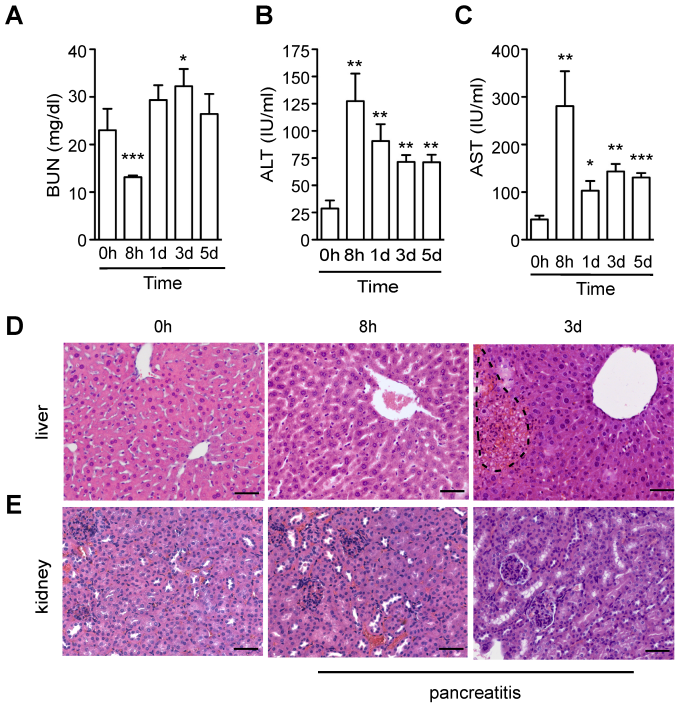

Figure 3-15: Liver and kidney damage during SAP: (**A-C**) Serum was removed for BUN, ALT and AST analysis at indicated time points. (**D**) and (**E**) Representative H&E sections of liver and kidney tissue of C57BL/6 mice during SAP at indicated time points. Necrotic cells were found after 3 days of AP in the liver tissue (dashed line). Results represent mean ± SD (n >4), *p < 0.05, **p < 0,005, ***p < 0,001 versus 0 hours. Scale bars represent 50µm.

Severe pulmonary damage was accompanied by an increase of IL-6 and Cxcl1 during onset of the disease, while both parameters returned to normal values as the disease progressed suggesting that IL-6 and Cxcl1 are accumulating in the lung (Figure 3-16 A and B).

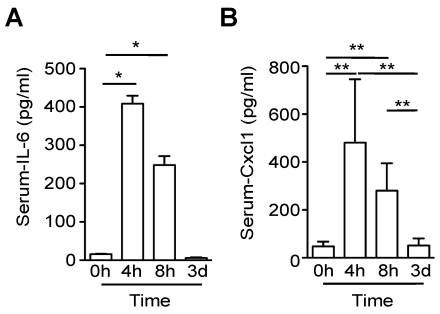

Figure 3-16: Changes in pro-inflammatory cytokines/chemokines (**A**) Serum IL-6 levels in C57BL/6 mice (n>5). (**B**) Serum CXCL1 levels in C57BL/6 mice (n>5). Results represent mean ± SD, *p< 0,05, **p < 0.005.

3.2.2 IL-6 links pancreatic damage to pulmonary damage

Several attempts have been made to identify parameters as predictors for SAP. Several associations of cytokines and chemokines with severity of AP have been described (Viedma, Perez-Mateo et al. 1992; Paajanen, Laato et al. 1995; Chen, Wang et al. 1999; Sathyanarayan, Garg et al. 2007). Among those only IL-6 and its downstream target C-reactive protein (CRP) turned out to be reliable parameters for severity of AP (Viedma, Perez-Mateo et al. 1992; Sathyanarayan, Garg et al. 2007). To evaluate the role of IL-6 in SAP-induced ALI, SAP was induced with cerulein in mice lacking IL-6 (*Il6*$^{-/-}$ mice). IL-6 deficient mice did not develop SAP-induced lethal ALI, while approximately 40% of the C57BL/6 control mice died. Moreover, mice injected once a day with recombinant 5µg IL-6 (i.v.; one hour before the last injection of cerulein) all succumbed to ALI. In contrast, single daily injections of IL-6 with 8 hourly injections of NaCl (0,9%) had no effect on survival (Figure 3-17).

These genetic and pharmacological data demonstrate that IL-6 is not only a marker for severity but also a relevant pathophysiological mediator of lethality in SAP with pulmonary damage

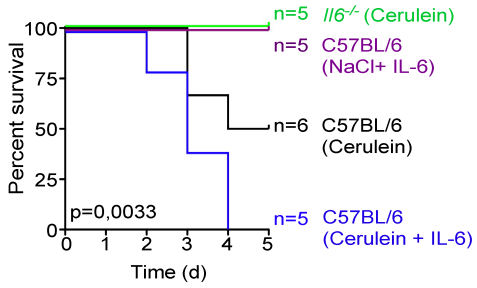

Figure 3-17: IL-6 is not only a marker for severity of AP, but a pathophysiological relevant mediator: Kaplan-Meier curves of cerulein-treated C57BL/6 (black), *Il6*$^{-/-}$ (green), C57BL/6 mice treated with recombinant IL-6 (blue; 5 µ g/day), and sham-treated C57BL/6 mice injected with IL-6 (purple; 5 µg/day).

To further investigate the mechanism of IL-6 in SAP-induced ALI, the onset of inflammation in *Il6*$^{-/-}$ mice was analyzed. In line with previous findings, pancreatic damage was increased in IL-6-deficient mice, as seen by the increase in amylase and lipase serum level as well as in the histology of pancreatic tissue (Figure 3-18 A-C) (Cuzzocrea, Mazzon et al. 2002). In contrast, lung injury was attenuated in *Il6*$^{-/-}$ mice as seen by less alveolar wall thickening and a decrease in MPO activity in the lung (Figure 3-18 D-F). Moreover, levels of the neutrophil-attracting chemokine Cxcl1 were significantly decreased in IL-6-deficient mice (Figure 3-18 G).

It has been shown that Cxcl1 is regulated by members of the gp130-Stat3 axis (Sander, Sackett et al. 2010). Since IL-6 also exerts its pro-inflammatory effects through the Jak2-dependent Stat3 pathway, the role of Stat3 activation was evaluated in *Il6*$^{-/-}$ mice. Phosphorylation of Stat3 and Stat1 was analyzed, using tissue homogenates of C57BL/6 and *Il6*$^{-/-}$ mice. Phosphorylation of Stat3^{Y705} was clearly attenuated in *Il6*$^{-/-}$ mice compared to C57BL/6 mice, while both genotypes failed to show any activation of Stat1 (Figure 3-18 H). Additional immunohistochemical staining of Stat3^{Y705} supported the immunoblot data, as mice lacking IL-6 failed to show Stat3 phosphorylation in acinar cells (Figure 3-18 I). Of note, immune cells in *Il6*$^{-/-}$ mice still demonstrated Stat3 activation.

In summary it can be stated, that Stat3 in the pancreas is a mediator of IL-6-dependent effects in SAP-associated ALI.

Hence the conclusion that IL-6 links the inciting event of AP to the secondary development of pulmonary damage with subsequent ALI via Stat3 activation in the pancreas.

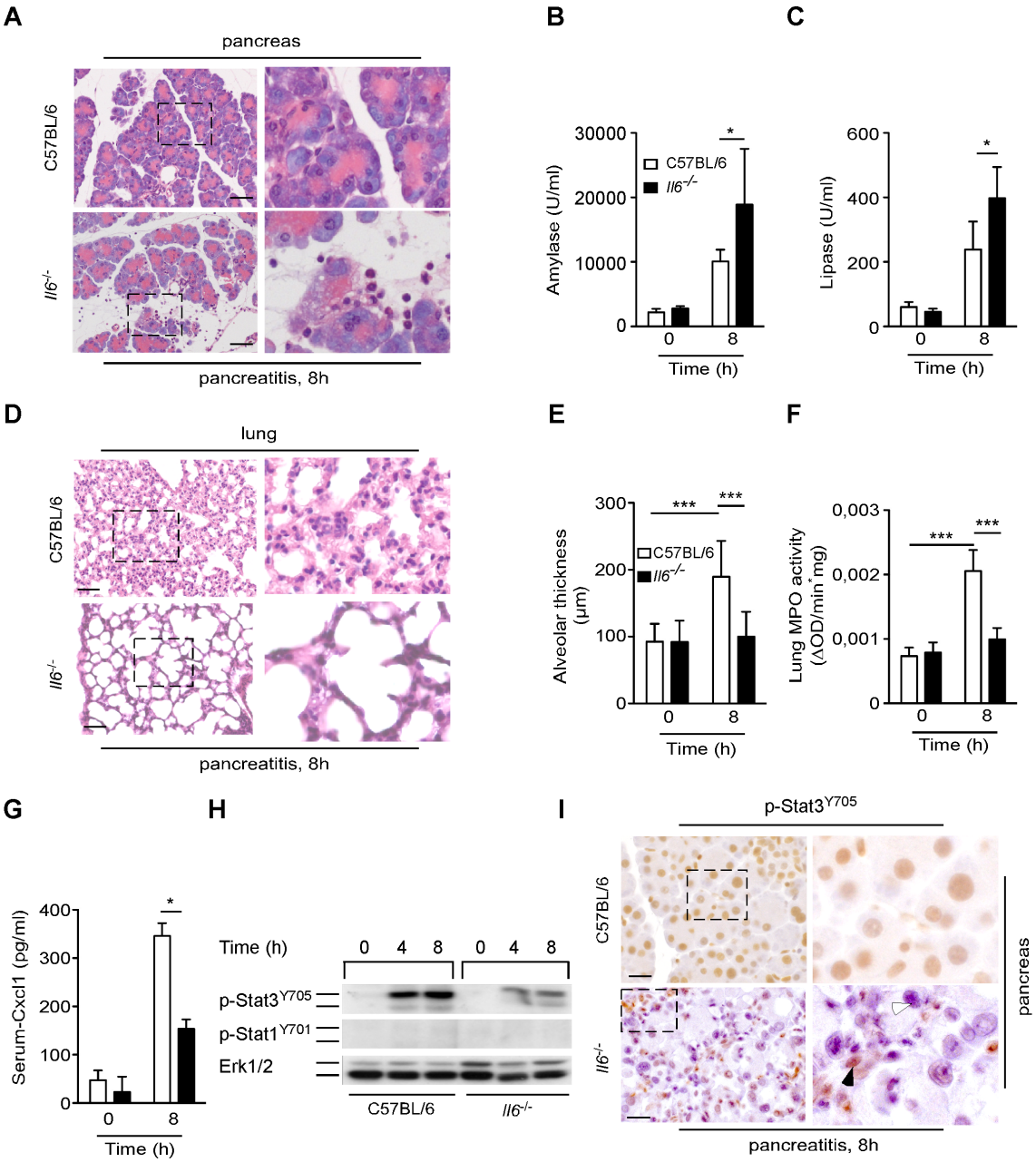

Figure 3-18: IL-6 links local damage to systemic complications: (**A**) Morphological analysis of H&E stained pancreatic tissue of C57BL/6 and *Il-6*$^{-/-}$ mice after 8 hours of AP. (**B**) and (**C**) Amylase and lipase levels in C57BL/6 and *Il-6*$^{-/-}$mice (n=4). (**D**) Histological sections of the lung tissue of C57BL/6 and *Il-6*$^{-/-}$ mice after 8 hours of AP. Note the increase of alveolar wall thickening and collapse in C57BL/6 mice (inset). (**E**) Capillary-alveolar membrane thickness in C57BL/6 and *Il-6*$^{-/-}$ mice (n=10). (**F**) MPO activity in the lung tissue of C57BL/6 and *Il-6*$^{-/-}$ mice (n>5). (**G**) Serum Cxcl1 level in C57BL/6 and *Il-6*$^{-/-}$ mice (n=4). (**H**) At 0, 4, and 8 hours, pancreatic tissue was isolated and homogenized to detect p-Stat3Y705 and p-Stat1Y701. Erk1/2 served as the loading control (representative blot; n=4 for each time point). (**I**) IHC staining of p-Stat3Y705 in pancreatic tissue of C57BL/6 and *Il-6*$^{-/-}$ mice. Only C57BL/6 mice revealed Stat3 activation in acinar cells, while *Il-6*$^{-/-}$ mice showed only phosphorylation of Stat3 in immune cells (inset, black arrow) and not in acinar cells (inset, white arrow). Results represent mean ± SD, *p < 0.05, ***p <0.001. Scale bars represent 50 µm.

3.2.3 IL-6 trans-signaling mediates pulmonary damage via Stat3 activation in the pancreas

As a next step the underlying mechanism of IL-6-dependent Stat3 activation was evaluated in isolated acinar cells. To test the hypothesis that IL-6 mediates Stat3 activation, acinar cells were stimulated for 2 hours with different concentrations of IL-6. Surprisingly, IL-6 alone did not induce robust Stat3 phosphorylation (Figure 3-19).

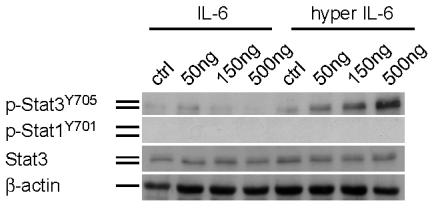

Figure 3-19: IL-6 trans-signaling is necessary to induce Stat3 phosphorylation in acinar cells. Immunoblot analysis of p-Stat3^{Y705} , p-Stat1^{Y701} and Stat3 of isolated acinar cells from C57BL/6 mice stimulated with different concentrations of IL-6 or hyper IL-6 for 2h. β-actin served as a loading control (representatitve blots, n=3 for each time point).

Notably, even supramaximal concentrations of the CCK analog cerulein failed to activate Stat3 in isolated acinar cells (Figure 3-20). IL-6 can activate Stat3 via two modes. The first mode entails classical signaling mechanisms characterized by the binding of IL-6 to the membrane-bound IL-6 receptor (mIL-6R) and gp130 on specific target cells. Alternatively, IL-6 binds to a naturally occurring soluble form of the IL-6R (sIL-6R), thereby forming a complex with IL-6 that initiates signaling in cells that lack membrane-bound IL-6R; this process is called IL-6 trans-signaling (Jostock, Mullberg et al. 2001). To test whether IL-6 mediates Stat3 activation in acinar cells via IL-6 trans-signaling, acinar cells were stimulated with different concentrations of the fusion protein hyper-IL-6, which consists of IL-6 and sIL-6R, for 2 hours (Fischer, Goldschmitt et al. 1997). Indeed, only hyper-IL-6 was sufficient to induce Stat3 phosphorylation in isolated acinar cells *in vitro* but not IL-6 alone (Figure 3-19).

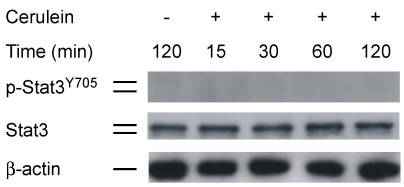

Figure 3-20: Cerulein is not able to phosphorylate Stat3 in acinar cells: Immunoblot analysis of p-Stat3^{Y705} and Stat3 of isolated acinar cells from C57BL/6 mice stimulated with cerulein for the indicated time

Conversely hepatocytes that express membrane-bound IL-6R respond to IL-6 (data not shown) (Sun, Jaruga et al. 2005). In fact, unlike hepatocytes, acinar cells showed only weak expression of the membrane-bound IL-6R (Figure 3-21).

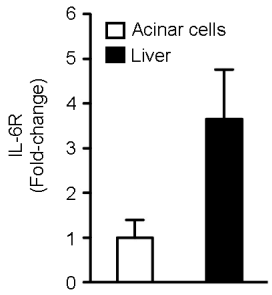

Figure 3-21: Acinar cells express only low levels of IL-6R: Levels of IL-6R mRNA of acinar cells or total liver tissue. Values are normalized to the level of cyclophillin mRNA and represent fold-change ± SD (n=3).

In contrast, circulating levels of sIL-6R in the serum increased during the onset of pancreatitis and returned to normal values as the disease progressed (Figure 3-22 A). However, sIL-6R in the BALF continued to increase during the disease (Figure 3-22 B). This kinetic and distribution resembles that of IL-6 and Cxcl1. Taken together, these *in vitro* data indicate that IL-6 trans-signaling rather than classical IL-6 signaling is required to activate Stat3 in acinar cells.

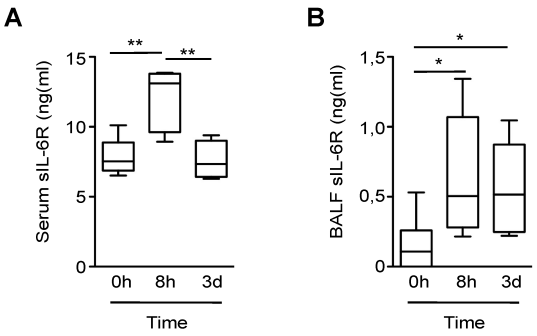

Figure 3-22: sIL-6R accumulates in the BALF: (**A**) Serum sIL-6R level in C57BL/6 mice during SAP (n=4). (**B**) BALF sIL-6R level in C57BL/6 mice during SAP (n=4). Results represent mean ± SD; **p < 0.005.

Previous studies showed that IL-6 trans-signaling plays a major role in the regulation of leukocyte recruitment, a process required for ALI (Atreya, Mudter et al. 2000; Chalaris, Rabe et al. 2007). To analyze whether specific inhibition of IL-6 trans-signaling *in vivo* has similar effects on ALI as in *Il-6*$^{-/-}$ mice, transgenic opt_*sgp130Fc* mice were analyzed. This mouse line has a liver-specific transgenic overexpression of a soluble gp130Fc (sgp130Fc); sgp130Fc inhibits IL-6 trans-signaling without affecting classical IL-6 signaling (Rabe, Chalaris et al. 2008; Jones, Scheller et al. 2011).

Similar to IL-6-deficient mice, ALI was clearly attenuated in opt_*sgp130Fc* mice. Morphologically, opt_*sgp130Fc* mice show less pulmonary damage compared to C57BL/6 mice (Figure 3-23 A). Alveolar wall thickening was significantly reduced and lung MPO levels were decreased in opt_*sgp130Fc* mice (Figure 3-23 B and C).

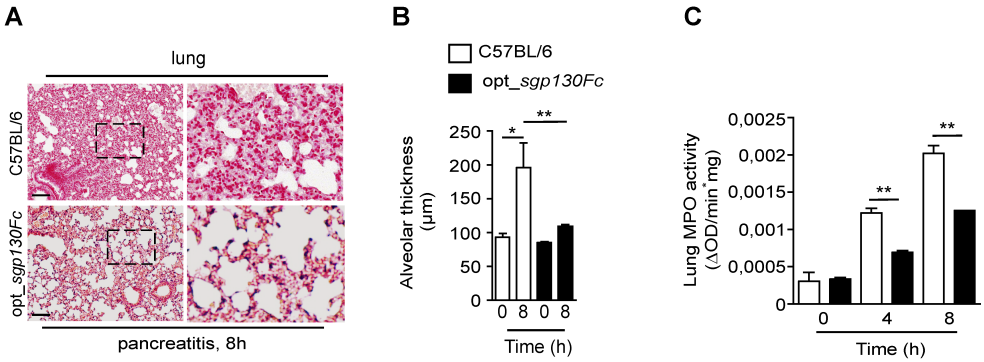

Figure 3-23: IL-6 trans-signaling is necessary for pulmonary damage: (**A**) Morphological analysis of representative H&E stainings reveals less alveolar collapse and thickness in opt_*sgp130Fc* mice as compared to C57BL/6 mice (inset) (**B**) Interstitial fluid accumulation. Capillary-alveolar membrane thickness in C57BL/6 and opt_*sgp130Fc* mice (n=5). (**C**) Lung tissue was removed to measure MPO activity in C57BL/6 and opt_*sgp130Fc* mice (n=5). Results represent mean ± SD, *p< 0,05, **p < 0.005. Scale bars represent 50µm.

Circulating levels of IL-6 in the serum were still high but with a significant decrease after 4 hours (Figure 3-24 A). Immunoblot analysis of Stat3 phosphorylation showed attenuated activation of Stat3 in opt_*sgp130Fc* mice, similar to the results obtained in *Il-6*$^{-/-}$ mice (Figure 3-24 B),.

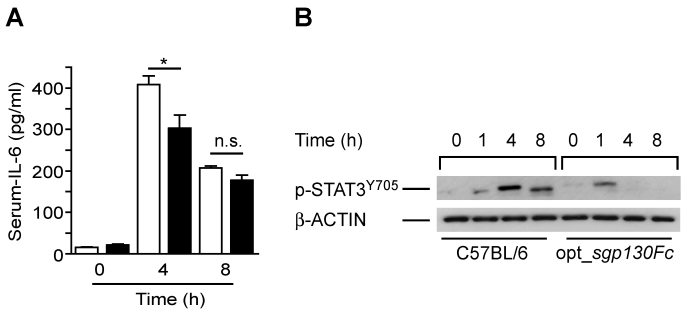

Figure 3-24: IL-6 trans-signaling is required for Stat3 phosphorylation in the pancreas: (**A**) Serum concentrations of IL-6 in C57BL/6 and opt_sgp130Fc mice (n=4). (**B**) At 0, 1, 4, and 8 hours, pancreatic tissue from C57BL/6 and opt_sgp130Fc mice was isolated and homogenized to detect p-Stat3^{Y705}. β-actin served as the loading control (representative blot; n=4 for each time point). Results represent mean ± SD, *p< 0,05.

In contrast to the findings in the IL-6-deficient mice, pancreatic damage was attenuated in opt_*sgp130Fc* mice, suggesting that classical IL-6 signaling possesses protective properties, thus attenuating pancreatic damage (Figure 3-25 A-C).

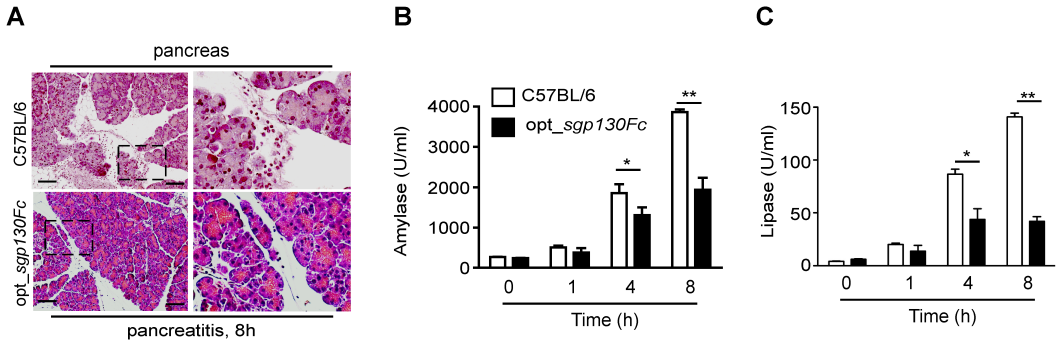

Figure 3-25: Lack of IL-6 trans-signaling improves pancreatic injury: (**A**) Morphological analysis of representative H&E stains reveal less pancreatic injury in opt_*sgp130Fc* mice as compared to C57BL/6 mice. (**B)** and (**C**) Serum analysis shows a significantly lower level of amylase and lipase after 4 hours and 8 hours in opt_*sgp130Fc* mice as compared to C57BL/6. Results represent mean ± SD, *p< 0,05, **p < 0.005. Scale bars represent 50µm.

Collectively, these data demonstrate that IL-6 trans-signaling, not classical IL-6 signaling, links the inciting event of AP to the secondary development of ALI. These data also implicate IL-6 trans-signaling-dependent Stat3 activation as the linking module.

3.2.4 Classical IL-6 signaling and IL-6 trans-signaling activate distinct pathways in the pancreas during inflammation.

While pulmonary damage was attenuated in *Il6*$^{-/-}$ and opt_*sgp130Fc* mice, the extent of local damage in the pancreas differed. To better understand the mechanisms underlying these findings, various signaling pathways involved in AP were analyzed *in vivo*. Interestingly, while Stat3^{Y705} phosphorylation was clearly diminished in *Il6*$^{-/-}$ and opt_*sgp130Fc* mice, serine phosphorylation at S727, which is known to attenuate reactive oxygen species (ROS) release from the electron transport chain, was dramatically phosphorylated in IL-6 deficient mice, suggesting an increase in ROS in these mice (Figure 3-26) (Szczepanek, Lesnefsky et al. 2012). This was not true for C57BL/6 and opt_*sgp130Fc* mice. Further, mice lacking IL-6 revealed strong phosphorylation of RelA in the pancreas. Likewise, the inhibitor proteins IκBα and IκBβ are rapidly degraded.

Transgenic opt_*sgp130Fc* mice revealed only slight activation of the IκB/NF-κB cascade. IκBα and IκBβ degradation was most prominent after 8 hours.

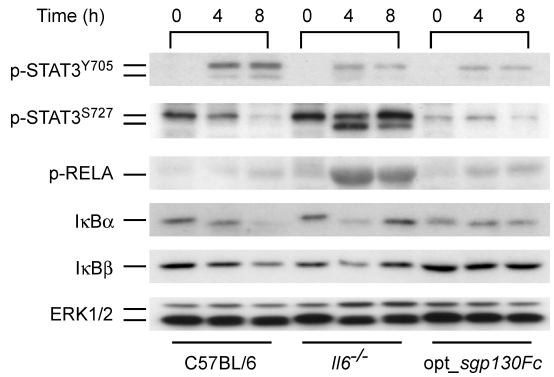

Figure 3-26: Classical IL-6 signaling and IL-6 trans-signaling activate different pathways in the pancreas during inflammation: At 0, 4, and 8 hours, pancreatic tissue from C57BL/6, Il6-/-, and opt_*sgp130Fc* mice was isolated and homogenized to detect p-Stat3^{Y705}, p-Stat3^{S727}, p-RelA, IκBα, and IκBβ. Erk1/2 served as the loading control (representative blot; n=4 for each time point).

In summary, while the inhibition of classical IL-6 signaling and IL-6 trans-signaling both reduced Stat3 phosphorylation at tyrosine 705 *in vivo*, these data implicate that different pathways are activated in the pancreas of *Il6*$^{-/-}$ and opt_*sgp130Fc* mice during inflammation. These findings provide an explanation for the different phenotypes in the pancreases of these mice.

3.2.5 Myeloid cells are the main source of IL-6

To specify the cellular source of increased pancreatic NF-κB activation, IHC stainings were performed. These stainings revealed that NF-κB activation is almost completely restricted to infiltrating cells as shown by nuclear localization of IκBα (Figure 3-27 A). In addition to NF-κB, myeloid cells turned out to be the main cellular source of local and systemic IL-6 (Figure 3-27 B).

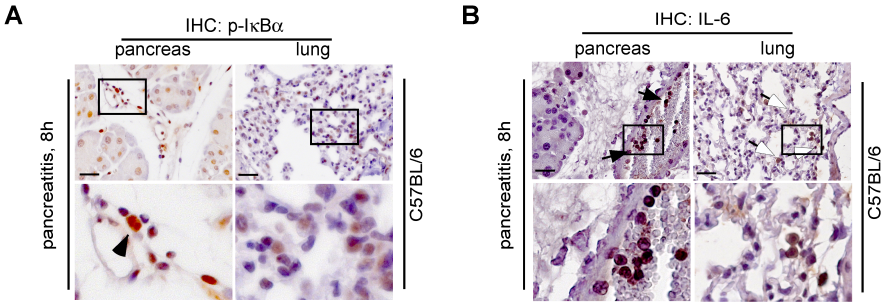

Figure 3-27: Macrophages are the cellular source of IL-6 during AP: (**A**) Immunohistochemical analyses were used to localize p-IκBα in the pancreas and lung tissues 8 hours after the first injection of cerulein. Positive nuclear staining for p-IκBα in the pancreas was mainly restricted to inflammatory cells (inset, black arrows). Alveolar cells show weak activation of p-IκBα. (**B**) IHC analyses were used to localize IL-6 in the pancreas and lung. Only inflammatory cells stained positive for IL-6 (black arrows). Alveolar macrophages express IL-6 in the lung (white arrows). Scale bars represent 50µm.

These data suggest that myeloid cells secrete IL-6 in a NF-κB-dependent manner.

3.2.6 Stat3 phosphorylation at Y705 modulates severity of inflammation and determines lethality.

To assess whether Stat3 activation in the pancreas is required to mediate lethal ALI, mice lacking either Stat3 or the suppressor of cytokine signaling 3 (Socs3) were generated using the Cre/LoxP system. *Stat3*$^{F/F}$ and *Socs3*$^{F/F}$ were crossed with *Ptf1aCre*^{ex1} mice, generating mice lacking Stat3 (*Stat3*$^{\Delta panc}$ mice) or Socs3 (*Stat3*$^{\Delta panc}$ mice) in the pancreas (Figure 3-28 A and B).

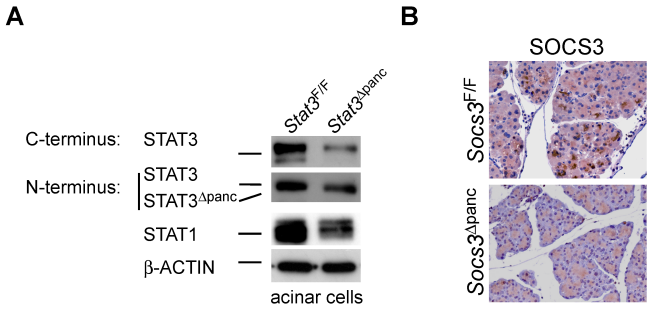

Figure 3-28: Conditional knockout of Stat3 and Socs3, respectively: (**A**) Immunoblot analysis of pancreatic acinar cells using different Stat3 antibodies. Stat3^{Y705} is directed against the tyrosine 705-containing domain in the C-terminus, while the second antibody detects the N-terminus (amino acid1-175) of truncated Stat3Δpanc and wild-type Stat3 (representative blot; n=3 mice). (**B**) Expression of Socs3 during AP. IHC analyses was used to localize Socs3 in mice undergoing AP. After 8 hours of AP expression of Socs3 was only detectable in acinar cells of *Socs3*$^{F/F}$ mice.

SAP was induced in *Stat3*$^{\Delta panc}$ and *Socs3*$^{\Delta panc}$ mice as well as floxed littermates (ctrl). While *Stat3*$^{\Delta panc}$ mice were resistant to SAP-induced lethal ALI, all *Socs3*$^{\Delta panc}$ mice succumbed to SAP (Figure 3-29).

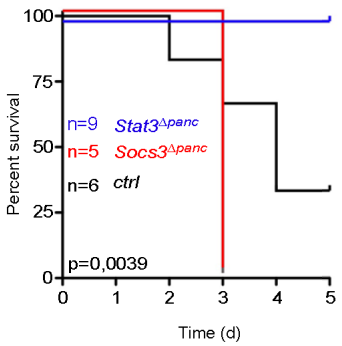

Figure 3-29: Stat3 phosphorylation on Y705 is linked to SAP-induced lethal ALI: Kaplan-Meier curves of *ctrl* (black), *Stat3*$^{\Delta panc}$ (blue), and *Socs3*$^{\Delta panc}$ (red) mice during SAP.

Altogether, these data support the assumption that phosphorylation of Stat3 on Y705 in the pancreas determines the severity of systemic complications and lethality.

3.2.7 Pharmacological inhibition of Stat3 or IL-6 trans-signaling mitigates SAP-induced lethal ALI.

The previous observations on SAP-induced ALI raised the possibility that pharmacological inhibition of IL-6 trans-signaling and its downstream effector Stat3, as well as Cxcl1 and its receptor Cxcr2 prevents SAP-induced lethal ALI. To examine this hypothesis, SAP was induced in C57BL/6 mice. In addition, these mice were injected with recombinant soluble gp130Fc, the small-molecule Stat3 inhibitor S3I-201, the Cxcr2 antagonist SB225002 or the anti-Cxcl1 antibody according to the treatment schedule in Figure 3-30.

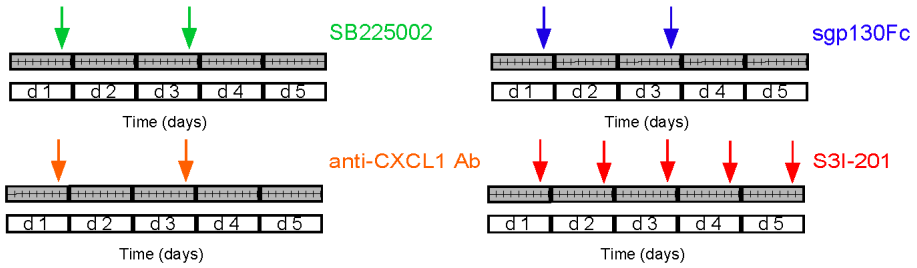

Figure 3-30: Schematic of treatment of SAP: Mice were either injected i.p. twice with recombinant soluble gp130Fc (150µg), the Cxcr2 antagonist SB225002, an anti-Cxcl1 antibody, or they were injected 5 times i.v. with the small-molecule Stat3 inhibitor S3I-201 (7.5 µ g/g body weight).

S3I-201 specifically inhibits the nuclear translocation of phosphorylated Stat3 *in vivo* (Siddiquee, Zhang et al. 2007). As shown in Figure 3-31, the administration of sgp130FC, S3I-201, SB225002 or anti-Cxcl1 antibody prevented all animals from SAP-induced lethal ALI.

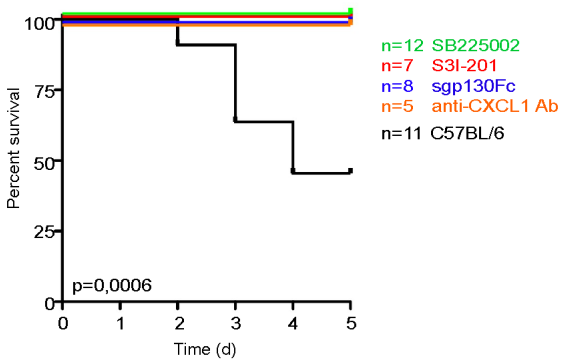

Figure 3-31: Pharmacological inhibition of Stat3, IL-6 trans-signaling and Cxcl1/Cxcr2 attenuates SAP-induced lethal ALI: Kaplan-Meier curves of C57BL/6 mice (black) and C57BL/6 mice treated with the Cxcr2 antagonist SB225002 (green), the Stat3 inhibitor S3I-201 (red), recombinant sgp130Fc (blue), or an anti-Cxcl1 antibody (orange) during SAP.

This demonstrates the involvement of the IL-6/Stat3 cascade in SAP-associated lethal ALI. Even the downstream effector Cxcl1 and its receptor Cxcr2 were critical for pancreatitis-associated pulmonary injury.

Morphologically, no changes in pancreatic damage were observed, while lung injury was clearly improved in all treatment groups (Figure 3-32 A and B).

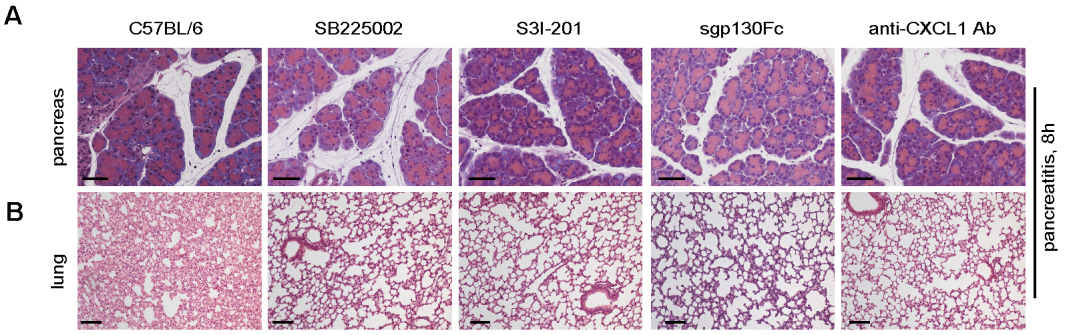

Figure 3-32: Inhibition of Stat3, IL-6 trans-signaling and Cxcl1/Cxcr2 attenuates lung damage: (**A**) and (**B**) Histological sections of pancreatic and lung tissue, respectively, of C57BL/6 mice and treated mice. Scale bars represent 50µm (**A**) or 100µm (**B**), respectively. Note the decrease in lung injury in treated mice as compared to C57BL/6 mice.

In serum analyses, there was no decrease in amylase and lipase level in any of the treatment groups (Figure 3-33 A and B). However, MPO activity in the lung was significantly decreased in all treatment groups, confirming the results from histology that pulmonary damage decreases after treatment (Figure 3-33 C).

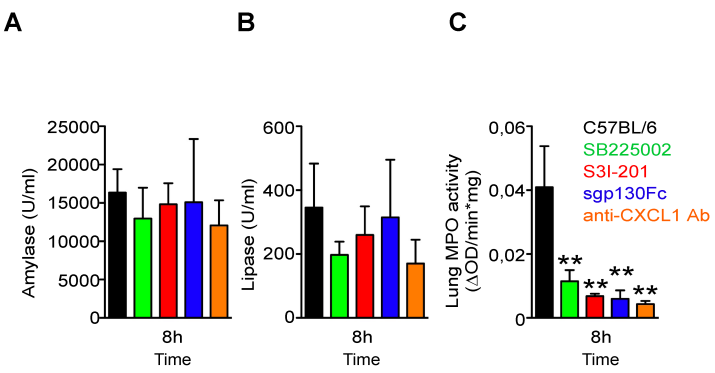

Figure 3-33:Pharmacological inhibition does not change local damage but improves lung injury: (**A**) and (**B**) Serum was analyzed for amylase and lipase activity at indicated time points (n=4). (**C**) MPO activity in the lung tissue of C57BL/6 mice or treated mice 8 hours after the first cerulein injection (n=4). Results represent mean ± SD, **p < 0.005.

Theses findings indicate that the IL-6/Stat3 pathway is crucial for SAP-associated lethal ALI, thereby providing a potential therapeutic target. The clinical relevance of these data was evaluated using plasma from patients with severe and mild AP (Table 7-2 and Table 7-3). IL-6 levels decrease as the disease progresses; therefore all samples were obtained within 50 hours after the onset of symptoms for both patient groups (Figure 3-34 A) (Leser, Gross et al. 1991; Inagaki, Hoshino et al. 1997). Similar to previous reports, IL-6 levels were significantly higher in plasma from individuals that later developed ALI as compared to that of patients with mild AP or control subjects (Figure 3-34 B) (Leser, Gross et al. 1991). However, the association between IL-6/sIL-6R and ALI was significant, reliably distinguishing patients with mild AP from those with pancreatitis-associated ALI (Figure 3-34 C and D) (von Bismarck, Claass et al. 2008). IL-8, a human ELR+CXC chemokine that activates neutrophils (i.e., like mouse Cxcl1), was also significantly elevated in the plasma of patients with SAP and organ failure (Figure 3-34 E) (Lin, Lin et al. 2010; Malmstrom, Hansen et al. 2011).

Collectively, these data demonstrate the involvement of the IL-6 trans-signaling/Stat3/Cxcl1 cascade in pancreatitis-associated ALI across species.

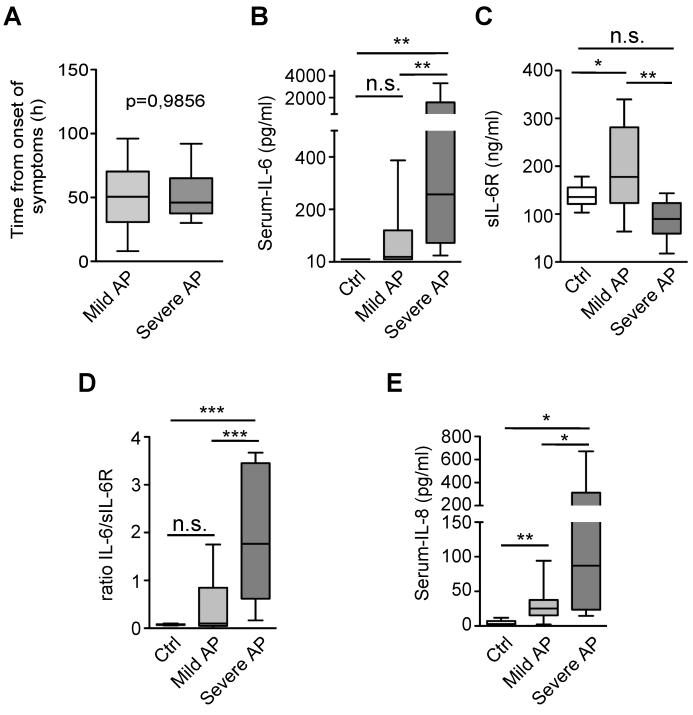

Figure 3-34: Trans-signaling in patients with acute pancreatitis: (A) Analysis of blood in individuals with mild and severe AP after the onset of symptoms. (**B**) and (**C**) Serum IL-6 and sIL-6R levels in control patients and patients with mild AP or SAP. (**D**) Ratio of IL-6/sIL-6R. (**E**) Serum IL-8 levels in control patients and patients with mild AP and SAP. Results represent mean ± SD (n>6), *p< 0,05, **p < 0.005, ***p < 0,001.

4 Discussion

Despite huge efforts and achievements in basic pancreatitis research, therapy of AP is still mostly symptomatic, focusing on pain-relief and intensive care medicine in severe cases (Bone 1991). Therefore, it is of the upmost importance to understand the molecular mechanisms of AP and the associated systemic complications to improve therapy.

The aim of this thesis was to investigate the role of the transcription factors NF-κB and Stat3 during AP. Transcription factors are proteins that control the transcription of genes by binding to their specific promoter or enhancer region. By binding to the DNA sequence transcription factors can either activate or block the expression of these genes.

NF-κB is a ubiquitous expressed pro-inflammatory transcription factor that is responsible for inflammation, embryonic development, tissue injury and repair (Rakonczay, Hegyi et al. 2008). NF-κB been shown to be activated in different animal models of AP, including cerulein-induced pancreatitis, taurocholate-induced pancreatitis and bile-pancreatic duct-ligation-induced pancreatitis, by pro-inflammatory cytokines, cholecystokinin and ROS (Dunn, Li et al. 1997; Meng, Ma et al. 2005; Algul, Treiber et al. 2007). While the role of NF-κB in the pathophysiology of AP has been under intense scrutiny in the past few years, little is known about Stat3. Stat3 is a transcription factor that is activated through phosphorylation by the Janus kinase 2 (Jak2) as well as growth factors receptors and non-receptor tyrosine kinases in response to various cytokines and growth factors. Several studies suggest that IL-6 mediates its effects of inflammation through the activation of the Stat3 pathway (Zhong, Wen et al. 1994; Pfitzner, Kliem et al. 2004). A previous study showed that activation of Stat3 increases pancreatic injury *in vitro* (Robinson, Vona-Davis et al. 2006). In keeping with these findings Chao et al. presented an increase of Stat3 phosphorylation in a severe model of AP that was IL-6-dependent (Chao, Chao et al. 2006).

4.1 The role of transcription factors in the local damage during AP

4.1.1 NF-κB and local damage

It is well established that the IKK/NF-κB/Rel pathway plays a significant role in the initiation of acute pancreatitis (Gukovsky, Gukovskaya et al. 1998; Steinle, Weidenbach et al. 1999; Weber and Adler 2001; Algul, Tando et al. 2002; Hayashi, Ishida et al. 2007). Recently, several animal models with either genetic inactivation or transgenic overexpression of different compartments of the NF-κB signaling pathway were generated to investigate the role of NF-κB in AP (Algul, Treiber et al. 2007; Baumann, Wagner et al. 2007). The results of these studies were at least in part contradictory, showing protective as well as deleterious effects. While several studies showed the degradation of the inhibitor protein IκBα during AP, its role during the disease has not been addressed genetically so far. To approach this issue, a mouse line was generated lacking IκBα in the pancreas as a part of the thesis. Pancreas-specific deletion of IκBα led to nuclear translocation of endogenous RelA. Surprisingly, deletion of IκBα resulted in an inflammatory phenotype characterized by upregulated pro-inflammatory factors and genesets, but no alterations in differentiation and morphology (Schwerdtfeger 2012). As shown for the epidermis, organ-specific deletion of IκBα and constitutive activation of NF-κB are not sufficient to induce local inflammation. Initiation and maintenance of skin inflammation require simultaneous IκBα deficiency in both the epidermal compartment and the immune system (Rebholz, Haase et al. 2007). Similarly, a complex crosstalk between acinar cells and immunocytes is required for inflammatory processes in the pancreas, especially during initiation (Vonlaufen, Apte et al. 2007). This data support this hypothesis and suggest that activation of RelA/p65 in the acinar cells is not sufficient to induce inflammation in the pancreas. In contrast, adenoviral-mediated transfer of RelA/p65 in the pancreas via the main duct induced an inflammatory response and acinar cell damage. However, this strategy might not only target acinar, but probably also

inflammatory cells thus launching inflammation in the organ (Chen, Ji et al. 2002). Similar effects have been observed, when constitutively active IKK2 was strongly overexpressed using the CMV promoter. This promoter, however, is not pancreas-specific, as it also affects other organs, including the thymus (Aleksic, Baumann et al. 2007; Baumann, Wagner et al. 2007).

In accordance with this concept, studies in other organs supported the concept that other pathways need to be activated in addition to NF-κB to obtain destructive inflammation (Guma, Stepniak et al. ; Rakonczay, Hegyi et al. 2008).

Acute experimental pancreatitis in IκBα-deficient mice results in an attenuated form of the disease. The amelioration of acute pancreatitis in mice with acinar cell-restricted deletion of IκBα depends on RelA/p65, since additional deletion of RelA/p65 in *Ikba*$^{\Delta panc}$ mice converts the mild pancreatitis into a severe form. Protective effects of NF-κB during inflammation have been described for other tissues as well. Loss of IKKβ in gastric epithelial cells and the subsequent inactivation of NF-κB, for example increased necrosis after *H. felis* infection, leading to a more severe chronic inflammation (Shibata, Takaishi et al.). The findings of this study are in line with a previous study in which deletion of RelA/p65 increased susceptibility of acinar cells to inflammation-associated cell death (Algul, Treiber et al. 2007). Thus, the IKK/NF-κB/Rel signaling pathway controls a highly regulated balance between pro-inflammatory and protective signaling pathways during inflammation.

4.1.2 NF-κB-dependent protective genes

Genome-wide analysis identified NF-κB/Rel-dependent genes that potentially exert protective effects in the pancreas. Indeed, in unstimulated organs the transcriptome reflected striking differences at baseline. Protective genes were clustered as those being differentially regulated in *Ikba*$^{\Delta panc}$ or *Rela*$^{\Delta panc}$ compared to *Ikba*$^{F/F}$ mice. Microarray analysis revealed several candidate genes that potentially possess protective capacities. Among these genes, the pancreatitis-associated protein 1 (*Pap1*) was identified as clearly differentially

regulated and highly expressed in *Ikba*$^{\Delta panc}$ mice. This was in line with previous results that identified *Pap1* as a NF-κB/Rel-dependent gene possessing anti-inflammatory capacities during pancreatitis (Algul, Treiber et al. 2007; Shigekawa, Hikita et al. 2012). Lentiviral overexpression of Pap1 clearly demonstrated that Pap1 exerts protective effects by reducing necrosis and acinar cell death, therefore attenuating AP (Algul, Treiber et al. 2007). Therefore, high levels of PAP1 in the pancreas of *Ikba*$^{\Delta panc}$ mice, at least partially, exert protective effects during experimental AP.

In addition to *Pap1*, the serine protease inhibitor 2A (*Spi2a*), the homologue of human a1-Antichymotrypsin (*AACT*), is highly upregulated in unstimulated *Ikba*$^{\Delta panc}$ mice. Spi2A is known to inhibit several cathepsins, like cathepsin B, V, L, K and H (Liu, Raja et al. 2003; Liu, Wang et al. 2004). Interestingly, Cathepsin B has been shown to be involved in intrapancreatic trypsinogen activation *in vitro* and *in vivo (Figarella, Miszczuk-Jamska et al. 1988; Halangk, Lerch et al. 2000; Lerch and Halangk 2006)*. In line with these findings, lentiviral expression of Spi2A in C57BL/6 mice lead to an alleviation of acute pancreatitis. This is paralleled by less necrosis and edema as well as a decrease in trypsin activity. Lentiviral-mediated expression of Spi2A led to an attenuation of AP, even in the severe phenotype of RelA deficient mice. A link between NF-κB and serine protease inhibitors is well established in vitro and in vivo (Greten, Arkan et al. 2007). Spi2A was identified as a physiological target of NF-κB/RelA in murine embryonic fibroblasts (Liu, Raja et al. 2003). In this setting, RelA-mediated induction of Spi2A was able to protect murine embryonic fibroblasts from TNFα–induced apoptosis. This was mainly due to abrogated caspase activity through inhibition of cathepsins in lysosomes. Thus, this mechanism by which NF-κB protects cells from lysosome-mediated apoptosis potentially is involved in trypsin activation in the pancreas. Although a recent study showed the impact of trypsin on inflammation and NF-κB activation, these data provide evidence for the reciprocal interaction of NF-κB and trypsin. NF-κB–dependent upregulation of Spi2A influences acinar cell integrity through modulation of trypsin activation rather than regulating inflammatory response only.

Several studies attempted to show a correlation between the NF-κB signaling pathway and trypsin activity in AP. Both NF-κB activation and intrapancreatic trypsinogen activation are early events during AP (Tando, Algul et al. 2002). A previous study however showed that cerulein-induced NF-κB activation and intraacinar trypsiongen activation are independent events in pancreatic acinar cells (Hietaranta, Saluja et al. 2001). In contrast, this study showed that pancreas-specific deletion of IκBα leads to the upregulation of Spi2A, which inhibits trypsin activity possibly through inhibition of cathepsin B. This clearly demonstrates that NF-κB and trypsinogen activation are linked *in vivo*. Collectively, these data reveal for the first time a direct link between trypsin activity and the NF-κB signaling pathway *in vivo*.

Despite the clear evidence for a protective role of Spi2A in AP human mutational analysis remains inconclusive. While mutations in the serine protease inhibitor Kazal 1 (*SPINK1*) in patients are associated with chronic pancreatitis (Witt, Luck et al. 2000), SNP analysis of *AACT*, the human homologue of *Spi2a*, failed to correlate with the severity of acute or chronic pancreatitis (Forsyth, Horvath et al. 2003). A possible explanation for this fact might be that Spi2A is not only expressed in the pancreas but also in other organs like liver, lung, kidney and hematopoetic stem cells. Genetic defects in the coding sequence of Spi2A would therefore not primarily cause susceptibility or resistance to AP but rather systemic disease.

Collectively, these data suggest that pancreas-specific inactivation of IκBα and the subsequent translocation of RelA attenuates AP by upregulation of Spi2A, which prevents the onset of AP by inhibiting trypsin activity.

4.1.3 The role of Stat3 during AP

While the role of NF-κB during AP is under constant debate there is little known about Stat3 in this setting. Stat3 is a transcription factor that is activated by members of the IL-6 and IL-10. It is involved in different inflammatory diseases, like inflammatory bowel disease, intestinal inflammation and lung inflammation (Gao and Ward 2007; Mitsuyama, Matsumoto et al. 2007; Atreya and Neurath

2008). Previous studies in patients with AP showed that IL-6 correlates with the severity of the disease. In addition, analysis of IL-6 knockout mice showed a potential relevance of IL-6 in the pathophysiology of AP, since mice lacking IL-6 showed a more severe form of AP after cerulein injections (Cuzzocrea, Mazzon et al. 2002). By the virtue of phosphorylating Stat3 on Y705, IL-6 confers pro-inflammatory effects locally and systemically as well as leucocyte recruitment. In the pancreas, a number of increased pro-inflammatory cytokines and chemokines were revealed, some of which have been validated by other studies as Stat3 target genes and whose high expression is correlated with severity of AP in mouse models as well as in humans. Indeed, the neutrophile-attractant chemokine Cxcl1 that is involved in monocyte/granulocyte traffic across endo- and eptihelial barriers is highly upregulated during AP (Klein, Wustefeld et al. 2005; Regner, Appelros et al. 2008; Quinton, Blahna et al. 2012). This study suggests that IL-6-induced Stat3 phosphorylation acts as an amplifier for the induction of Cxcl1. The ELR+CXC chemokine Cxcl1 binds to the Cxcr2 receptor to orchestrate extravasation of leukocytes from the vascular system to the site of inflammation. In addition to pro-inflammatory cytokines and chemokines, Stat3 regulates the expression of its own inhibitor, the suppressor of cytokine signaling 3 (Socs3) (Aggarwal, Kunnumakkara et al. 2009).

Although analysis of the downstream target of IL-6, Stat3 showed an increase of Stat3 phosphorylation during severe AP, Stat3 has not been investigated genetically in this setting (Chao, Chao et al. 2006). Pancreas-specific knockout of Stat3 attenuates AP significantly, possibly by increased apoptosis within the acinar cells (unpublished data). Knocking out Socs3, the negative regulator of Stat3, as a proof of principle supported the results obtained in the Stat3 knockout mice. Here, mice displayed an aggravated pancreatic damage compared to floxed littermates, suggesting a pro-inflammatory effect of Stat3 activation within the pancreas.

Evaluation of Stat3 during AP demonstrated that severity of the disease depends on the activation of Stat3 within the pancreas.

4.2 Stat3 and NF-κB cooperate to promote ALI

The causal link between the inflammatory process of severe acute pancreatitis (SAP) and the concomitant evolving lethal ALI has long been recognized in clinical daily routine, the underlying molecular mechanisms however remain unclear so far.

To investigate this connection, a new SAP model was needed. The requirements for the new model were a sterile infection of the pancreas that results in severe inflammatory response syndrome (SIRS) with subsequent damage of distant organs and lethality comparable to the clinical situation. There are several models for AP used in pancreatitis research, with pros and cons for every model (Su, Cuthbertson et al. 2006). Invasive, surgical models like duct ligation and duct injections require technical expertise, are very expensive, do not show clinical and pathological relevance and are infectious and not SIRS based (Su, Cuthbertson et al. 2006; Samuel 2008). Non invasive models include the L-arginine and cerulein-induced pancreatitis (Elder, Saccone et al. 2012). While both models are well established and used for several studies, the mechanism underlying the L-arginine-induced pancreatitis is not clear so far. While lung inflammation could be measured, it is not clear if the pulmonary damage is a result of pancreatic injury or a direct effect of L-arginine toxicity (Kubisch, Sans et al. 2006; Elder, Saccone et al. 2011). The other relevant non-invasive model for experimental pancreatitis is the cerulein-induced pancreatitis model, which is well established and results in pancreatic damage that resembles the clinical situation (Watanabe, Baccino et al. 1984; Algul, Tando et al. 2002). Cerulein injections lead to mild lung injury that resembles early stages of acute respiratory distress syndrome (ARDS). However, the pulmonary damage is not sufficient to allow protein permeability and substantially alter respiratory mechanics (Elder, Saccone et al. 2011). To establish a new model for SAP with concomitant ALI the cerulein model was modified. Instead of 8 hourly injections on one day, mice received 8 hourly injections for five consecutive days. While the pancreas shows first signs of regeneration after 3 days, the pulmonary damage increases as the disease

progresses. The model had mortality rates of 50% that were comparable with the clinical situation in the human disease (Whitcomb 2006). Other systemic complications like sepsis and hypotension could be explained, proposing ALI as the main reason for the lethality.

4.2.1 The IL-6 signaling pathway links local damage to systemic complications via the Stat3 pathway

Using tissue-specific gain- and loss-of-function approaches in this new model of SAP and ALI, this study provides direct genetic and pharmacological evidence that IL-6-trans-signaling and not classical IL-6 signaling, links the inciting event of SAP to the subsequential systemic complication of ALI. Mechanistically, IL-6 forms complexes with the soluble IL-6R (sIL-6R) to activate Stat3 in the pancreas. This amplifyies inflammation by further release of pro-inflammatory factors during SAP. Persistent Stat3 activation confers to high levels of Cxcl1 to mediate infiltration of granulocytes into the lung, thus promoting lethal ALI. This axis seems to be present in individuals with SAP and ALI; evidence that this mechanism exists across species.

While the role of IL-6 in acute pancreatitis has been extensively analyzed, showing that deletion or inhibition of IL-6 leads to more severe pancreatic damage, IL-6-trans-signaling has so far not been addressed in this context (Cuzzocrea, Mazzon et al. 2002; Chao, Chao et al. 2006). This study demonstrates a new role of IL-6 trans-signaling in SAP with concomitant ALI showing that IL-6 is not marely a marker for the severity of AP, but a relevant pathophysiological factor (Leser, Gross et al. 1991; Viedma, Perez-Mateo et al. 1992). IL-6 exerts its effects during SAP and lethal ALI predominantly via IL-6-trans-signaling. This type of activation renders virtually all cells capable of responding to IL-6/sIL-6R complexes, making for a large new spectrum of IL-6 activities (Jones, Richards et al. 2005). In humans, sIL-6R is generated through differential mRNA splicing but primarily through ADAM17-mediated proteolytic cleavage and subsequent shedding of membrane-bound IL-6R, whereas in the mouse, sIL-6R is exclusively generated by proteolysis (Jones, Horiuchi et al. 2001). sIL-6R is found at high concentrations in serum and urine. The formation

of an IL-6/sIL-6R complex protects IL-6 from degradation thus prolonging its half-life in circulation (Peters, Jacobs et al. 1996). Moreover, IL-6 trans-signaling has been shown to regulate processes localized to the site of inflammation. This mode of activation enhances IL-6 responsiveness and drives inflammatory events. In addition to its pro-inflammatory capacities, classical IL-6 signaling coordinates homeostatic properties of IL-6, such as neutropenia, changes in cholesterol, and weight gain (Jones, Scheller et al. 2011). Beyond the phosphorylation of $Stat3^{Y705}$, classical IL-6 signaling and IL-6 trans-signaling are likely involved in distinct and different pathways during inflammation (Scheller, Chalaris et al. 2011). More importantly, IL-6 has been shown to play a crucial anti-inflammatory role in both local and systemic acute inflammatory responses by controlling the level of pro-inflammatory but not anti-inflammatory cytokines. Moreover, the strong phosphorylation of serine residue 727 on Stat3 and the phosphorylation of RelA in the pancreatic tissue were observed in IL-6 deficient mice; this phosphorylation was not detectable in control or transgenic opt_*sgp130Fc* mice. These transgenic mice overexpress the fusion protein sgp130Fc that leads to a blockage of IL-6 trans-signaling without affecting classical IL-6 signaling. The phosphorylation of $Stat3^{S727}$, for example, was found to be localized in the mitochondria for the optimal function of the electron transport chain (Szczepanek, Lesnefsky et al. 2012). In fact, IL-6 has pleiotropic effects being not only involved in inflammation and infection responses but also in the regulation of metabolic, regenerative, and neural processes. While the pro-inflammatory effects are mediated by IL-6 trans-signaling, other functions of IL-6 such as metabolic control in the liver and regeneration of the epithelium in the intestine seem to be facilitated via the membrane-bound IL-6 receptor (Jones, Scheller et al. 2011). These data suggest that unlike blocking IL-6 trans-signaling, the genetic inhibition of classical IL-6 signaling likely eliminates protective mechanisms during inflammation. Such effects might also be of relevance in the pancreas. These observations might account for the differences in pancreatic damage observed in *Il6*$^{-/-}$ and opt_*sgp130Fc* mice.

4.2.2 Myeloid cells produce IL-6 in a NF-κB-dependent manner

Furthermore, IL-6 deficient mice revealed an increase in NF-κB activation. IHC showed that in addition to acinar cells, myeloid cells displayed a strong activation of the NF-κB pathway. Besides NF-κB activation, myeloid cells turned out to be the cellular source of local and systemic IL-6 during AP, suggesting that IL-6 is produced in a NF-κB-dependent manner. These data are in line with a previously published study that showed that CD11b positive cells display an enhanced secretion of pro-inflammatory cytokines (e.g. IL-6 and CCL3) in patients with urothelial and renal carcinomas (Eruslanov, Stoffs et al. 2013). Another study showed that NF-κB-dependent production of IL-6 by Kupffer cells is required for DEN-induced hepatocellular carcinoma (Naugler, Sakurai et al. 2007).

Correlation of IL-6/sIL-6R trans-signaling driven Stat3 phosphorylation in the injured pancreas with the extent of ALI observed here suggest a novel role for Stat3. Whereas deletion studies in mice confirm that activation of Stat3 in the acinar cells leads to lethal ALI during SAP, the protective role of Stat3 in the lung has been demonstrated across multiple models of acute pulmonary inflammation and injury (Hokuto, Ikegami et al. 2004). Activation of Stat3 in epithelial cells of the lung has been demonstrated to exert cytoprotective roles when exposed to various noxious and infectious agents (Meng, Dyer et al. 2001; Ikegami, Falcone et al. 2008). However, IL-6 trans-signaling-dependent Stat3 activation at the site of distant inflammation (e.g. acinar cells) is likely to promote pulmonary damage during SAP (Gao, Guo et al. 2004; Tang, Yan et al. 2011). Whether the circulating IL-6/sIL-6R complex is sufficient to mediate all these effects or whether it requires additional local release of IL-6 and sIL-6R from activated neutrophils remains to be determined (Chalaris, Rabe et al. 2007).

4.3 Therapeutic strategies and diagnosis

In patients with SAP and concomitant ALI, high levels of IL-6 were observed, while levels of sIL-6R were significantly decreased compared to individuals with

mild AP or controls. This potentially reflects the complexation of IL-6 with the soluble receptor providing evidence for IL-6 trans-signaling even in the human disease. It was further demonstrated that the ratio of IL-6/sIL-6R in the serum is useful to distinguish patients with a mild pancreatitis from patients with SAP and subsequent ALI. Interestingly, in analysis of bronchoalveolar lavage fluid from patients with acute lung injury sIL-6R and IL-6 levels were also shown to be elevated (Park, Goodman et al. 2001). In addition, IL-8, a member of the CXC chemokine family, a neutrophile attractant that is similar to murine Cxcl1, was increased in patients with SAP. These data were in line with the results obtained in the murine SAP model suggesting an across species phenomenon.

Previous studies revealed the therapeutic potential of the IL-6-trans-signaling/Stat3/Cxcl1 cascade in other diseases. The monoclonal anti-IL-6R antibody Tocilizumab was shown to decrease disease severity in patients with rheumatoid arthritis (Choy, Isenberg et al. 2002). While Tocilizumab blocks both, the anti-inflammatory and pro-inflammatory activities of IL-6, sgp130Fc binds only to IL-6 molecules that are bound by the sIL-6R, thus blocking IL-6 trans-signaling without affecting classical signaling. First clinical trials investigating sgp130Fc will start in the beginning of 2013 (Rose-John 2012).

Several strategies were used to evaluate the therapeutic potential of the IL-6-trans-signaling/Stat3/Cxcl1 cascade in the murine model of SAP-associated ALI. The inhibition of Cxcl1 or the Cxcr2 receptor, by anti-Cxcl1 antibody or by the Cxcr2 antagonist SB225002, was sufficient to prevent death independent from the local damage in the pancreas. Moreover, specific blocking of IL-6 trans-signaling by sgp130FC injections during SAP as well as inhibiting Stat3 signaling with S3I-201 improved survival. Here, the pivotal role of the Stat3-dependent Cxcl1/Cxcr2 axis in linking pancreatic damage to ALI was demonstrated. Interestingly, this concept seems to be relevant even in other settings of ALI (Konrad and Reutershan 2012).

The IL-6-trans-signaling/Stat3/Cxcl1 cascade does not only define a specific and promising target that links local to systemic inflammation, its activation opens a therapeutic window, especially in patients with an ongoing SAP and ALI. Whether the circulating IL-6/sIL-6R complex is sufficient to mediate these

effects or requires additional local release of IL-6 and sIL-6R from activated neutrophils remains to be determined (Chalaris, Rabe et al. 2007). With the development of Stat3 inhibitors, specific IL-6/IL-6R antibodies and soluble recombinant gp130 proteins at hand, it is reasonable to test such substances in patients with SAP and ALI (Siddiquee, Zhang et al. 2007).

4.4 Conclusions

These data increases our understanding of the role of the transcription factors NF-κB and Stat3 during AP.

Constitutive activation of NF-κB in the pancreas attenuates pancreatitis, possibly through upregulation of NF-κB-dependent protective genes. Among those genes *Pap1* and *Spi2a* seem to play a key role in ameliorating the disease. While *Pap1* has been identified in previous studies, *Spi2a* is as a new promising target gene that might decrease trypsin activity through inhibition of cathepsin B. However, SNP analysis of *AACT*, the human homologue of *Spi2a*, in patients with AP and CP failed to reveal any correlation between single mutations and disease severity.

Activation of Stat3 via IL-6 trans-signaling in the pancreas seem to link the local damage of AP to distantly mediated ALI. This effect is supported by the release of IL-6 by infiltrating macrophages in a NF-κB-dependent manner. Furthermore, inhibiting IL-6 trans-signaling and its downstream effector Stat3 during lethal SAP is a specific and promising target that links local inflammation in the pancreas to respiratory failure. In this study, the significance of the IL-6-trans-signaling/Stat3 pathway was demonstrated in pancreatitis-associated ALI across species and suggests a mechanism of how distant organ damage is linked to lethal ALI (Figure 4-1) (Matthay and Zemans 2011).

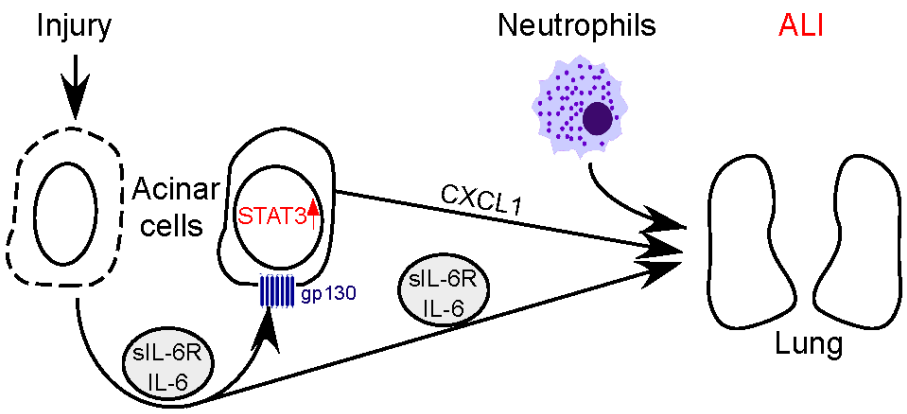

Figure 4-1: Scheme of the central role of IL-6 trans-signaling during SAP-associated ALI.

5 Summary

The focus of this thesis was the investigation of molecular mechanisms of acute pancreatitis (AP) in different mouse models. While several studies investigated transcription factors in AP, the function of NF-κB and Stat3 need to be addressed more closely. The first project of this thesis was to evaluate the role of IκBα during AP. Preliminary data of pancreas-specific IκBα knockout mice showed constitutive activation of RelA; severity of AP in these mice was attenuated with reduced trypsin activity. Microarray analysis in pancreas-specific RelA and IκBα knockout mice helped to identify NF-κB-dependent genes that might have a protective effect during AP. One of the genes found in theses analysis was the serine protease inhibitor 2A (Spi2A). SNP analysis of *alpha-1-antichymotrypsin*, the human homologue of *Spi2a*, however, did not show any correlation with disease severity.

The second project of this thesis was the evaluation of the role of IL-6 during AP. It is well established that IL-6 levels in patients correlate with disease severity. Whether IL-6 is only a marker or has pathophysiological relevance is not known. To investigate the role of IL-6 in pancreatitis-associated lung injury, a new model for severe acute pancreatitis (SAP) was established. The data from this model showed that serum IL-6 level correlate with lethality. Additional experiments indicated that IL-6 trans-signaling and not classical IL-6 signaling is necessary to link the local pancreatic damage to the systemic complications of acute lung injury (ALI). Pancreas-specific inactivation of Stat3 or Socs3 revealed the involvement of the IL-6-trans-signaling/gp130/Stat3 signaling cascade in this model. Pharmacological inhibition experiments emphasize the importance of this signaling cascade as a possible target for therapy. Serum analyses of patients with mild or severe pancreatitis did support the results obtained from the mouse studies.

6 References

Aggarwal, B. B., A. B. Kunnumakkara, et al. (2009). "Signal transducer and activator of transcription-3, inflammation, and cancer: how intimate is the relationship?" Ann N Y Acad Sci **1171**: 59-76.

Aho, H. J., S. M. Koskensalo, et al. (1980). "Experimental pancreatitis in the rat. Sodium taurocholate-induced acute haemorrhagic pancreatitis." Scand J Gastroenterol **15**(4): 411-416.

Ahuja, N., A. Andres-Hernando, et al. (2012). "Circulating IL-6 mediates lung injury via CXCL1 production after acute kidney injury in mice." Am J Physiol Renal Physiol **303**(6): F864-872.

Aleksic, T., B. Baumann, et al. (2007). "Cellular immune reaction in the pancreas is induced by constitutively active IkappaB kinase-2." Gut **56**(2): 227-236.

Algul, H., Y. Tando, et al. (2002). "Acute experimental pancreatitis and NF-kappaB/Rel activation." Pancreatology **2**(6): 503-509.

Algul, H., M. Treiber, et al. (2007). "Pancreas-specific RelA/p65 truncation increases susceptibility of acini to inflammation-associated cell death following cerulein pancreatitis." J Clin Invest **117**(6): 1490-1501.

Ammann, R. W., H. Buehler, et al. (1987). "Differences in the natural history of idiopathic (nonalcoholic) and alcoholic chronic pancreatitis. A comparative long-term study of 287 patients." Pancreas **2**(4): 368-377.

Antonarakis, S. E. (1998). "Recommendations for a nomenclature system for human gene mutations. Nomenclature Working Group." Hum Mutat **11**(1): 1-3.

Apte, M. V. and J. S. Wilson (2004). "Mechanisms of pancreatic fibrosis." Dig Dis **22**(3): 273-279.

Atreya, R., J. Mudter, et al. (2000). "Blockade of interleukin 6 trans signaling suppresses T-cell resistance against apoptosis in chronic intestinal inflammation: evidence in crohn disease and experimental colitis in vivo." Nat Med **6**(5): 583-588.

Atreya, R. and M. F. Neurath (2008). "Signaling molecules: the pathogenic role of the IL-6/STAT-3 trans signaling pathway in intestinal inflammation and in colonic cancer." Curr Drug Targets **9**(5): 369-374.

Awla, D., A. Abdulla, et al. (2011). "TLR4 but not TLR2 regulates inflammation and tissue damage in acute pancreatitis induced by retrograde infusion of taurocholate." Inflamm Res **60**(12): 1093-1098.

Baron, T. H. and D. E. Morgan (1999). "Acute necrotizing pancreatitis." N Engl J Med **340**(18): 1412-1417.

Baumann, B., M. Wagner, et al. (2007). "Constitutive IKK2 activation in acinar cells is sufficient to induce pancreatitis in vivo." J Clin Invest **117**(6): 1502-1513.

Baxter, J. N., S. A. Jenkins, et al. (1985). "Effects of somatostatin and a long-acting somatostatin analogue on the prevention and treatment of experimentally induced acute pancreatitis in the rat." Br J Surg **72**(5): 382-385.

Bollrath, J. and F. R. Greten (2009). "IKK/NF-kappaB and STAT3 pathways: central signalling hubs in inflammation-mediated tumour promotion and metastasis." EMBO Rep **10**(12): 1314-1319.

Bone, R. C. (1991). "Sepsis, the sepsis syndrome, multi-organ failure: a plea for comparable definitions." Ann Intern Med **114**(4): 332-333.

Bradley, E. L., 3rd (1993). "A clinically based classification system for acute pancreatitis. Summary of the International Symposium on Acute Pancreatitis, Atlanta, Ga, September 11 through 13, 1992." Arch Surg **128**(5): 586-590.

Chalaris, A., J. Gewiese, et al. (2010). "ADAM17-mediated shedding of the IL6R induces cleavage of the membrane stub by gamma-secretase." Biochim Biophys Acta **1803**(2): 234-245.

Chalaris, A., B. Rabe, et al. (2007). "Apoptosis is a natural stimulus of IL6R shedding and contributes to the proinflammatory trans-signaling function of neutrophils." Blood **110**(6): 1748-1755.

Chao, K. C., K. F. Chao, et al. (2006). "Blockade of interleukin 6 accelerates acinar cell apoptosis and attenuates experimental acute pancreatitis in vivo." Br J Surg **93**(3): 332-338.

Chen, C. C., S. S. Wang, et al. (1999). "Serum interleukin 10 and interleukin 11 in patients with acute pancreatitis." Gut **45**(6): 895-899.

Chen, X., B. Ji, et al. (2002). "NF-kappaB activation in pancreas induces pancreatic and systemic inflammatory response." Gastroenterology **122**(2): 448-457.

Chiari, H. (1896). "Über Selbstverdauung des menschlichen Pankreas." Zeitschrift für Heilkunde **17**: 69-96.

Choy, E. H., D. A. Isenberg, et al. (2002). "Therapeutic benefit of blocking interleukin-6 activity with an anti-interleukin-6 receptor monoclonal antibody in rheumatoid arthritis: a randomized, double-blind, placebo-controlled, dose-escalation trial." Arthritis Rheum **46**(12): 3143-3150.

Cuzzocrea, S., E. Mazzon, et al. (2002). "Absence of endogenous interleukin-6 enhances the inflammatory response during acute pancreatitis induced by cerulein in mice." Cytokine **18**(5): 274-285.

Dann, S. M., M. E. Spehlmann, et al. (2008). "IL-6-dependent mucosal protection prevents establishment of a microbial niche for attaching/effacing lesion-forming enteric bacterial pathogens." J Immunol **180**(10): 6816-6826.

Darnell, J. E., Jr., I. M. Kerr, et al. (1994). "Jak-STAT pathways and transcriptional activation in response to IFNs and other extracellular signaling proteins." Science **264**(5164): 1415-1421.

Dawra, R., R. Sharif, et al. (2007). "Development of a new mouse model of acute pancreatitis induced by administration of L-arginine." Am J Physiol Gastrointest Liver Physiol **292**(4): G1009-1018.

Dunn, J. A., C. Li, et al. (1997). "Therapeutic modification of nuclear factor kappa B binding activity and tumor necrosis factor-alpha gene expression during acute biliary pancreatitis." Am Surg **63**(12): 1036-1043; discussion 1043-1034.

Durbec, J. P. and H. Sarles (1978). "Multicenter survey of the etiology of pancreatic diseases. Relationship between the relative risk of developing

chronic pancreaitis and alcohol, protein and lipid consumption." Digestion **18**(5-6): 337-350.
Elder, A. S., G. T. Saccone, et al. (2011). "Caerulein-induced acute pancreatitis results in mild lung inflammation and altered respiratory mechanics." Exp Lung Res **37**(2): 69-77.
Elder, A. S., G. T. Saccone, et al. (2011). "L-Arginine-induced acute pancreatitis results in mild lung inflammation without altered respiratory mechanics." Exp Lung Res **37**(1): 1-9.
Elder, A. S., G. T. Saccone, et al. (2012). "Lung injury in acute pancreatitis: mechanisms underlying augmented secondary injury." Pancreatology **12**(1): 49-56.
Eruslanov, E., T. Stoffs, et al. (2013). "Expansion of CCR8+ Inflammatory Myeloid Cells in Cancer Patients with Urothelial and Renal Carcinomas." Clin Cancer Res **19**(7): 1670-1680.
Figarella, C., B. Miszczuk-Jamska, et al. (1988). "Possible lysosomal activation of pancreatic zymogens. Activation of both human trypsinogens by cathepsin B and spontaneous acid. Activation of human trypsinogen 1." Biol Chem Hoppe Seyler **369 Suppl**: 293-298.
Fischer, M., J. Goldschmitt, et al. (1997). "I. A bioactive designer cytokine for human hematopoietic progenitor cell expansion." Nat Biotechnol **15**(2): 142-145.
Forsyth, S., A. Horvath, et al. (2003). "A review and comparison of the murine alpha1-antitrypsin and alpha1-antichymotrypsin multigene clusters with the human clade A serpins." Genomics **81**(3): 336-345.
Frossard, J. L., M. L. Steer, et al. (2008). "Acute pancreatitis." Lancet **371**(9607): 143-152.
Gao, H., R. F. Guo, et al. (2004). "Stat3 activation in acute lung injury." J Immunol **172**(12): 7703-7712.
Gao, H. and P. A. Ward (2007). "STAT3 and suppressor of cytokine signaling 3: potential targets in lung inflammatory responses." Expert Opin Ther Targets **11**(7): 869-880.
Greten, F. R., M. C. Arkan, et al. (2007). "NF-kappaB is a negative regulator of IL-1beta secretion as revealed by genetic and pharmacological inhibition of IKKbeta." Cell **130**(5): 918-931.
Grivennikov, S., E. Karin, et al. (2009). "IL-6 and Stat3 are required for survival of intestinal epithelial cells and development of colitis-associated cancer." Cancer Cell **15**(2): 103-113.
Guice, K. S., K. T. Oldham, et al. (1988). "Pancreatitis-induced acute lung injury. An ARDS model." Ann Surg **208**(1): 71-77.
Gukovsky, I., A. S. Gukovskaya, et al. (1998). "Early NF-kappaB activation is associated with hormone-induced pancreatitis." Am J Physiol **275**(6 Pt 1): G1402-1414.
Guma, M., D. Stepniak, et al. "Constitutive intestinal NF-kappaB does not trigger destructive inflammation unless accompanied by MAPK activation." J Exp Med **208**(9): 1889-1900.
Halangk, W. and M. M. Lerch (2004). "Early events in acute pancreatitis." Gastroenterol Clin North Am **33**(4): 717-731.

Halangk, W., M. M. Lerch, et al. (2000). "Role of cathepsin B in intracellular trypsinogen activation and the onset of acute pancreatitis." J Clin Invest **106**(6): 773-781.
Hayashi, T., Y. Ishida, et al. (2007). "IFN-gamma protects cerulein-induced acute pancreatitis by repressing NF-kappa B activation." J Immunol **178**(11): 7385-7394.
Heinrich, P. C., I. Behrmann, et al. (2003). "Principles of interleukin (IL)-6-type cytokine signalling and its regulation." Biochem J **374**(Pt 1): 1-20.
Hietaranta, A. J., A. K. Saluja, et al. (2001). "Relationship between NF-kappaB and trypsinogen activation in rat pancreas after supramaximal caerulein stimulation." Biochem Biophys Res Commun **280**(1): 388-395.
Hokuto, I., M. Ikegami, et al. (2004). "Stat-3 is required for pulmonary homeostasis during hyperoxia." J Clin Invest **113**(1): 28-37.
Hoth, J. J., J. D. Wells, et al. (2011). "Mechanism of neutrophil recruitment to the lung after pulmonary contusion." Shock **35**(6): 604-609.
Huang, L., M. H. Wang, et al. (2012). "Effects of Chai-Qin-Cheng-Qi decoction () on acute pancreatitis-associated lung injury in mice with acute necrotizing pancreatitis." Chin J Integr Med.
Ikegami, M., A. Falcone, et al. (2008). "STAT-3 regulates surfactant phospholipid homeostasis in normal lung and during endotoxin-mediated lung injury." J Appl Physiol **104**(6): 1753-1760.
Inagaki, T., M. Hoshino, et al. (1997). "Interleukin-6 is a useful marker for early prediction of the severity of acute pancreatitis." Pancreas **14**(1): 1-8.
Jones, S. A., S. Horiuchi, et al. (2001). "The soluble interleukin 6 receptor: mechanisms of production and implications in disease." FASEB J **15**(1): 43-58.
Jones, S. A., P. J. Richards, et al. (2005). "IL-6 transsignaling: the in vivo consequences." J Interferon Cytokine Res **25**(5): 241-253.
Jones, S. A., J. Scheller, et al. (2011). "Therapeutic strategies for the clinical blockade of IL-6/gp130 signaling." J Clin Invest **121**(9): 3375-3383.
Jostock, T., J. Mullberg, et al. (2001). "Soluble gp130 is the natural inhibitor of soluble interleukin-6 receptor transsignaling responses." Eur J Biochem **268**(1): 160-167.
Karin, M. (2008). "The IkappaB kinase - a bridge between inflammation and cancer." Cell Res **18**(3): 334-342.
Klein, C., T. Wustefeld, et al. (2005). "The IL-6-gp130-STAT3 pathway in hepatocytes triggers liver protection in T cell-mediated liver injury." J Clin Invest **115**(4): 860-869.
Konrad, F. M. and J. Reutershan (2012). "CXCR2 in acute lung injury." Mediators Inflamm **2012**: 740987.
Kopf, M., H. Baumann, et al. (1994). "Impaired immune and acute-phase responses in interleukin-6-deficient mice." Nature **368**(6469): 339-342.
Krebs, D. L. and D. J. Hilton (2001). "SOCS proteins: negative regulators of cytokine signaling." Stem Cells **19**(5): 378-387.
Kubisch, C. H., M. D. Sans, et al. (2006). "Early activation of endoplasmic reticulum stress is associated with arginine-induced acute pancreatitis." Am J Physiol Gastrointest Liver Physiol **291**(2): G238-245.

Lampel, M. and H. F. Kern (1977). "Acute interstitial pancreatitis in the rat induced by excessive doses of a pancreatic secretagogue." Virchows Arch A Pathol Anat Histol **373**(2): 97-117.
Lerch, M. M. and W. Halangk (2006). "Human pancreatitis and the role of cathepsin B." Gut **55**(9): 1228-1230.
Leser, H. G., V. Gross, et al. (1991). "Elevation of serum interleukin-6 concentration precedes acute-phase response and reflects severity in acute pancreatitis." Gastroenterology **101**(3): 782-785.
Levy, D. and J. E. Darnell, Jr. (1990). "Interferon-dependent transcriptional activation: signal transduction without second messenger involvement?" New Biol **2**(10): 923-928.
Lin, W. C., C. F. Lin, et al. (2010). "Prediction of outcome in patients with acute respiratory distress syndrome by bronchoalveolar lavage inflammatory mediators." Exp Biol Med (Maywood) **235**(1): 57-65.
Liu, N., S. M. Raja, et al. (2003). "NF-kappaB protects from the lysosomal pathway of cell death." Embo J **22**(19): 5313-5322.
Liu, N., Y. Wang, et al. (2004). "Serine protease inhibitor 2A inhibits caspase-independent cell death." FEBS Lett **569**(1-3): 49-53.
Lust, J. A., K. A. Donovan, et al. (1992). "Isolation of an mRNA encoding a soluble form of the human interleukin-6 receptor." Cytokine **4**(2): 96-100.
Madrid, L. V., C. Y. Wang, et al. (2000). "Akt suppresses apoptosis by stimulating the transactivation potential of the RelA/p65 subunit of NF-kappaB." Mol Cell Biol **20**(5): 1626-1638.
Malmstrom, M. L., M. B. Hansen, et al. (2011). "Cytokines and Organ Failure in Acute Pancreatitis: Inflammatory Response in Acute Pancreatitis." Pancreas.
Matsumoto, S., T. Hara, et al. (2010). "Essential roles of IL-6 trans-signaling in colonic epithelial cells, induced by the IL-6/soluble-IL-6 receptor derived from lamina propria macrophages, on the development of colitis-associated premalignant cancer in a murine model." J Immunol **184**(3): 1543-1551.
Matthay, M. A. and R. L. Zemans (2011). "The acute respiratory distress syndrome: pathogenesis and treatment." Annu Rev Pathol **6**: 147-163.
Matthews, V., B. Schuster, et al. (2003). "Cellular cholesterol depletion triggers shedding of the human interleukin-6 receptor by ADAM10 and ADAM17 (TACE)." J Biol Chem **278**(40): 38829-38839.
McFarland-Mancini, M. M., H. M. Funk, et al. (2010). "Differences in wound healing in mice with deficiency of IL-6 versus IL-6 receptor." J Immunol **184**(12): 7219-7228.
Meng, Y., Q. Y. Ma, et al. (2005). "Effect of resveratrol on activation of nuclear factor kappa-B and inflammatory factors in rat model of acute pancreatitis." World J Gastroenterol **11**(4): 525-528.
Meng, Z. H., K. Dyer, et al. (2001). "Essential role for IL-6 in postresuscitation inflammation in hemorrhagic shock." Am J Physiol Cell Physiol **280**(2): C343-351.
Mitsuyama, K., S. Matsumoto, et al. (2007). "Therapeutic strategies for targeting the IL-6/STAT3 cytokine signaling pathway in inflammatory bowel disease." Anticancer Res **27**(6A): 3749-3756.

Mullberg, J., E. Dittrich, et al. (1993). "Differential shedding of the two subunits of the interleukin-6 receptor." FEBS Lett **332**(1-2): 174-178.
Mullberg, J., H. Schooltink, et al. (1993). "The soluble interleukin-6 receptor is generated by shedding." Eur J Immunol **23**(2): 473-480.
Mullhaupt, B., K. Truninger, et al. (2005). "Impact of etiology on the painful early stage of chronic pancreatitis: a long-term prospective study." Z Gastroenterol **43**(12): 1293-1301.
Nakhai, H., S. Sel, et al. (2007). "Ptf1a is essential for the differentiation of GABAergic and glycinergic amacrine cells and horizontal cells in the mouse retina." Development **134**(6): 1151-1160.
Naugler, W. E., T. Sakurai, et al. (2007). "Gender disparity in liver cancer due to sex differences in MyD88-dependent IL-6 production." Science **317**(5834): 121-124.
Niederau, C., L. D. Ferrell, et al. (1985). "Caerulein-induced acute necrotizing pancreatitis in mice: protective effects of proglumide, benzotript, and secretin." Gastroenterology **88**(5 Pt 1): 1192-1204.
Nowell, M. A., P. J. Richards, et al. (2003). "Soluble IL-6 receptor governs IL-6 activity in experimental arthritis: blockade of arthritis severity by soluble glycoprotein 130." J Immunol **171**(6): 3202-3209.
Nowell, M. A., A. S. Williams, et al. (2009). "Therapeutic targeting of IL-6 trans signaling counteracts STAT3 control of experimental inflammatory arthritis." J Immunol **182**(1): 613-622.
Paajanen, H., M. Laato, et al. (1995). "Serum tumour necrosis factor compared with C-reactive protein in the early assessment of severity of acute pancreatitis." Br J Surg **82**(2): 271-273.
Pandol, S. J., A. K. Saluja, et al. (2007). "Acute pancreatitis: bench to the bedside." Gastroenterology **132**(3): 1127-1151.
Paonessa, G., R. Graziani, et al. (1995). "Two distinct and independent sites on IL-6 trigger gp 130 dimer formation and signalling." Embo J **14**(9): 1942-1951.
Park, W. Y., R. B. Goodman, et al. (2001). "Cytokine balance in the lungs of patients with acute respiratory distress syndrome." Am J Respir Crit Care Med **164**(10 Pt 1): 1896-1903.
Peters, M., S. Jacobs, et al. (1996). "The function of the soluble interleukin 6 (IL-6) receptor in vivo: sensitization of human soluble IL-6 receptor transgenic mice towards IL-6 and prolongation of the plasma half-life of IL-6." J Exp Med **183**(4): 1399-1406.
Pfitzner, E., S. Kliem, et al. (2004). "The role of STATs in inflammation and inflammatory diseases." Curr Pharm Des **10**(23): 2839-2850.
Quinton, L. J., M. T. Blahna, et al. (2012). "Hepatocyte-specific mutation of both NF-kappaB RelA and STAT3 abrogates the acute phase response in mice." J Clin Invest **122**(5): 1758-1763.
Rabe, B., A. Chalaris, et al. (2008). "Transgenic blockade of interleukin 6 transsignaling abrogates inflammation." Blood **111**(3): 1021-1028.
Rakonczay, Z., Jr., P. Hegyi, et al. (2008). "The role of NF-kappaB activation in the pathogenesis of acute pancreatitis." Gut **57**(2): 259-267.

Rebholz, B., I. Haase, et al. (2007). "Crosstalk between keratinocytes and adaptive immune cells in an IkappaBalpha protein-mediated inflammatory disease of the skin." Immunity **27**(2): 296-307.
Regner, S., S. Appelros, et al. (2008). "Monocyte chemoattractant protein 1, active carboxypeptidase B and CAPAP at hospital admission are predictive markers for severe acute pancreatitis." Pancreatology **8**(1): 42-49.
Renner, I. G. and J. R. Wisner, Jr. (1986). "Ceruletide-induced acute pancreatitis in the dog and its amelioration by exogenous secretin." Int J Pancreatol **1**(1): 39-49.
Rinderknecht, H. (1986). "Activation of pancreatic zymogens. Normal activation, premature intrapancreatic activation, protective mechanisms against inappropriate activation." Dig Dis Sci **31**(3): 314-321.
Robinson, K., L. Vona-Davis, et al. (2006). "Peptide YY attenuates STAT1 and STAT3 activation induced by TNF-alpha in acinar cell line AR42J." J Am Coll Surg **202**(5): 788-796.
Rose-John, S. (2012). "IL-6 trans-signaling via the soluble IL-6 receptor: importance for the pro-inflammatory activities of IL-6." Int J Biol Sci **8**(9): 1237-1247.
Rosendahl, J., H. Witt, et al. (2008). "Chymotrypsin C (CTRC) variants that diminish activity or secretion are associated with chronic pancreatitis." Nat Genet **40**(1): 78-82.
Rupec, R. A., F. Jundt, et al. (2005). "Stroma-mediated dysregulation of myelopoiesis in mice lacking I kappa B alpha." Immunity **22**(4): 479-491.
Samuel, I. (2008). "Bile and pancreatic juice exclusion activates acinar stress kinases and exacerbates gallstone pancreatitis." Surgery **143**(3): 434-440.
Sander, L. E., S. D. Sackett, et al. (2010). "Hepatic acute-phase proteins control innate immune responses during infection by promoting myeloid-derived suppressor cell function." J Exp Med **207**(7): 1453-1464.
Sathyanarayan, G., P. K. Garg, et al. (2007). "Elevated level of interleukin-6 predicts organ failure and severe disease in patients with acute pancreatitis." J Gastroenterol Hepatol **22**(4): 550-554.
Scheller, J., A. Chalaris, et al. (2011). "The pro- and anti-inflammatory properties of the cytokine interleukin-6." Biochim Biophys Acta **1813**(5): 878-888.
Schwerdtfeger, C. (2012). Pankreas-spezifische Deletion von IkBa – Implikationen für Pankreasentwicklung und Ausprägung des Schweregrades einer akuten experimentellen Pankreatitis. Dr. med. Dissertation, TU München.
Shi, C., X. Zhao, et al. (2005). "Role of nuclear factor-kappaB, reactive oxygen species and cellular signaling in the early phase of acute pancreatitis." Scand J Gastroenterol **40**(1): 103-108.
Shibata, W., S. Takaishi, et al. "Conditional deletion of IkappaB-kinase-beta accelerates helicobacter-dependent gastric apoptosis, proliferation, and preneoplasia." Gastroenterology **138**(3): 1022-1034 e1021-1010.

Shigekawa, M., H. Hikita, et al. (2012). "Pancreatic STAT3 Protects Mice against Caerulein-Induced Pancreatitis via PAP1 Induction." Am J Pathol **181**(6): 2105-2113.
Siddiquee, K., S. Zhang, et al. (2007). "Selective chemical probe inhibitor of Stat3, identified through structure-based virtual screening, induces antitumor activity." Proc Natl Acad Sci U S A **104**(18): 7391-7396.
Steer, M. L. and J. Meldolesi (1987). "The cell biology of experimental pancreatitis." N Engl J Med **316**(3): 144-150.
Steinle, A. U., H. Weidenbach, et al. (1999). "NF-kappaB/Rel activation in cerulein pancreatitis." Gastroenterology **116**(2): 420-430.
Su, K. H., C. Cuthbertson, et al. (2006). "Review of experimental animal models of acute pancreatitis." HPB (Oxford) **8**(4): 264-286.
Sun, R., B. Jaruga, et al. (2005). "IL-6 modulates hepatocyte proliferation via induction of HGF/p21cip1: regulation by SOCS3." Biochem Biophys Res Commun **338**(4): 1943-1949.
Szczepanek, K., E. J. Lesnefsky, et al. (2012). "Multi-tasking: nuclear transcription factors with novel roles in the mitochondria." Trends Cell Biol **22**(8): 429-437.
Szmola, R. and M. Sahin-Toth (2007). "Chymotrypsin C (caldecrin) promotes degradation of human cationic trypsin: identity with Rinderknecht's enzyme Y." Proc Natl Acad Sci U S A **104**(27): 11227-11232.
Taga, T. and T. Kishimoto (1997). "Gp130 and the interleukin-6 family of cytokines." Annu Rev Immunol **15**: 797-819.
Takeda, K., T. Kaisho, et al. (1998). "Stat3 activation is responsible for IL-6-dependent T cell proliferation through preventing apoptosis: generation and characterization of T cell-specific Stat3-deficient mice." J Immunol **161**(9): 4652-4660.
Takeda, K., K. Noguchi, et al. (1997). "Targeted disruption of the mouse Stat3 gene leads to early embryonic lethality." Proc Natl Acad Sci U S A **94**(8): 3801-3804.
Tanaka, M., M. Kishimura, et al. (2000). "Cloning of novel soluble gp130 and detection of its neutralizing autoantibodies in rheumatoid arthritis." J Clin Invest **106**(1): 137-144.
Tando, Y., H. Algul, et al. (2002). "Induction of IkappaB-kinase by cholecystokinin is mediated by trypsinogen activation in rat pancreatic lobules." Digestion **66**(4): 237-245.
Tang, H., C. Yan, et al. (2011). "An essential role for Stat3 in regulating IgG immune complex-induced pulmonary inflammation." FASEB J **25**(12): 4292-4300.
Teich, N., J. Rosendahl, et al. (2006). "Mutations of human cationic trypsinogen (PRSS1) and chronic pancreatitis." Hum Mutat **27**(8): 721-730.
Traenckner, E. B., H. L. Pahl, et al. (1995). "Phosphorylation of human I kappa B-alpha on serines 32 and 36 controls I kappa B-alpha proteolysis and NF-kappa B activation in response to diverse stimuli." Embo J **14**(12): 2876-2883.
Viedma, J. A., M. Perez-Mateo, et al. (1992). "Role of interleukin-6 in acute pancreatitis. Comparison with C-reactive protein and phospholipase A." Gut **33**(9): 1264-1267.

von Bismarck, P., A. Claass, et al. (2008). "Altered pulmonary interleukin-6 signaling in preterm infants developing bronchopulmonary dysplasia." Exp Lung Res **34**(10): 694-706.
Vonlaufen, A., M. V. Apte, et al. (2007). "The role of inflammatory and parenchymal cells in acute pancreatitis." J Pathol **213**(3): 239-248.
Watanabe, O., F. M. Baccino, et al. (1984). "Supramaximal caerulein stimulation and ultrastructure of rat pancreatic acinar cell: early morphological changes during development of experimental pancreatitis." Am J Physiol **246**(4 Pt 1): G457-467.
Weber, C. K. and G. Adler (2001). "From acinar cell damage to systemic inflammatory response: current concepts in pancreatitis." Pancreatology **1**(4): 356-362.
Whitcomb, D. C. (2006). "Clinical practice. Acute pancreatitis." N Engl J Med **354**(20): 2142-2150.
Whitcomb, D. C., M. C. Gorry, et al. (1996). "Hereditary pancreatitis is caused by a mutation in the cationic trypsinogen gene." Nat Genet **14**(2): 141-145.
Witt, H. (2003). "Chronic pancreatitis and cystic fibrosis." Gut **52 Suppl 2**: ii31-41.
Witt, H., M. V. Apte, et al. (2007). "Chronic pancreatitis: challenges and advances in pathogenesis, genetics, diagnosis, and therapy." Gastroenterology **132**(4): 1557-1573.
Witt, H., W. Luck, et al. (2000). "Mutations in the gene encoding the serine protease inhibitor, Kazal type 1 are associated with chronic pancreatitis." Nat Genet **25**(2): 213-216.
Yasukawa, H., M. Ohishi, et al. (2003). "IL-6 induces an anti-inflammatory response in the absence of SOCS3 in macrophages." Nat Immunol **4**(6): 551-556.
Yoshida, N. and T. Yoshikawa (2008). "Basic and translational research on proteinase-activated receptors: implication of proteinase/proteinase-activated receptor in gastrointestinal inflammation." J Pharmacol Sci **108**(4): 415-421.
Yu, J. H., K. H. Kim, et al. (2006). "Suppression of IL-1beta expression by the Jak 2 inhibitor AG490 in cerulein-stimulated pancreatic acinar cells." Biochem Pharmacol **72**(11): 1555-1562.
Yu, J. H., J. W. Lim, et al. (2002). "Suppression of cerulein-induced cytokine expression by antioxidants in pancreatic acinar cells." Lab Invest **82**(10): 1359-1368.
Zhong, Z., Z. Wen, et al. (1994). "Stat3: a STAT family member activated by tyrosine phosphorylation in response to epidermal growth factor and interleukin-6." Science **264**(5155): 95-98.

7 Supplemental material

7.1 Supplemental Figures and tables

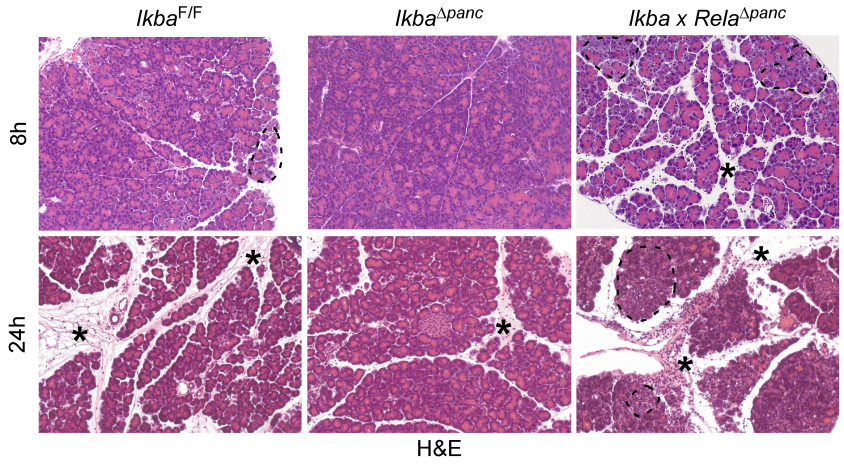

Figure 7-1: Histologic sections of the pancreas of *Ikba*$^{F/F}$, *Ikba*$^{\Delta panc}$, and *Ikba x Rela*$^{\Delta panc}$ mice were analyzed after 8 and 24 hours of cerulein administration. *Ikba x Rela*$^{\Delta panc}$ mice showed increased edema (black stars) and necrosis (dashed line). Adapted from (Schwerdtfeger 2012).

Table 7-1: *SERPINA3* (*AACT*) coding variants in subjects with acute pancreatitis, chronic pancreatitis and healthy controls CP, chronic pancreatitis; het, heterozygous; homo, homozygous; NS, not significant * one subject was homozygous for c.303A>G; ** two subjects were homozygous for c.303A>G

	Acute Pancreatitis				**CP**	**Controls**	*P* value
Degree of Severity	**1**	**2**	**3**	**Total**			
c.8G>A (p.R3K)	0/36 (0%)	0/116 (0%)	0/67 (0%)	0/219 (0%)	0/242 (0%)	1/401 (0.3%)	NS
c.25G>A (p.9AA)	13/36 (36.1%)	24/116 (20.7%)	19/67 (28.4%)	56/219 (25.6%)	64/242 (26.5%)	92/401 (22.9%)	NS
c.25G>A (p.9AT)	13/36 (36.1%)	61/116 (52.6%)	28/67 (41.8%)	102/219 (46.6%)	115/242 (47.5%)	211/401 (52.6%)	NS
c.25G>A (p.9TT)	10/36 (27.8%)	31/116 (26.7%)	20/67 (29.9%)	61/219 (27.9%)	63/242 (26%)	98/401 (24.4%)	NS
c.25G (p.9A)	39/72 (54.2%)	109/232 (47%)	66/134 (49.3%)	214/438 (48.9%)	243/484 (50.2%)	395/802 (49.3%)	NS
c.25A (p.9T)	33/72 (45.8%)	123/232 (53%)	68/134 (50.7%)	224/438 (51.1%)	241/484 (49.8%)	407/802 (50.8%)	NS
c.36C>T (p.L12L)	0/36 (0%)	4/116 (3.5%)	0/67 (0%)	4/219 (1.8%)	2/242 (0.8%)	7/401 (1.8%)	NS
c.122G>A (p.R41Q)	0/36 (0%)	0/116 (0%)	0/67 (0%)	0/219 (0%)	0/242 (0%)	1/401 (0.3%)	NS
c.153C>T (p.S51S)	0/36 (0%)	0/116 (0%)	0/67 (0%)	0/219 (0%)	1/242 (0.4%)	0/401 (0%)	NS
c.303A>G (p.K101K)	9/36 (25%)	17/116 (14.7%)*	9/67 (13.4%)	35/219 (16.0%)*	50/242 (20.7%)	74/401 (18.5%)**	NS
c.754C>G (p.P252A)					0/242 (0%)	1/52 (1.9%)	NS
c.786C>A (p.T262T)					1/242 (0.4%)	0/52 (0%)	NS
c.798G>A (p.L266L)					5/242 (2.1%)	1/52 (1.9%)	NS
c.819C>T (p.S273S)					12/242 (5.0%)	3/52 (5.8%)	NS
c.822A>C (p.A274A)					3/242 (1.2%)	1/52 (1.9%)	NS
c.843A>T (p.Q281H)					1/242 (0.4%)	0/52 (0%)	NS
c.1041A>G (p.T347T)					5/242 (2.1%)	2/52 (3.9%)	NS

Table 7-2: Patients with severe acute pancreatitis and respiratory failure. Etiology: Biliary:0, Alcohol:1, ERCP:2, Drugs:3, Other:4, Unknown:5

Patient ID	Gender	Age	Severity Atlanta	Etiology
1	m	56	severe	5
2	m	89	severe	2
3	m	92	severe	0
4	m	31	severe	1
5	f	57	severe	0
6	m	77	severe	0
27	f	81	severe	0
28	f	62	severe	2
29	m	81	severe	5
30	f		severe	2

Table 7-3: Patients with mild acute pancreatitis. Etiology: Biliary:0, Alcohol:1, ERCP:2, Drugs:3, Other:4, Unknown:5

Patient ID	Gender	Age	Severity Atlanta	Etiology
7	f	57	mild	0
8	m	74	mild	0
9	f	47	mild	0
10	f	55	mild	5
11	f	78	mild	4
12	m	30	mild	0
13	f	37	mild	2
14	m	84	mild	5
15	m	67	mild	0
16	f	71	mild	2
17	f	56	mild	0
18	m		mild	1
19	m	83	mild	5
20	m	64	mild	0
21	f	29	mild	1
22	f	54	mild	4
23	f	19	mild	3
24	f	30	mild	3
25	m	21	mild	5
26	m	45	mild	2

8 Appendix

8.1 List of abbreviations

AACT	Alpha-1-antichymotrypsin
AKT	v-akt murine thymoma viral oncogene homolog
ALB1	Albumin
ALI	Acute lung injury
ALT	Alanine aminotransferase
AP	Acute pancreatits
ARDS	Acute respiratory distress syndrome
AST	Aspartate aminotransferase
BALF	Bronchoalveolar lavage fluid
bp	base pairs
BUN	Blood urea nitrogen
CCK	Cholecystokinin
CP	Chronic pancreatitis
Cxcl1	chemokine (C-X-C motif) ligand 1
Da	Dalton
ERCP	Endoscopic retrograde cholangiopancreatography
ERK	Extracellular signal-related protein kinase
FACS	fluorescence activated cell sorting
FD4	Fluorescein isothiocyante dextran 4
FFPE	Formalin-fixed, paraffin-embedded
H & E	Hematoxylin and eosin
IF	Immunofluorescence
Ifu	Infectious unit
IHC	Immunohistochemistry
IκBα	inhibitor of kappa B
IKK	IκB kinase
IL-6	Interleukin 6
IL-6R	Interleukin 6 receptor
LAL	Limulus amebocyte lysate

MAPK	Mitogen activated protein kinase
MOF	Multiple organ failure
MPO	Myeloperoxidase
NF-κB	nuclear factor 'kappa-light-chain-enhancer' of activated B-cells
PAP1	Pancreatitis-associated protein 1
PMN	Polymorphonuclear macrophages
PTF1a	pancreas specific transcription factor, 1a
RelA/p65	v-rel reticuloendotheliosis viral oncogene homolog A
ROS	reactive oxygen species
RT-PCR	Reverse transcription-Polymerase-chain reaction
SAP	Severe acute pancreatitis
SIRS	systemic inflammatory response syndrome
SNP	Single Nucleotide Polymorphism
Socs3	suppressor of cytokine signaling 3
Spi2A	Serine protease inhibitor 2A
Stat3	signal transducer and activator of transcription 3
WT	Wild type

8.2 Acknowledgements – Danksagungen

Mein besonderer Dank gilt PD Dr. Hana Algül für die Möglichkeit diese Arbeit in seiner Arbeitsgruppe durchzuführen. Danke auch für die gute und motivierende Betreuung und die Unterstützung während meiner Doktorarbeit.

Außerdem möchte ich mich ganz herzlich bei Prof. Dr. Heiko Witt für seine bereitwillige und sehr hilfreiche Betreuung meiner Doktorarbeit und die Durchführung der SNP Analysen bedanken.

Vielen Dank auch an Prof. Dr. Roland Schmid für die tolle Atmosphäre in der 2 Medizinischen Klinik und die vielen netten Ausflüge zum Skifahren, Wandern und zum Oktoberfest.

Auch möchte ich mich ganz herzlich bei den Mitgliedern meiner Arbeitsgruppe bedanken. Matthias, Karen, Song, Magda, Hong, Sonja, Nina, Chantal, Marina und auch Pawel und Barbara aus der AG Siveke, vielen Dank für die schöne Zeit und hilfreichen Diskussionen. Vor allem bei Matthias möchte ich mich für seine Unterstützung und für die vielen hilfreichen Diskussionen bedanken.

Mein Dank gilt auch Prof. Dr. Walter Halangk und Dr. Thomas Wartmann für die Hilfe bei der Trypsinbestimmung und Prof. Dr. Stefan Rose-John und Prof. Dr. Björn Rabe für die Zusammenarbeit beim Trans-signaling Projekt.

Vor allem möchte ich mich bei meiner Familie und meinen Freunden für Ihre großartige Unterstützung bedanken.